2015-12-01

Shaking Table Testing to Evaluate Effectiveness of Prefabricated Vertical Drains for Liquefaction Mitigation

Caleb Robert Oakes
Brigham Young University

Shaking Table Testing to Evaluate Effectiveness of Prefabricated Vertical Drains for Liquefaction Mitigation

Caleb Robert Oakes

A thesis submitted to the faculty of
Brigham Young University
in partial fulfillment of the requirements for the degree of

Master of Science

Kyle M. Rollins, Chair
Norman L. Jones
Kevin W. Franke

Department of Civil and Environmental Engineering

Brigham Young University

December 2015

ABSTRACT

Shaking Table Testing to Evaluate Effectiveness of Prefabricated Vertical Drains for Liquefaction Mitigation

Caleb Robert Oakes
Department of Civil and Environmental Engineering, BYU
Master of Science

This study was designed to evaluate the ability of vertical drains to prevent liquefaction and limit associated settlement. Drain performance was investigated using full-scale tests with vertical drains in liquefiable sand using a laminar shear box with acceleration time histories applied at the base. Performance of the sand box with drains in these tests was compared with performance of the sane box without drains in previous tests. The test data was also used to create case histories which can be used for further research and calibration of computer models.

Although some investigations regarding vertical drains have been performed with centrifuge tests, no full-scale drain installation had been tested previously. Two drain geometries were investigated, first with drains spaced at 4 feet and second with drains spaced at 3 feet, to determine the effect of spacing on drain effectiveness.

Sand was hydraulically placed at a relative density of about 40%. Sensors to monitor pore water pressure, settlement, lateral displacement, and acceleration were placed in the laminar shear box. Three rounds of testing were performed with each drain configuration. Each round consisted of three tests, with peak sinusoidal acceleration levels of 0.05g, 0.1g, and 0.2g respectively, with 15 sinusoidal cycles in each case. A cone penetration test sounding was performed between each round as well as before and after testing to characterize the soil properties for each round.

Prefabricated drains were effective at reducing excess pore pressure generation during shaking and increasing the rate of dissipation immediately following the shaking. Liquefaction induced settlement was typically reduced by about 50% relative to tests without drains. These results are in good agreement with results from previous centrifuge testing. Drains spaced closer together reduced the excess pore pressure that generated during shaking and increased the rate of pore pressure dissipation relative to tests with drains spaced further apart, but post-liquefaction settlements were similar. As the soil became denser, settlement decreased significantly, as did the time for pore pressures to dissipate.

Keywords: Caleb Oakes, Kyle Rollins, liquefaction, liquefaction mitigation, drains

ACKNOWLEDGEMENTS

I would like to thank Dr. Rollins, without which I would not have a master's thesis, nor much of my knowledge of Geotechnical Engineering. I would especially like to thank my wife, Natalie, who has been with me and by my side through even some of my classes, but all of the work to complete my Master's degree. I would also like to thank Dr. Franke and Dr. Jones for being members of my committee and answering my questions, as well as taking an interest in me.

Funding for this study was provided by Grant No. CMMI 1052645 from the National Science Foundation and by FHWA pooled fund study TPF-5(244) supported by Departments of Transportation from the states of Alaska, California, New York, and Utah. Utah served as the lead agency with David Stevens as the project manager. This support is gratefully acknowledged; however, the opinions, conclusions and recommendations in this paper do not necessarily represent those of the sponsoring organizations. The testing program was conducted at the NEES@UB laboratory at the State University of New York-Buffalo with support from the George Brown Network for Earthquake Engineering Simulation (NEES). The assistance of the laboratory staff at NEES@Buffalo is greatly appreciated.

TABLE OF CONTENTS

LIST OF TABLES

LIST OF FIGURES

1 INTRODUCTION

Liquefaction of loose saturated sand results in significant damage to transportation systems in nearly every major earthquake event. Liquefaction and the resulting loss of shear strength can lead to landslides, lateral spreading of bridge abutments and wharfs, loss of vertical and lateral bearing support for foundations, and excessive foundation settlement and rotation. Liquefaction resulted in nearly $1 billion worth of damage during the 1964 Niigata Japan earthquake (NRC, 1985), $99 million damage in the 1989 Loma Prieta earthquake (Holzer, 1998), and over $11.8 billion in damage just to ports and wharf facilities in the 1995 Kobe earthquake (EQE,1995). The loss of these major port facilities subsequently led to significant indirect economic losses. Port facilities in Oakland, Los Angeles and Seattle are vulnerable to similar losses.

Typically, liquefaction hazards have been mitigated by densifying the soil in-situ using techniques such as vibrocompaction, stone columns, compaction grouting, dynamic compaction, or explosives. An alternative to densifying the sand is to provide drainage so that the excess pore water pressures generated by the earthquake shaking are rapidly dissipated, thereby preventing liquefaction. The excess pore pressure ratio (r_u = excess pore pressure divided by the vertical effective stress) must normally be kept below 0.4 to prevent excessive settlement due to increases in compressibility (Albaisa and Lee 1974, Seed and Booker, 1977)

Vertical drains allow for pore pressure dissipation through horizontal flow which significantly decreases the drainage path length. This feature becomes particularly important when drainage is impeded by a horizontal silt or clay layer and a water interlayer forms further increasing the potential for sliding (Kulasingam et al. 2004). As shown in Figure 1 vertical drains can relieve these pressures, prevent the formation of a water interlayer, and reduce the potential for lateral spreading and slope instability.

The concept of using vertical gravel drains for liquefaction mitigation was pioneered by Seed and Booker (1977). They developed design charts that could be used to determine drain diameter and spacing. Improved curves which account for head losses were developed by Onoue (1988). Although gravel drains or stone columns have been utilized at many sites for liquefaction mitigation, most designers have relied on the densification provided by the stone column installation rather than the drainage. Some investigators suspect that significant settlement might still occur even if drainage prevents liquefaction. In addition, investigators have found that sand infiltration can reduce the hydraulic conductivity and flow capacity of gravel drains in practice relative to lab values (Boulanger et al. 1997).

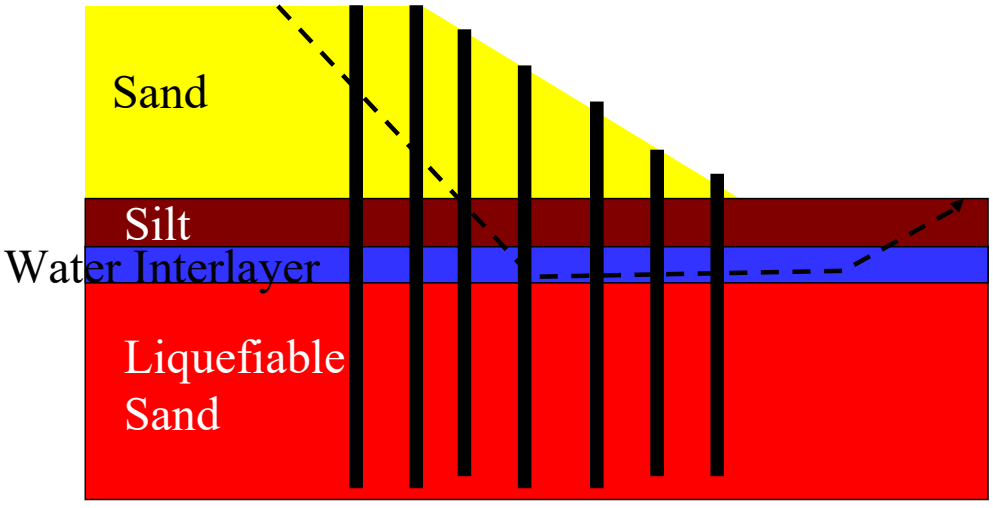

Figure 1 Schematic Drawing Showing the Potential for Vertical Drains to Relieve Pore Pressures and Intercept Water Interlayers Which May Form Below a Low Permeability Silt Layer

One recent innovation for providing drainage is the geo-composite drain (Rollins 2003). As shown in Figure 2, geo-composite drains are vertical, slotted plastic drain pipes also known as "EQ drains" which are typically 75 to 150 mm in diameter. These drains are installed with a vibrating steel mandrel in much the same way that smaller pre-fabricated vertical drains (PVDs) are installed for consolidation of clays. The geocomposite drains are typically placed in a triangular grid pattern at center-to-center spacings of 1 to 2 m depending on the permeability of the treated soil. In contrast to conventional PVDs, which have limited flow capacity (2.83×10^{-5} m^3/sec, for a gradient of 0.25), a 100 mm diameter drain can theoretically carry very large flow volumes (0.093 m^3/sec) with the potential to relieve water pressure in sands. This flow volume is more than 10 times greater than that provided by a typical 1 m diameter stone column (6.51×10^{-3} m^3/sec). Filter fabric sleeves are placed around the drains to prevent infiltration of sand.

Figure 2 (a) EQ Drain Without Filter Fabric Showing Slots Illuminated by Light Inside Pipe and (b) EQ Drain with Filter Fabric and Anchor Plate at the End (Rollins et al, 2004).

Unfortunately, no field performance data is available to show how vertical drains actually perform when subjected to earthquake motions. In the absence of earthquake performance data, investigators have used a number of methods to investigate the effectiveness of vertical geo-composite drains. These methods include: field tests involving controlled blasting or vibrations to induced liquefaction, centrifuge testing with scaled models which are accelerated to simulate the stress levels existing under field conditions and numerical methods. While each of these methods can be used to obtain useful information about the performance of earthquake drains, a full scale test should be performed to validate the results found in the other tests which are only analogues of the actual field conditions.

1.1 Project Objectives and Scope

The objectives of this project are to:

1. Evaluate the ability of pre-fabricated vertical drains to reduce excess pore pressure and settlement for level ground conditions at progressively higher acceleration levels.
2. Define the influence of drain spacing on the effectiveness of the drains for mitigating liquefaction hazard.
3. Provide well-documented case histories which can be used to calibrate/validate numerical models for predicting the performance of pre-fabricated vertical drains.

To accomplish the project objectives, full scale testing was performed using the laminar shear box at the State University of New York-Buffalo. This "shared-use" facility was made available through the George Brown Network for Earthquake Engineering Simulation (NEES) program of the National Science Foundation. Sand within the laminar box extended to a depth of 14.5 to 16.5 ft and 3-inch diameter corrugated drain pipes extended to the base of the sand. One series of tests were performed with a center to center drain spacing of 4 ft while a second series of

tests involved drains at 3 ft spacing. Comparisons between the two spacings will help determine whether the smaller spacing is significantly better at reducing pore pressures and settlement. A total of nine shaking tests were applied to each sand model with base input motions consisting of 15 cycles with peak accelerations ranging from 0.05g to 0.2g.

The project will determine whether earthquake drains can effectively reduce excess pore pressures and settlement due to liquefaction. This was determined by measuring pore pressure ratios using pore pressure transducers in three columns with the transducers spaced at 2.5' vertical intervals. Settlement was measured at the surface with string potentiometers, through the profile using Sondex settlement profilometers, and by measuring the water vacated during the test.

This project includes setup and performance of the test at the University at Buffalo NEES facility, as well as data reduction to produce case histories of earthquake drains under earthquake loading. Further evaluation of the test data to match the results with current numerical models will be performed in the future by other students and is not included in the scope of this thesis.

2 LITERATURE REVIEW

In this chapter, studies relevant to the thesis are presented. This includes (1) field testing involving controlled blasting or vibrations to induce liquefaction with and without vertical drains, (2) centrifuge testing with scaled models which are accelerated to simulate the stress levels existing under field conditions with and without drains, and (3) numerical models to investigate vertical drain performance. In addition, tests performed previously with the laminar shear box without earthquake drains are summarized so that they can be compared subsequently with laminar box tests conducted as part of this study.

2.1 Field Testing to Evaluate Vertical Drains for Liquefaction Remediation

Rollins et al (2003) employed controlled blasting techniques to generate excess pore pressures to test full-scale EQ drains at a test site on Treasure Island in San Francisco Bay. These tests investigated the pore pressure dissipation properties of EQ drains and the densification produced during drain installation. The test site consisted of two rings of blast holes with several test regions surrounding the blast holes. Each test region contained a cluster of seven EQ drains installed in a triangular grid pattern, incorporating various combinations of drain spacing, use of a filter sock, and amount of vibration used during installation. Installation settlement was dependent on the vibration energy and reached as much as 0.3 m. This densification increased the cone penetration resistance by about 25%.

Due to the rapid loading rate from the explosive changes, the EQ drains were unable to prevent liquefaction. However, dissipation rates were substantially increased as shown in Figure 3.

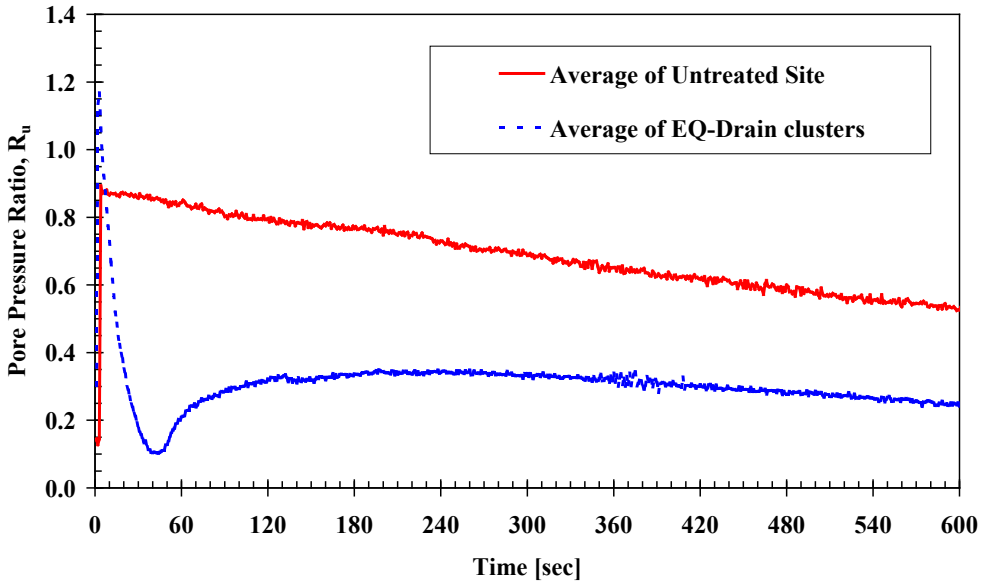

Figure 3 Comparison of Excess Pore Pressure Ratio as a Function of Time at Sites Treated with EQ Drains Relative to an Untreated Test Site (Rollins et al. 2003).

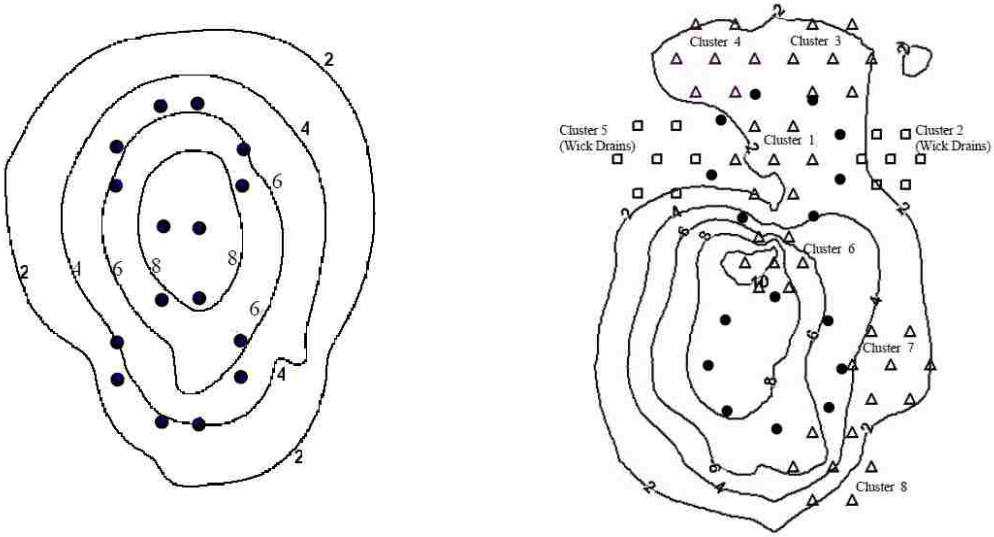

Figure 4 Contours of Measured Settlement (in cm) for (A) Untreated Site and (B) Site Treated with Clusters of EQ Drains After Detonation of 16 Explosive Charges Around Two 4.3 M Diameter Rings. Rollins et al, (2003).

Furthermore, post-liquefaction settlements were reduced from about 100 mm in the untreated region to less than 25 mm in several of the regions treated with drains (see Figure 4). The increase in the pore pressure ratio after initial dissipation for the drain test areas in Figure 3 appears to result from sand infiltration due to inadequate filter fabric. Several of the drains filled with sand.

Subsequently, blast liquefaction experiments with EQ drains were reported by Rollins et al. (2004) at a site south of Vancouver, BC, Canada. EQ drain performance was evaluated by installing a cluster of 35 EQ drains at one test site as shown in Figure 5 and comparing the pore pressure and settlement behavior with an adjacent, untreated control site. The drains were installed using a vibratory mandrel in a triangular grid pattern with a center-to-center spacing of 1.22 m. Drain installation caused the soil within the boundaries of the cluster to settle with a maximum settlement of over 350 mm. The relative density of the treated sand was increased from an initial value of 40% to a final value of about 50% by the drain installation.

Sixteen explosive charges in four blast holes were used to induce liquefaction. Although a 0.5 second delay was used between blasts, the charges were very large (1.8 kg to 2.7 kg) and induced liquefaction within 2 seconds. Nevertheless, pore pressure dissipation rates were much faster with the drains than without as shown in Figure 6. The drains were also able to reduce the total amount of settlement by about 40% when compared to the untreated site.

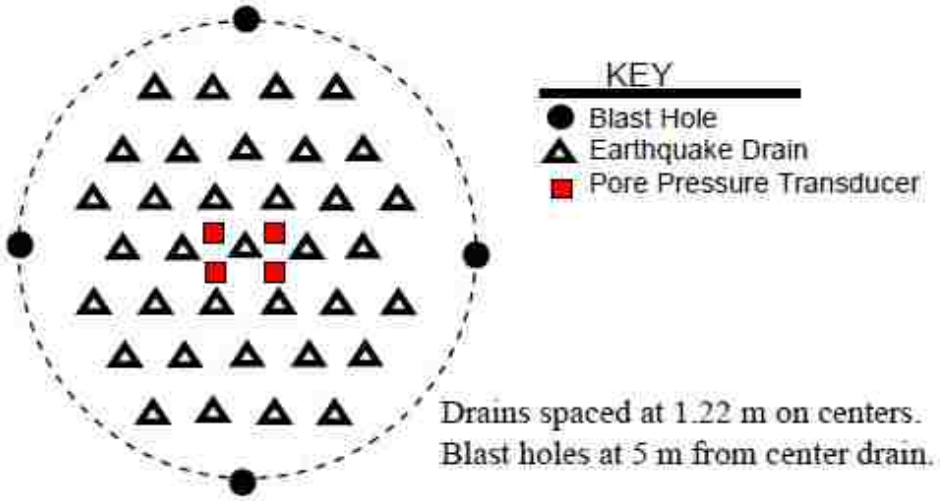

Figure 5 Layout of EQ Drains, Blast Holes and Pore Pressure Transducers to Monitor Effectiveness of Drains for Liquefaction Remediation.

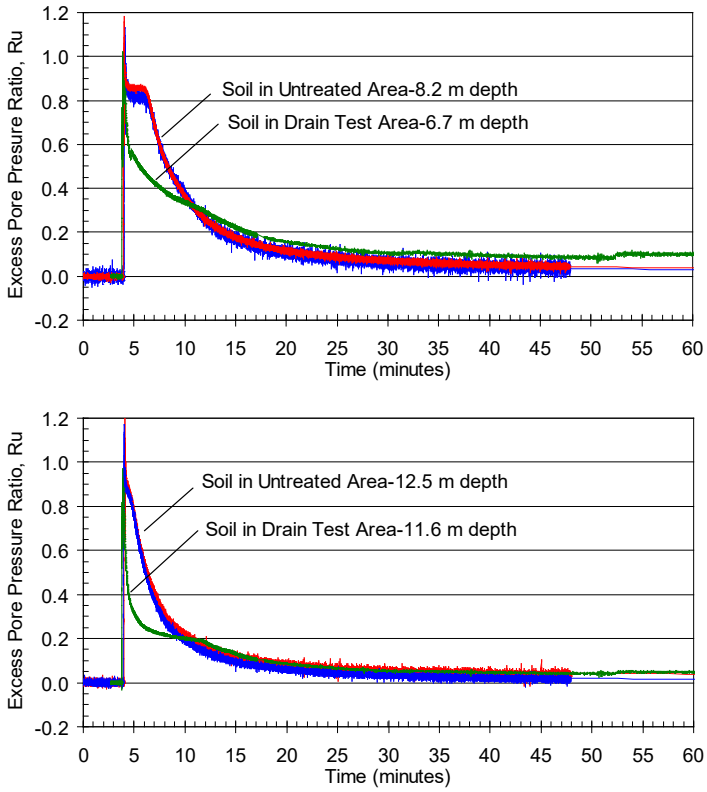

Figure 6 Comparison of Measured Excess Pore Pressure Ratio vs. Time Following Blasting at Two Depths with and Without Drains in Place (Rollins et al. 2004).

Chang et al. (2004) performed field tests on a volume of reconstituted, saturated sand measuring 1.2 m x 1.2 m x 1.2 m, surrounded by an impervious membrane. Tests were conducted with and without an EQ drain in the center of the test volume. The relative density of the sand for both tests was approximately 35%. Stress cycles were applied using a large Vibroseis Oil prospecting truck from the NEES-Univ. of Texas site and pore pressures and accelerations were measured at several points within the test volume.

Plots of the measured excess pore pressure ratio with and without a drain from this test are presented in Figure 7. Without a drain, liquefaction was produced during the application of 60 stress cycles (3 second total duration), while the excess pore pressure ratio did not exceed 0.25 (25%) for the test volume with a drain subjected to the same vibrations.

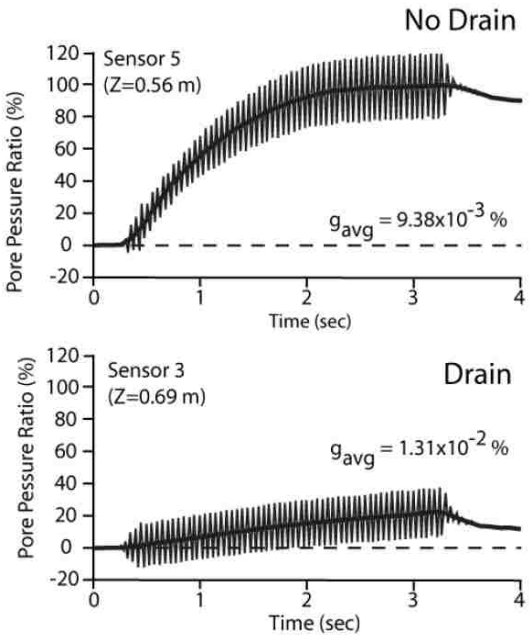

Figure 7 Comparison of Excess Pore Pressure Ratio at Test Sites with and Without a Drain While Subject to Cyclic Strain from the NEES@UT-Austin Vibroseis Truck (Chang et al, 2004).

Volumetric strain decreased from 2.1% without a drain to less than 0.5% with a drain in place. While the EQ drain successfully prevented liquefaction for this shallow soil layer, drainage of a thicker layer would be more difficult. In addition, the applied strain amplitude was relatively small and a more severe motion could produce different results.

In 2010, full scale dynamic testing was performed using a vibratory hammer excitation source in an attempt to evaluate how effective EQ drains were in dissipating excess pore water pressures (Marinucci et al. 2010). The subsurface profile beneath the topsoil consisted of relatively clean loose-to-medium dense sand underlain by silt and clay, though it was interbedded and highly variable with a water table at approximately 2 feet below ground surface (bgs). The liquefaction sensors consisted of both miniature pore water pressure transducers and tri-axial accelerometers. Crosshole seismic testing was performed to assess the saturation of the soil. The average shear wave velocities indicated that the soil was not liquefiable, but the average stress-corrected CPT tip stress values indicated the soil was highly liquefiable. The discrepancy between the two in situ test parameters was attributed to the age and cementation of the Pleistocene era sand.

The vertical EQ drains were installed using a vibratory mandrel, followed by dynamic testing that vibrated on opposite sides of the test area at various distances from the centerline. The layout of test is shown in Figure 8. The vibratory installation of one drain was used as a test of the untreated condition. Shear wave velocity decreased after the installation and testing of the drains. Significant settlement during installation of the drains indicated considerable densification of the sand, which contributed to the reduced dynamic and pore pressure responses. This densification was presumably due to breaking of cementation bonds within the sand.

Although lower excess pore pressure and settlements were generated in the treated ground relative to the untreated ground, the comparisons are not definitive. Unfortunately, the vibratory

hammer also produced significantly lower accelerations in the treated ground so that it was not possible to say conclusively whether the improved performance came from improved drainage or the reduced acceleration levels.

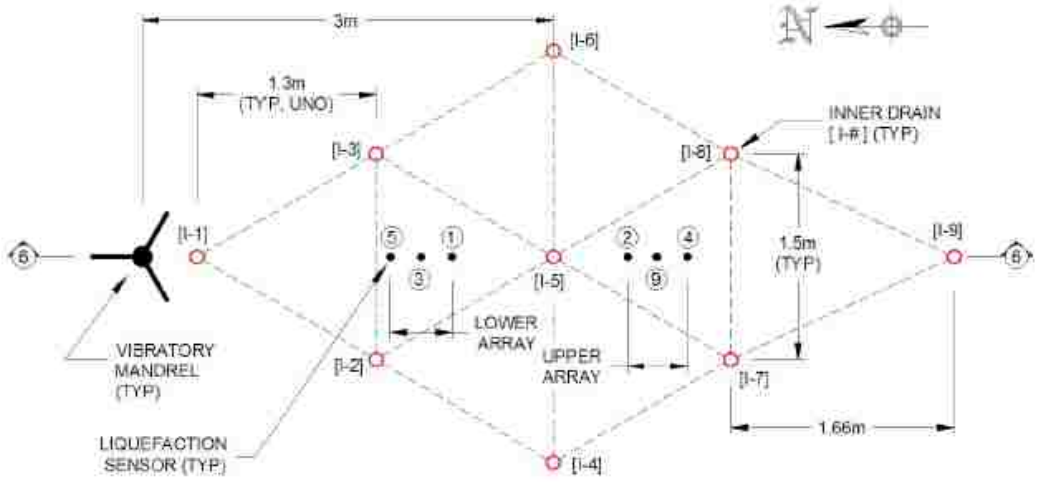

Figure 8 Plan View of the Instrumentation and Vertical Drain Geometry. The Vibratory Mandrel Source is Shown at only One Position for Clarity (Marinucci et al. 2010).

2.2 Centrifuge Testing to Evaluate Vertical Drains for Liquefaction Remediation

As part of a NEESR grand challenge study, three dynamic centrifuge tests were performed to evaluate EQ drain performance when subjected to various time histories of acceleration based on ground displacement and excess pore water pressure (Δu). Results from the first test were discussed by Kamai et al. (2007), Marinucci et al. (2008), Howell et al. (2009a), and Marinucci (2010), and results from the second test were discussed by Kamai et al. (2008) and Marinucci (2008). The first centrifuge test was used to investigate the ability of vertical drains to prevent lateral spreading. Testing was performed to compare performance of two 3° slopes, one with and one without vertical drains. At prototype scale, the soil profile consisted of a 5.5-m thick liquefiable sand overlain by a 0.5-m thick silt layer. At acceleration levels between 0.11g and

0.15g full liquefaction and some soil deformations occurred on the untreated slope while smaller pore pressures and less deformation occurred on the slope with the vertical drains.

The second centrifuge test also involved the effect of prefabricated drains on lateral spreading with a 3° slope. At prototype scale, the profile consisted of a 4.8-m thick liquefiable zone (D_r=40%), but with a 1.0-m thick clay layer overlying it. The slopes were subjected to three significant earthquake motions, with peak ground accelerations of 0.06 g, 0.11 g and 0.28g. Figure 9 presents plots of the excess pore pressure as a function of depth at various times during the 0.28 g shaking event for (a) the treated and (b) the untreated slopes. While liquefaction (excess pore pressure equal to the initial vertical effective stress line) was produced in the untreated slope, excess pore pressures were reduced by the presence of the drains. However, the drainage appears to have been more effective restricting excess pore pressures in the lower half of the profile than in the upper half.

Figure 10 provides plots of (a) the horizontal settlement and (b) the vertical settlement of the treated and untreated slopes for the series of tests with various peak ground acceleration levels. Although the vertical drains were not successful in eliminating all movement, they were effective in reducing horizontal displacements to about 20% of those for the untreated slope and vertical settlements to about 50% of the untreated slope for the acceleration levels involved.

The third centrifuge test reported by Howell, et al. (2012) consisted of three treatment areas: one untreated, one untreated but containing non-draining tubes (to confirm soil pinning was not an issue), and one drain treated. Figure 11 shows the plan view and the half of the cross section that contained the vertical drains, although the other half would mirror it to the right minus the drains. This test had a steeper slope (10° rather than 3°) and a thicker clay layer (1.5 m) over the liquefiable sand zone which was 5.5-m thick with a relative density of 40%.

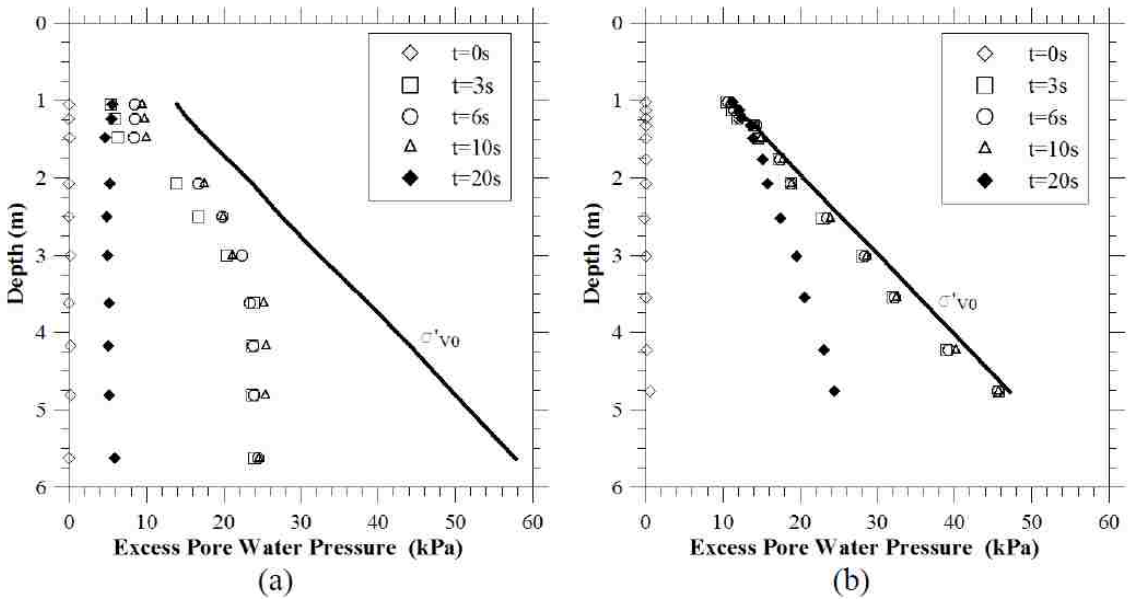

Figure 9 Excess Pore Water Pressure Profile for Varying Times for PGA=0.28g Event for (A) Treated and (B) Untreated Sides. (Note: "T=0s" Corresponds to Start of Shaking.) (Marinucci et al 2008)

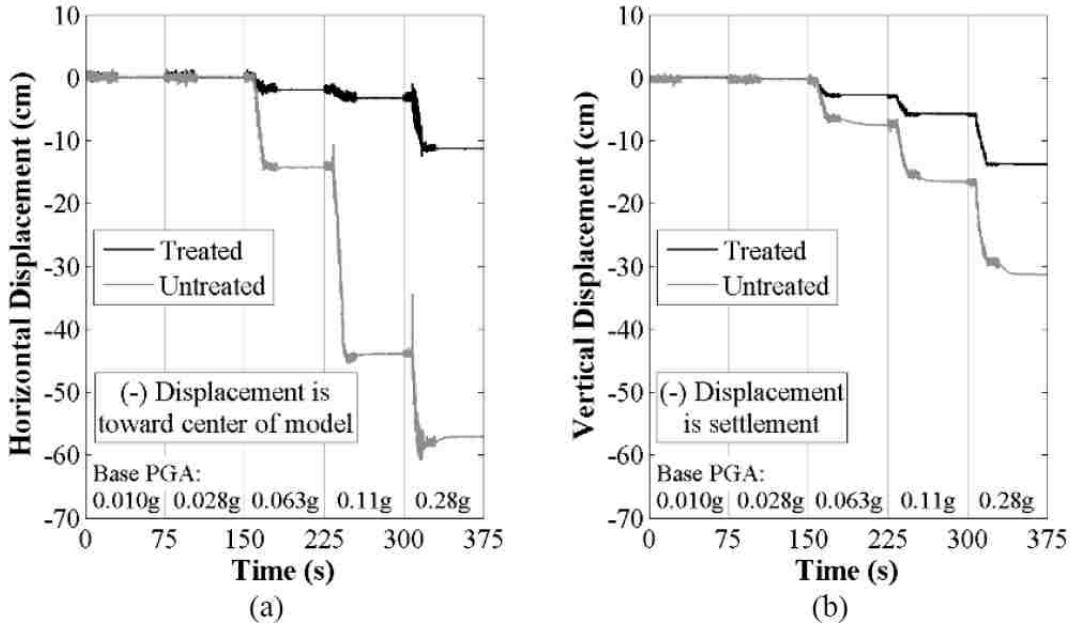

Figure 10 Shaking-Induced Deformation: (A) Horizontal and (B) Vertical Directions for Untreated and Treated Slopes. (Marinucci et al, 2008).

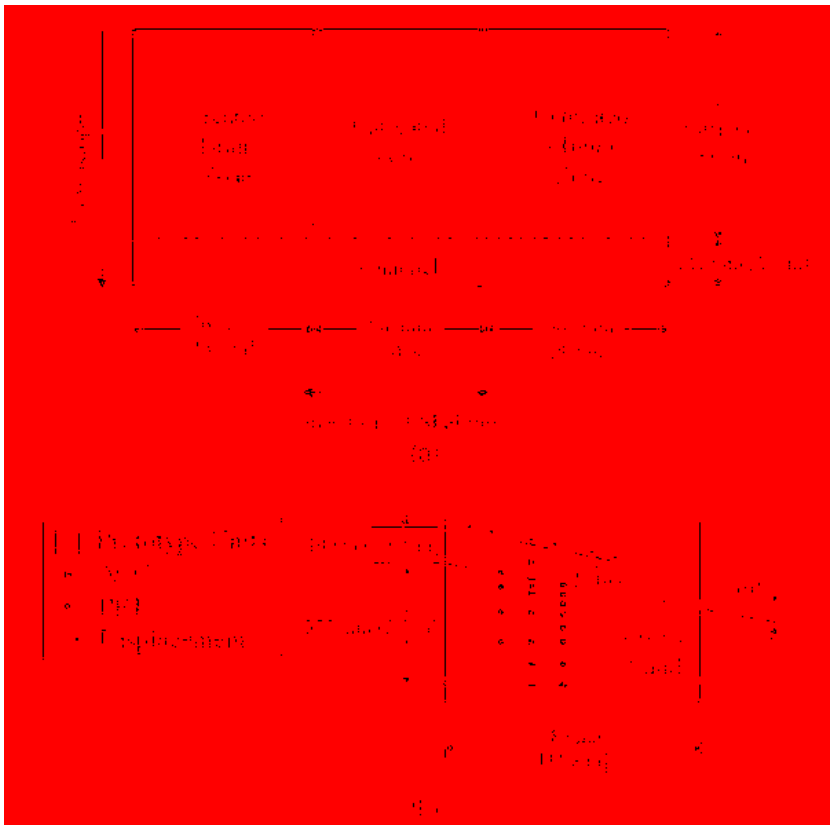

Figure 11 Layout for Centrifuge Test Comparing Behavior of Slopes in Liquefiable Sand with and Without Vertical Drains to Mitigate Liquefaction Hazard: (A) Plan; (B) Cross Section (Howell et al. 2012).

Water was used as the pore fluid for these tests out of concern about how well a more viscous fluid would flow through the model drains, which also meant that scaling laws for diffusion and dynamic response were not simultaneously satisfied (Kutter 1995). Scaling laws still apply for dynamics, and the hydraulic conductivity of the fine Nevada sand can be scaled upward by a factor of 15 to correspond to values typical of medium to coarse sands. The vertical drains were spaced at 1.5 m center to center. The slopes were subjected to progressively higher accelerations levels ranging from 0.10g to 0.95g. No appreciable difference was observed between the performance of the untreated slope and the slope with non-draining tubes so the effect of pinning was considered to be inconsequential.

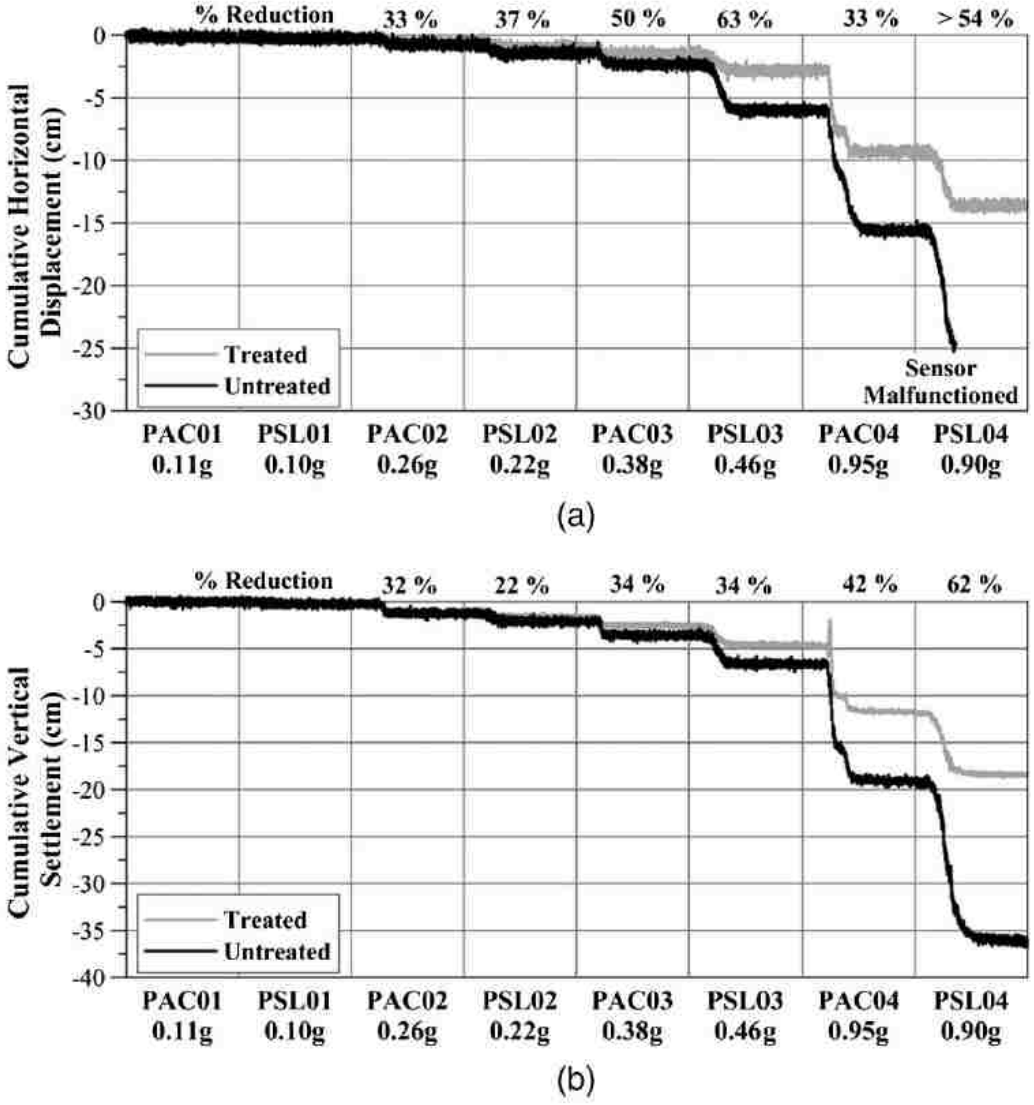

Figure 12 Cumulative (A) Horizontal and (B) Vertical Displacements at Mid-Slope in the Untreated and Treated Areas for All Shaking Events. (After Howell et al, 2012).

The vertical drains were effective in reducing the measured deformations during shaking by dissipating the excess pore water pressures both during and after the shaking event. Plots showing the cumulative (a) horizontal and (b) vertical displacements for the treated and untreated slopes for the various events are shown in Figure 12. The percent reduction in settlement is summarized in Figure 12 along with the peak ground acceleration (PGA) of the earthquake event.

The reduction in settlement for the treated slopes with drains was typically 30% to 60% of that for the untreated slopes without drains.

As indicated in Figure 12, there was often a significant variation in the reduction in deformation obtained for various records and acceleration levels. As shown in Figure 13, Howell et al (2012) found that much of this variation could be explained by plotting the displacement as a function of the elapsed time between the first and last exceedance of r_u=0.5. Therefore, the longer the soil remained in a quasi-fluid state the greater the horizontal and vertical settlement for a given soil profile. This finding demonstrates the importance of vertical drains in reducing the potential for settlement and lateral spreading.

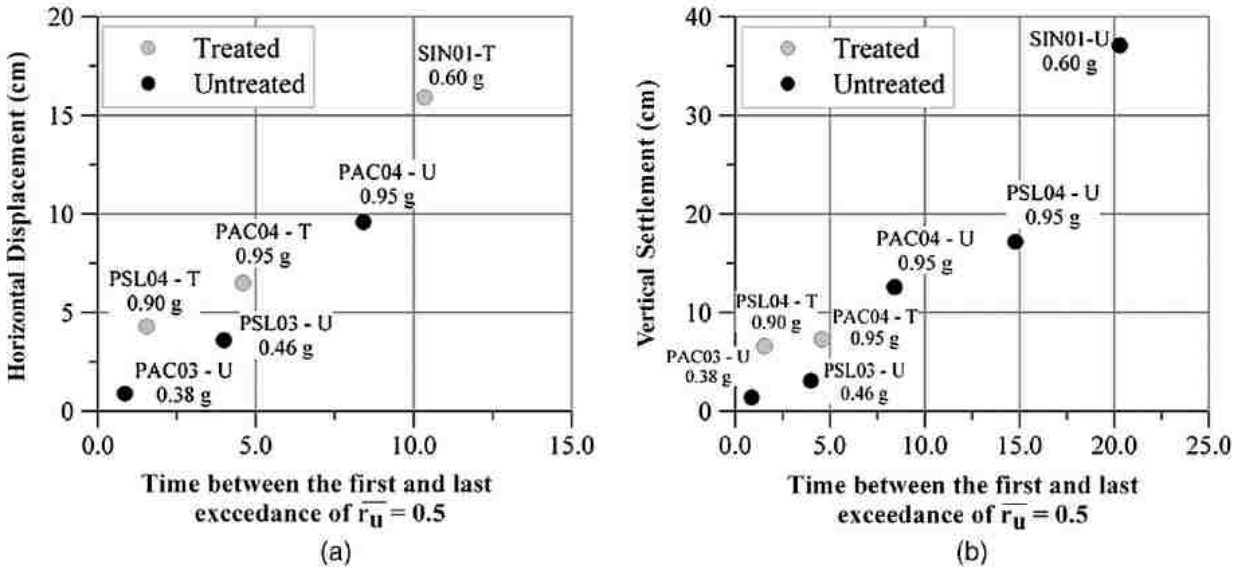

Figure 13 Horizontal and Vertical Deformations at Midslope in the Untreated and Treated Areas: (A) Horizontal Displacement, (B) Vertical Displacements as a Function of Time Between The First And Last Exceedance Of R_u=0.5. (Howell et al. 2012).

Howell also plotted time histories of r_u using different earthquake events, including a sine wave acceleration input as well as two earthquake time histories. The results are shown in Figure 14 and it may be noted that the treated r_u time history has very large oscillations for the sine wave

input motion (SIN01). Howell attributed these spikes in r_u to dilation at large strain. Howell concluded that drains are effective at reducing pore pressures both during and after shaking, even with the large dilation spikes as in the SIN01 event. With an input motion with equal intensity it is hard to realize the full impact of the drains until shaking stops because of the oscillatory nature of the excess pore pressure response.

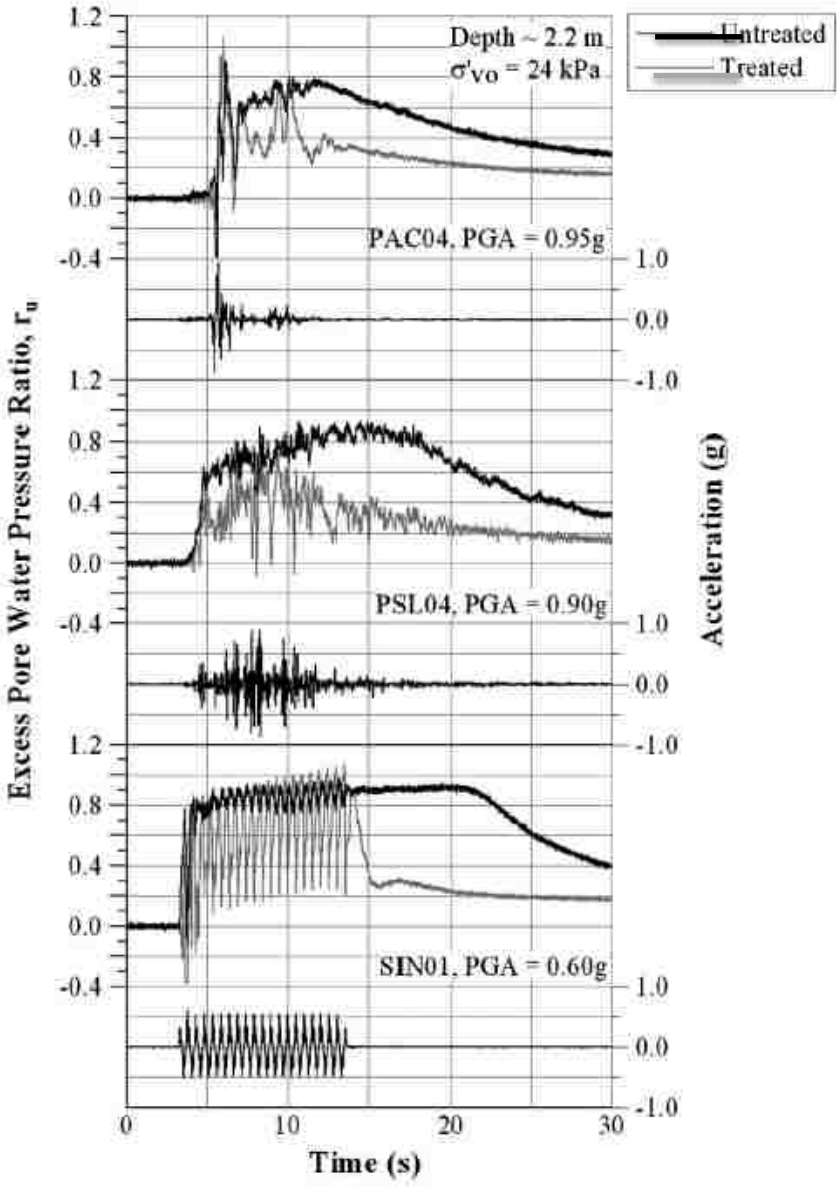

Figure 14 Excess Pore Water Pressure (r_u) Versus Time for PAC04, PSL04, and SIN01 Events (Howell et al. 2012).

2.3 Numerical Analyses Conducted to Evaluate Liquefaction Remediation with Drains

Because the blast testing approach produced liquefaction much more rapidly than an earthquake, there was less time for pore pressure dissipation and the effectiveness of drains in an earthquake might be obscured. For example, the blast sequence at the Vancouver test site took only 2 or 3 seconds to produce liquefaction while destructive earthquakes might take 10 to 60 seconds to produce liquefaction. The longer time for pore pressure buildup allows the earthquake drains to operate more effectively in limiting pore pressure generation.

To provide increased understanding of the behavior of the drains in an earthquake, Rollins et al (2004) performed numerical analyses using the computer program FEQDrain (Pestana et al, 1997). The computer model was first calibrated using the measured settlement and pore pressure response from the blast test. Then, the calibrated soil properties were held constant while the duration of shaking was increased to match typical earthquake durations. The soil layering used in the model was based on the CPT soundings. The initial estimate of permeability (k_x and k_y) for each layer was based on borehole permeability testing that was performed with a double packer inside several of the earthquake drains prior to the blast testing. The modulus of compressibility and duration of earthquake shaking were estimated using guidelines provided by Pestana et al (1997). Relatively small variations in these parameters were generally sufficient to obtain a reasonable match with the measured pore pressure dissipation and settlement time histories. In addition, calibrated parameters were within the range of measured values. Figure 15 presents plots showing (a) the computed and measured r_u vs time curves and (b) the computed and measured settlement versus time curves. In both cases the agreement is relatively good.

Analyses were then performed using the same soil profile and properties but with durations typical of various earthquakes. The ratio of equivalent earthquake stress cycles to cycles producing

liquefaction (N_q/N_l) was estimated based on magnitude and guidelines suggested by Youd et al (2001). Table 1 provides a summary of the maximum computed r_u and settlement for various earthquake events and drain spacings. Table 1 suggests that appropriately designed drains can significantly reduce excess pore pressure and settlement.

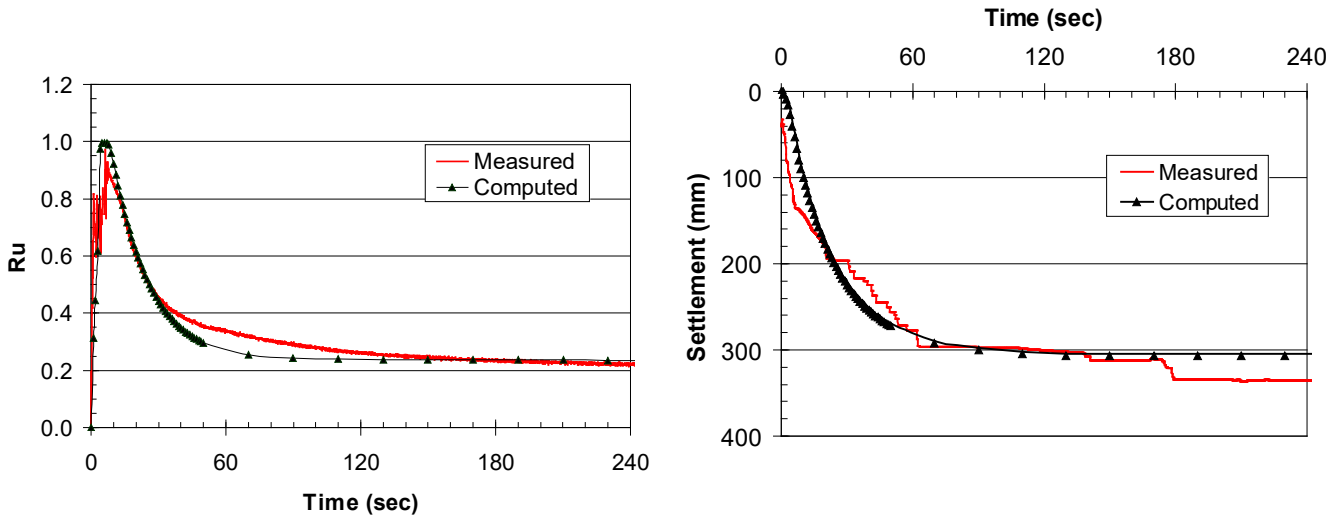

Figure 15 Comparison of (a) Measured and Computed Excess Pore Pressure Ratio (r_u) Versus Time at a Depth of 11.8 m and (b) Measured and Computed Settlement Versus Time Curves for the Vancouver Test Site. (Rollins et al, 2004).

Table 1 Summary of Computed Maximum r_u and Settlement for Various Earthquake Events and Drain Spacings at the Vancouver Site.

Magnitude	Duration (sec)	N_q/N_l	Drain Spacing (m)	Maximum. r_u	Settlement (mm)
Blast	8	4.0	1.22	1.0	310
6.0	8	2.0	0.91	0.40	31
6.75	17	2.0	0.91	0.47	35
6.75	17	3.0	0.91	0.61	48
7.5	35	2.0	0.91	0.65	53

Recent numerical simulations by Vytiniotis et al. (2013) compared slope deformations with and without EQ drains for 58 reference seismic ground motions. Using finite element software a model was created to simulate boundary conditions and ground motions to evaluate EQ drain effectiveness in reducing earthquake-induced permanent slope deformations for a partially submerged saturated sandy slope. The geometry of the model is shown in Figure 16. One of the key findings is that EQ drains show no correlation to the Arias Intensity, meaning that EQ drains will be similarly effective under different acceleration time-histories. The numerical simulations also demonstrated that EQ drains are effective in reducing earthquake-induced permanent slope deformations for sloped, loose granular, liquefiable soils such as are commonly found in U.S. ports. Though the EQ drains are behind the crest of the partially submerged slope, they reduce slope deformations by prohibiting the diffusion of excess pore pressures from the far field to the slope.

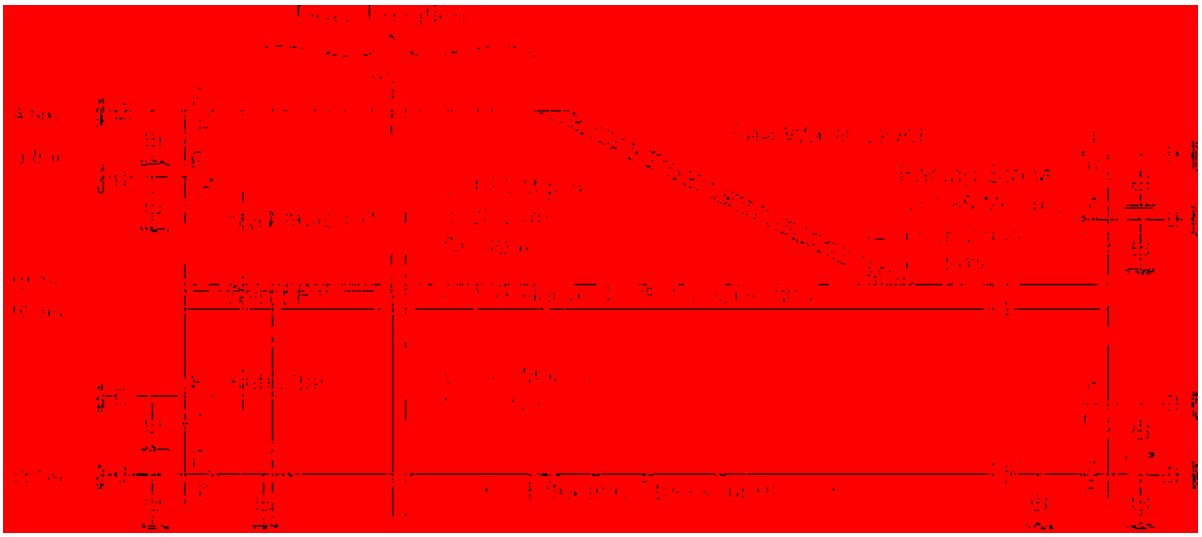

Figure 16 Analyzed Section with Details of the Properties of the Finite Element Numerical Model (Vytiniotis et al. 2013).

2.4 Previous Laminar Shear Box Testing

Prior to the testing program described in the thesis, some large-scale testing was performed using the NEES Buffalo site laminar shear box without drains, notably Level Ground Test LG0, (Bethapudi, 2008), Level Ground Test LG1 (Dobry and Thevanayagam, 2013) and Induced Partial Saturation Test IPS-1 (Yegian, 2015). In general, the soil profile consisted of 4.9m (16 ft) of loose saturated sand at a relative density of about 40%. Specified acceleration time histories were produced by two hydraulic actuators at the base of the model. These tests are valuable as comparisons for tests with drains to determine the reduction in settlement and pore pressures.

LG0 consisted of one test using sinusoidal input motions with progressively higher acceleration levels. The input motions for LG0 ranged from 0.01g to 0.30g as shown in Figure 17. The test was designed to determine the response of liquefied soil in a level ground environment. The pore pressure response to the input motions in LG0 is shown in Figure 18(a), while excess pore pressure ratios are shown in Figure 18(b) at various times during the test. As shown in Figure 18(b), after 6 seconds, the excess pore pressure ratio is approximately 1.0 down to a depth of 3.25 meters, or 10.7 feet. This liquefaction occurred 1 second into shaking at 0.05g acceleration, or after 2 loading cycles. The entire profile exceeds $r_u = 0.80$ after 10 seconds (ten 0.05g cycles) and is nearly 1.0 after 156 (20 0.05g cycles).

Time histories of excess pore pressures are shown in Figure 19 for three depths in the profile. The excess pore pressure rapidly increases until it reaches the vertical effective stress (indicating liquefaction) and remain essentially constant during cyclic loading. After cyclic loading ceases at 35 seconds, an additional 170 seconds is typically required for the excess pore pressures to dissipate to less than 10% of the maximum value at liquefaction. Dissipation appears to occur from the bottom up as a result of the upward flow of water. After the end of shaking, the

sand remains essentially liquefied for an additional 85s, 60s, and 25s at depths of 1.32m (4.3), 2.52m (8.25ft), and 3.9m(12.8ft), respectively.

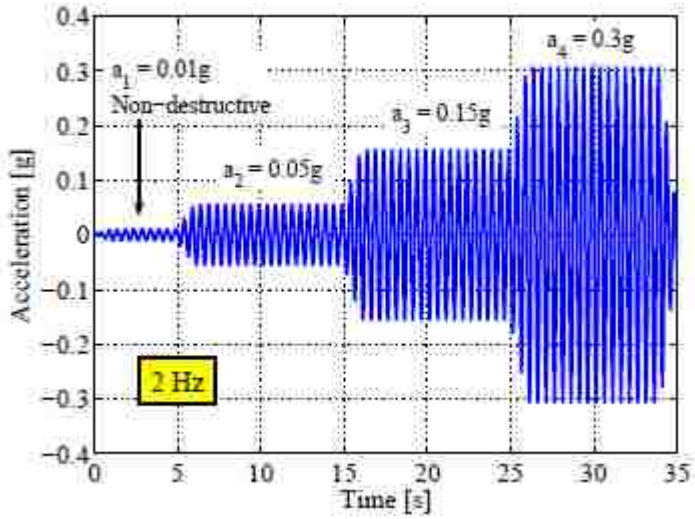

Figure 17 Input Motions for LG0 (Bethapudi 2008).

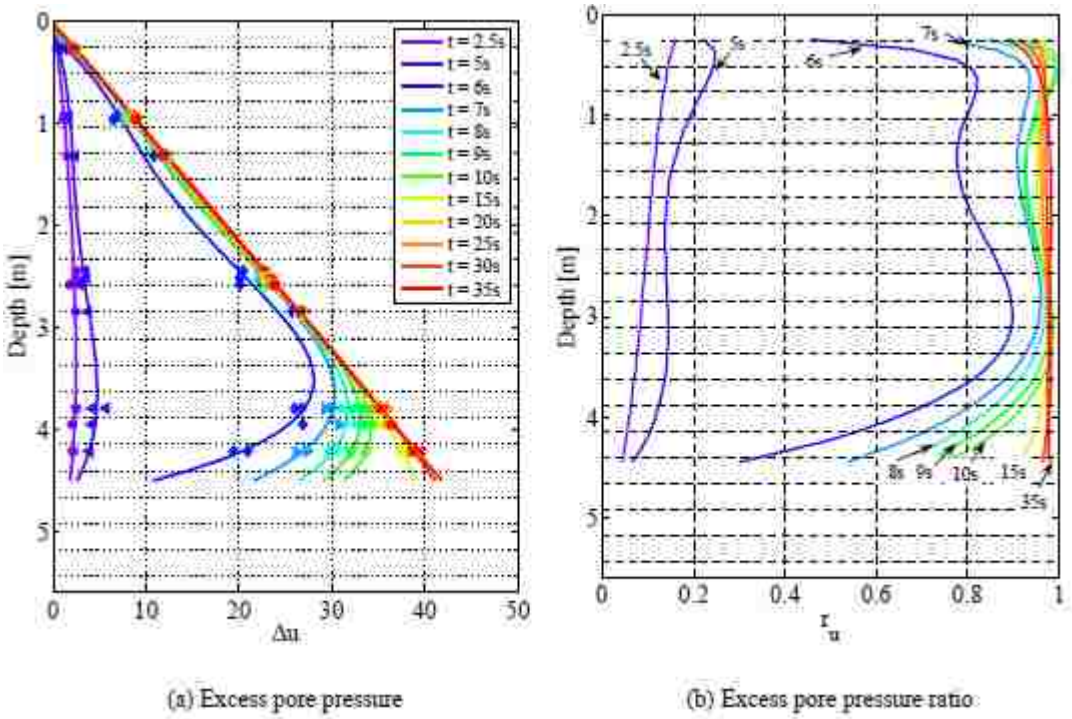

(a) Excess pore pressure (b) Excess pore pressure ratio

Figure 18 Excess Pore Pressure Profiles for LG0 (Bethapudi 2008).

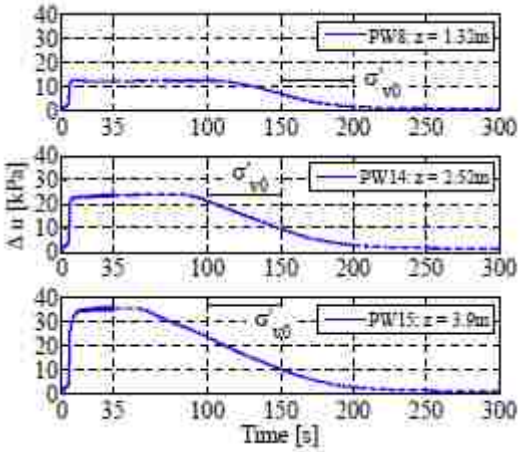

Figure 19 Excess Pore Pressure Histories Bethapudi (2008).

The ground surface settlement measured by three string potentiometers during the LG0 test is plotted in Figure 20. The average settlement at the end of shaking (35 seconds) was 1.57 inches. The total settlement after 300 seconds was 3.81 inches. The amount of settlement that occurred during shaking was 41%. The pore pressure transducer near the surface (1.32m) reached r_u=0.5 at about 175 seconds, which is about when the settlement slowed significantly as shown in Figure 20. Essentially 95% of the measured settlement has been completed at this point.

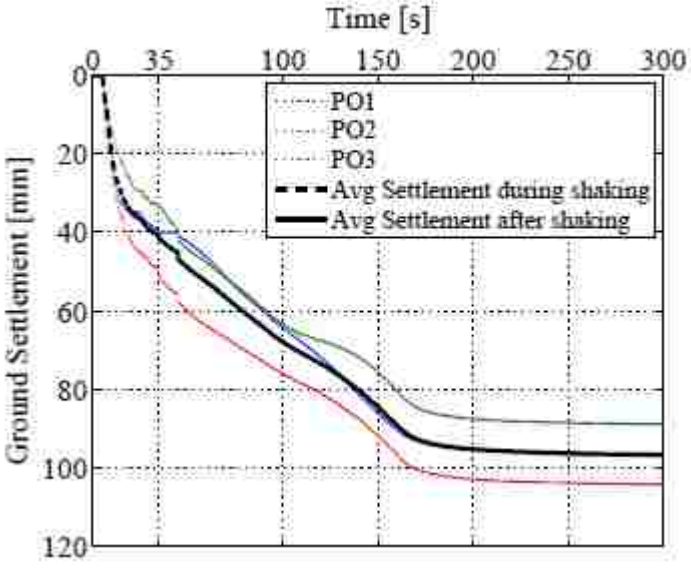

Figure 20 Settlement Histories (Bethapudi, 2008)

In the LG1 tests reported by Dobry and Thevanayagam (2013), repeated cycles of shaking were performed to observe the gain in liquefaction resistance with number of cycles. The initial relative density of the sand was 40%, which should be similar for all laminar shear box testing. LG1 used acceleration levels of 0.03g to 0.1g. An initial round of only one test at 0.03g with 15 cycles and one test with 0.1g with 15 cycles was first performed. Then, seven rounds of testing are performed in the following manner: five 0.03g tests with 5 cycles each, followed by a test at 0.03g with 15 cycles, and finally a test at 0.1g with 15 cycles. The settlement observed in LG1 for each shaking event is shown in Figure 21. Settlement gradually decreases as the number of shaking events increases and the soil slowly becomes more compact.

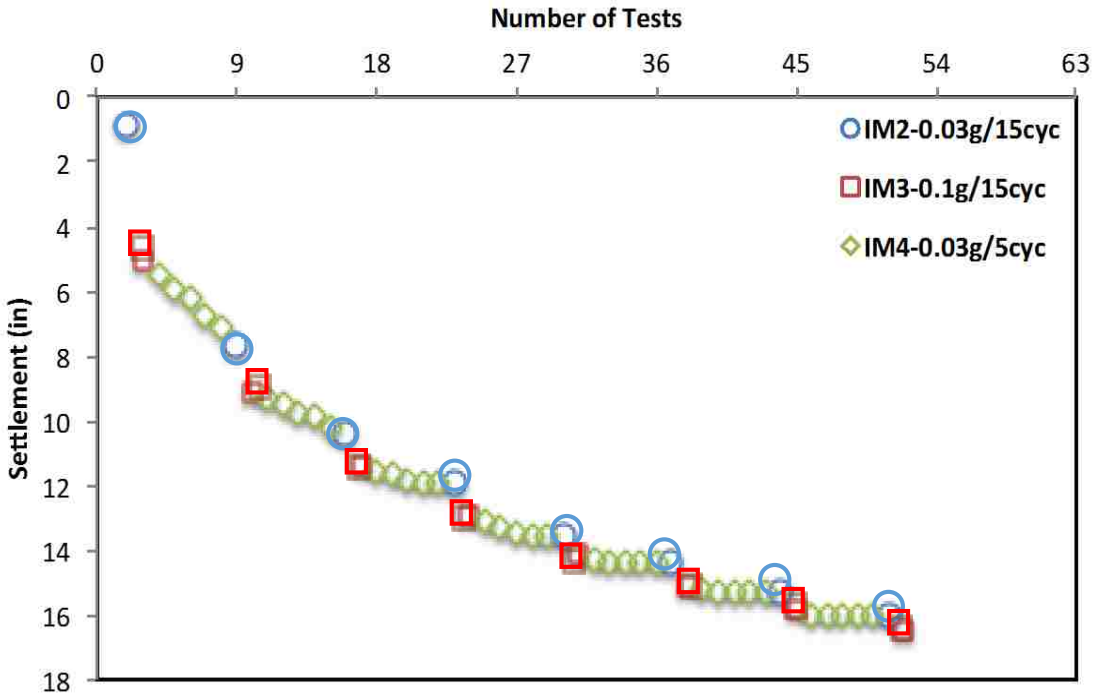

Figure 21 Settlement Due to Number of Cycles (Dobry and Thevanayagam, 2013).

For comparison with this study, all settlement attributed to the 0.03g tests are attributed to the 0.1g test following it, such that a graph of cumulative settlement vs. number of 0.10g tests is

produced as shown in Figure 22. This presumes that the small settlement associated with the six intermediate 0.03g tests "pre-strain" the soil and reduce the settlement that subsequently occurs for the 0.10g test. Therefore Figure 22 as the same shape as Figure 21 except that the number of tests would be eight rather than 54.

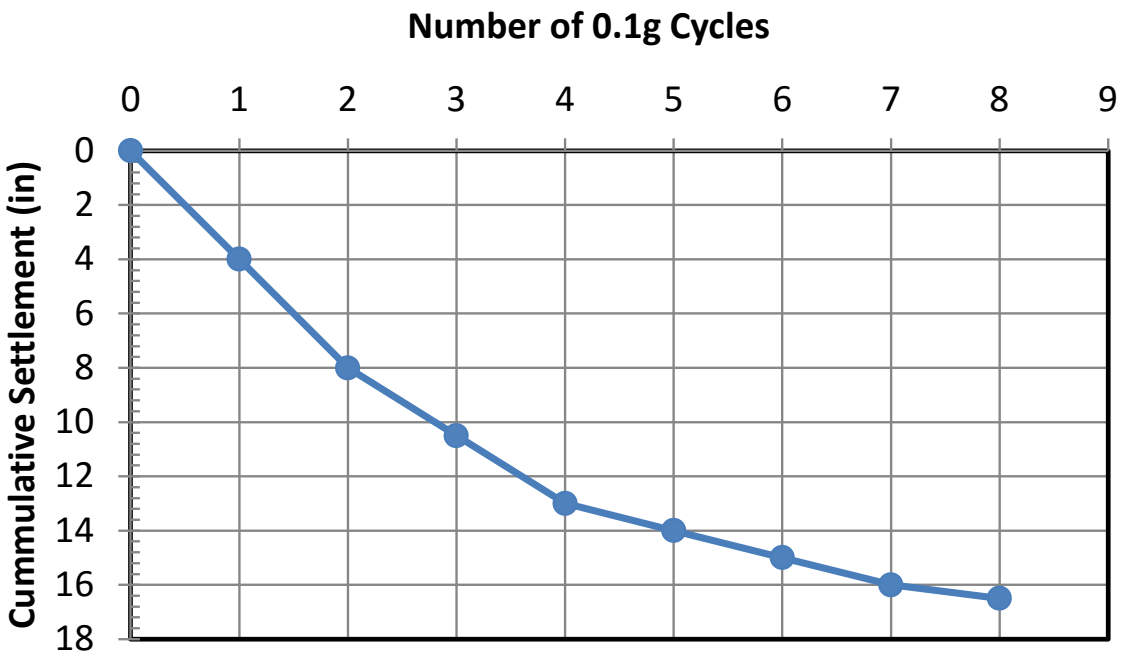

Figure 22 Settlement Versus Number of 0.1g Test Cycles (Dobry and Thevanayagam, 2013).

In the IPS1 tests, investigators from Northeastern University (Yegian, 2015) investigated the potential for increasing the liquefaction resistance using Induced Partial with the laminar shear box. Yegian treated the ground with a compound that produced air bubbles after injection, which pushed water out of the pore space and partially desaturated the sand. In IPS1, Yegian treated only the top 10 feet of soil, leaving the bottom 6.5 feet of soil untreated. Six 0.1g tests with 15 cycles were performed, followed by two 0.2g tests with 15 cycles. The cumulative settlement for the tests is shown in Figure 23. Assuming that essentially all of the settlement occurred in the untreated

zone, the settlement can be scaled up from 6.5’ layer to equal that of a full 16’ untreated layer. This settlement can then be compared to the settlement measured in LG1 and other tests in the laminar shear box. Subsequent tests performed when the entire 16’ thick layer was treated generally confirmed that the treated soil experience very little settlement. A plot of the scaled cumulative settlement versus number of shaking tests for IPS1 results is shown in Figure 24 and the agreement with the cumulative settlement curve from the LG1 test sequence is remarkably good. It should be noted, however, that the two curves diverge significantly when 0.20g loading cycles were applied to the base of the model

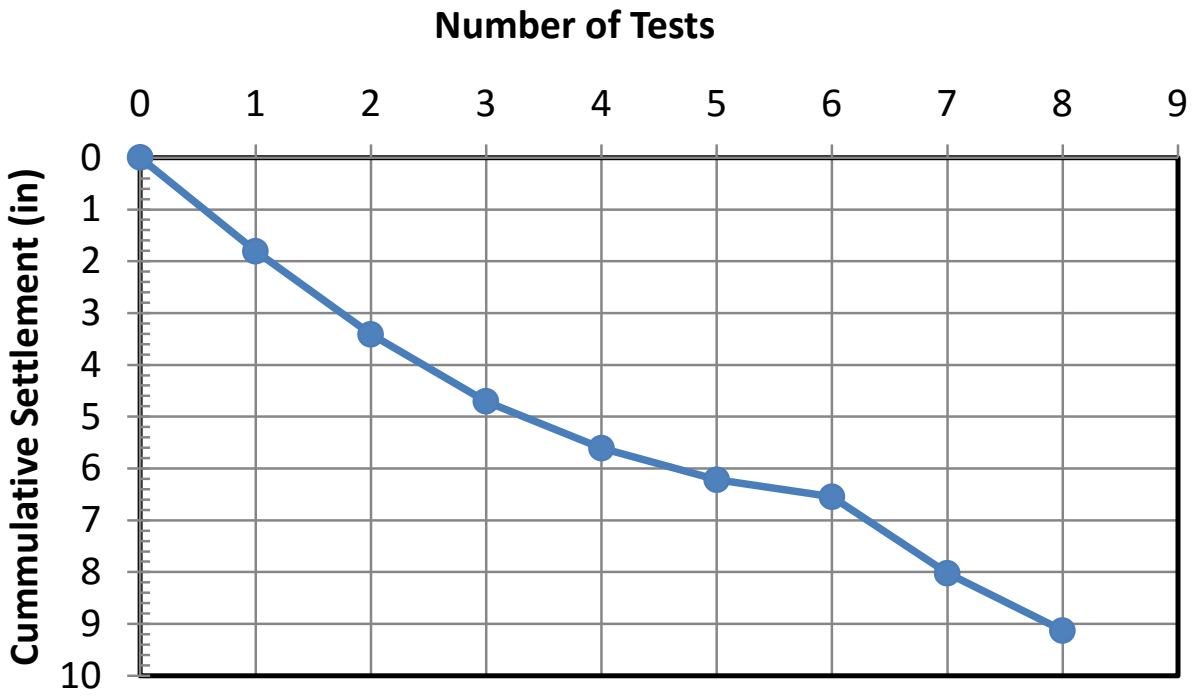

Figure 23 Settlement Versus Number of Tests, IPS1 (Yegian, 2015).

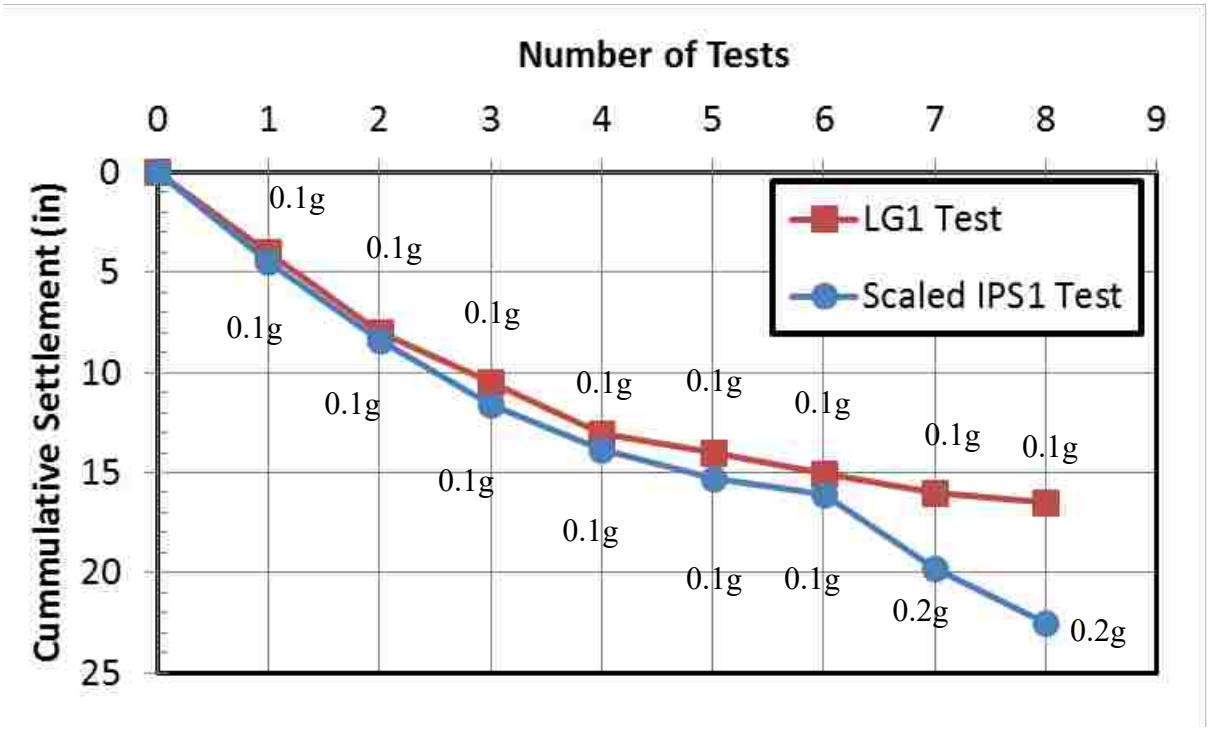

Figure 24 Settlement Versus Number of Tests for IPS with Scaled Settlement (Yegian, 2015).

2.5 Limitations of Previous Studies

Although the previous studies clearly highlight the potential effectiveness of earthquake drains, they are all limited in one way or another. Moreover, these limitations represent a significant impediment to the implementation of drainage as a more routine mitigation strategy. For example, the blast liquefaction testing involves native sand under full-scale conditions which is desirable, but the blast charges produce a very intense dynamic load that is applied much more rapidly than an earthquake and it is difficult to translate the observed performance during blasting to a magnitude and peak acceleration for earthquake conditions.

Centrifuge testing can simulate realistic earthquake shaking conditions; however, similitude issues are always a concern and it is difficult to reproduce the aging and natural "structure" of sands in the field. As a result, flow failures which have been observed in nature have not typically been observed in centrifuge tests, even with very loose sand, without

strategically placing low permeability layers. In contrast, very dense sands have experienced liquefaction and exhibited significant settlement in centrifuge tests while this poor performance has not been observed in nature (Knappett and Madabhushi, 2008). These departures from field performance make it difficult to directly apply results from centrifuge tests to design practice. Furthermore, in the centrifuge tests involving drains reported by Marinucci et al. (2010) and Howell et al (2012), water was used as the pore fluid so that the permeability of the sand under prototype conditions was equivalent to that of coarser sand. Performance could be considerably different for sand with a permeability 50 to 100 times lower.

The numerical simulations by Vytiniotis et al. (2013) and Rollins et al (2004) demonstrate the effectiveness of EQ drains in reducing deformations for partially submerged saturated sandy slopes, but further field testing is needed to validate the models. While the tests with the Vibroseis trucks involved full-scale conditions, the sand thickness was limited to 1.5 m and induced shear strains were so low that 40 strain cycles were required to induce liquefaction. For higher strain levels, more typical of earthquake shaking, and thicker zones of potentially liquefiable sand typical of many field sites, the drain performance would be expected to be less robust. In the full-scale field tests by Marinucci et al. (2010), breaking of cementation bonds within the sand during drain installation resulted in significant settlement, making it hard to isolate the effect of densification from the effect of drainage provided by the EQ drains.

3 TEST EQUIPMENT, LAYOUT, AND PROCEDURES

The test equipment, layout, and procedures in this section give the general set-up of the tests. More specific layout and procedures for each test are provided in the section for that test.

3.1 Test Equipment

Equipment and lab technicians for this test were provided by the NEES laboratory at the University at Buffalo campus. Equipment used for this test include the laminar shear box, which will be discussed in section 3.2.1, the SCRAMNET DAQ for data acquisition, the hydraulic power supply which was used to create the input motions for the laminar shear box, the pumps and pipes used to pump sand from the holding tanks into the laminar shear box, and video cameras to capture video of the event from multiple views. Instrumentation such as pore pressure transducers, accelerometers and potentiometers were provided by the University at Buffalo NEES facility. However, some additional pore pressure transducers were provided by the Brigham Young University Civil & Environmental Engineering department, and others were provided by the University at Buffalo Civil Engineering department.

3.2 Test Layout

3.2.1 Laminar Shear Box and Sand Deposition

Plan and elevation views of the laminar shear box are provided in Figure 25. The laminar box consists of 40 stacked rectangular rings with dimensions as shown in Figure 25. Each ring is 6 inches (150 mm) tall and is supported by a series of roller bearings which allows each ring to move independently in the horizontal direction so that the movement was largely controlled by the mass of the soil inside the box. In this fashion, the soil had the potential to respond as it might in the field during earthquake shaking. Two flexible rubber membrane liners were placed inside the laminar box to allow the sand to be saturated and undrained during the cyclic loading. Acceleration time histories can be imposed on the bottom of the laminar box using two high-speed hydraulic actuators using a hydraulic accumulator system. Photographs of the laminar box and the actuators at the base of the box are provided in Figure 26.

The basic layout of the test is defined by the laminar shear box used to perform the test. The laminar shear box is 16'-4 ¾" by 9' with a depth of 20'. Sand is pumped into the box as a slurry from a holding tank. The end of the pipe has a diffuser to ensure that the sand is placed by pluviation rather than allowing scouring by the material exiting the pipe. To provide a consistent relative density, the water level is maintained at a consistent hight above the sand and the diffuser is placed at a consistent height above the water level. The final height of the sand inside the box is typically between 14.5-17', usually around 16' to 16.5'. The relative density of the sand placed in this manner is expected to be between 35 and 50%. Buckets are placed in the box as it is being filled and are weighed upon filling of the bucket with sand to measure the density of the sand at that location. This is repeated at various depths as the box is filled with sand.

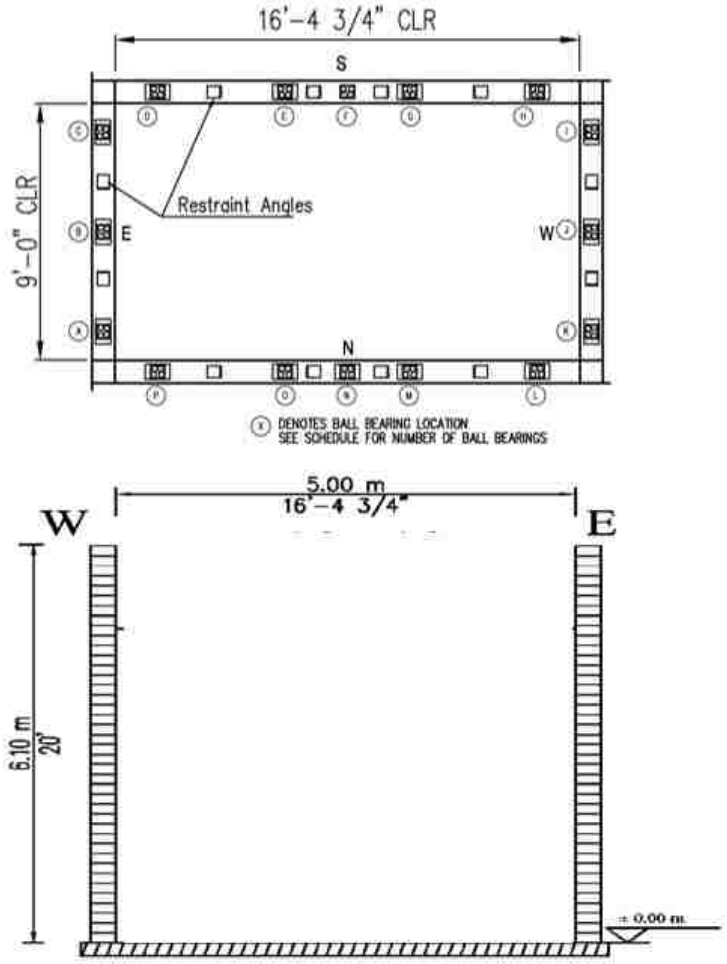

Figure 25 Profile and Plan View of Laminar Shear Box.

Figure 26 Photographs of the Laminar Shear Box and Hydraulic Actuators at the Base

3.3 Sondex Settlement Profilometers

To create a profile of settlement in the laminar box due to shaking, special pipes were installed in the laminar box as outlined in each test. These pipes consisted of corrugated plastic pipes approximately 4 inches in diameter with metal rings around the pipe located at intervals of 2 feet. A smaller pipe was inserted inside the corrugated pipe to allow a sensor to be lowered down the inner pipe. A sensor that can detect the metal rings was slowly moved down the length of the pipe. The depth of each ring is then recorded relative to a reference elevation. This is illustrated in Figure 27.

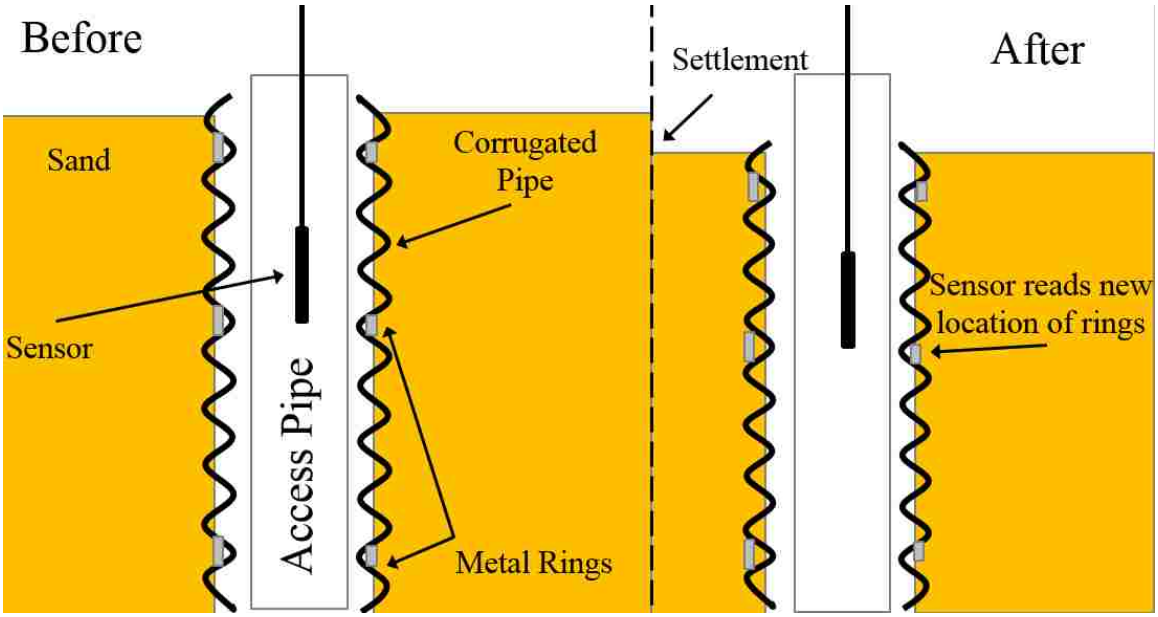

Figure 27 Profile View of Sondex Settlement Profilometer

After each test, the locations of the metal rings shifted down as the sand settled because the corrugation of the outside pipe interlocks with the sand and moves with it. If certain sections move more than others, the corrugated pipe compresses only in that area, and the distance between the rings is less than two feet. By taking the difference between the initial and final locatins of the metal rings after each test, a profile of settlement can be obtained as a function of depth.

3.4 Procedures

To perform the test, the laminar box must first be empty. The pre-fabricated vertical drains are installed before the box is filled with sand. The drains are fastened to a grid at the bottom of the box and hung from a framework at the top of the box at the desired locations. Pore pressure monitors are strung together and hung and fastened in a similar manner. Other instrumentation installed in this manner prior to filling the box includes Sondex profilometers and pipes for

measuring hydraulic conductivity. After all instrumentation is secured in place, the box can be filled with sand.

The box is filled with Ottawa sand held in holding tanks in a slurry. The slurry is pumped into the box over the course of 3 to 5 days. As the filling is taking place, buckets are filled inside the box and weighed to determine the density of the sand. Knowing the properties of the sand, the relative density is calculated from these density measurements.

A CPT test is done after filling the box to get another gage of density. A seismic test is done using a hammer and a steel plate to measure the shear wave velocity. The CPT is not standard. It is a device created by the NEES facility specifically for the laminar shear box. The device bolts to a frame on top of the box. The cone is mounted in this manner, and is driven using a pulley system connected to a winch. Because it is not a standard CPT device, it may not be as accurate, but it is the best possible way to do so in the laminar shear box. The CPT sounding is pushed in at 2cm/s rate, reacted off a beam above the box.

Once the laminar shear box is prepared for testing, a test run is performed. This test run is a very low magnitude shake, usually a sign wave with 0.015g maximum acceleration. Once the test run is performed and the operators are sure everything is working, the shear box is immediately ready for operation.

Once the box is ready for testing, the DAQ system is set to record, and the operator begins the test. During the test water is evacuated from the ground as the sand settles. After the test run is over and is no longer being recorded, the water must be removed from the box before a new test can begin. The water is pumped from the box to an outside drain. Water removed from the box is measured by filling 5-gallon buckets, giving an approximate measurement of the settlement of the sand in the box. After the water is removed to slightly below the ground surface more testing can

be done. For this study, tests are run at 0.05g, 0.1g, and 0.2g before another CPT is done. Then another round of 0.05g, 0.1g, and 0.2g tests is performed, followed by another CPT. Finally, a third round of the same tests is performed, followed by the final CPT.

After all three rounds of testing are complete, the sand is removed by pumping the sand in a slurry back into the holding tanks the sand was taken from to fill the box. All instrumentation is then removed, and the box is ready for a new project.

4 PVD-1

4.1 Layout of Drains and Instrumentation

4.1.1 Vertical Drain Plan

The layout of the prefabricated vertical drains in plan and profile views is shown in Figure 28 and the positions are detailed in Table 2 with coordinates relative to the center of the box. The drains are 3 inch diameter corrugated plastic pipes with an outside diameter of approximately 3.7 inches which are surrounded by a filter fabric sock to prevent infiltration of sand. The fabric sock was sealed closed at the bottom with tape, and stapled shut before placing a plastic foot over the bottom of the pipe.

Prior to sand placement, the drains are hung from a framework above the top of the box and tied to the bottom PVD grid with wire to prevent uplift in the event of liquefaction. After the sand fill is placed, the drains are cut off about 2 to 3 inches above the ground surface to allow the water to freely dissipate at the surface.

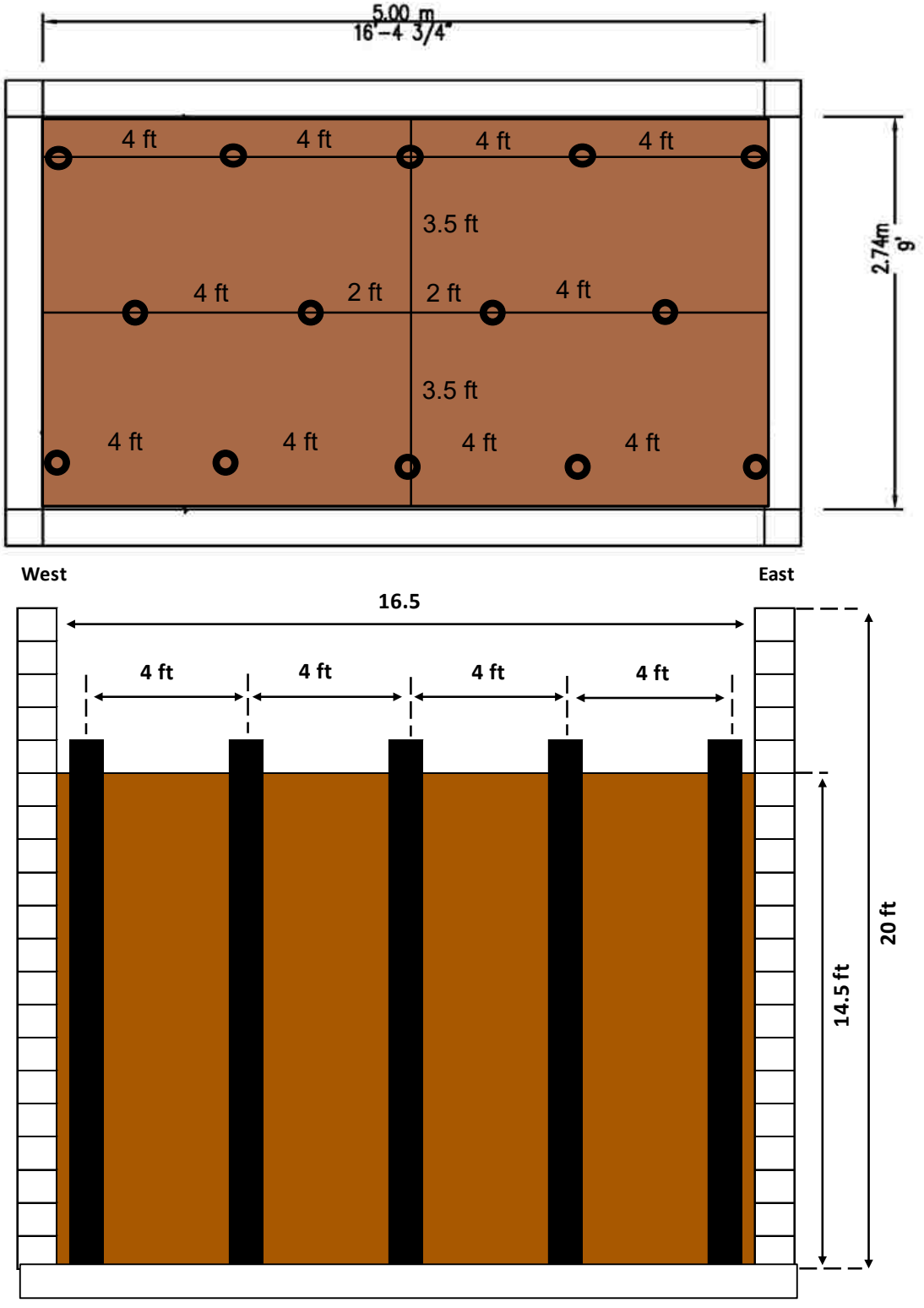

Figure 28 Plan and Elevation View of Laminar Shear Box

Table 2 Coordinates of Prefabricated Vertical Drains (PVDs) for PVD-1

Drains	x (in)	y (in)
1	-72	0
2	-24	0
3	20	0
4	72	0
5	-96	42
6	-48	42
7	0	42
8	48	42
9	96	42
10	-96	-42
11	-48	-42
12	0	-42
13	48	-42
14	96	-42

4.1.2 Instrumentation Plan

Figure 29 and Figure 30 show plan and profile views, respectively, of the locations of the various sensors. Table 3 shows the number of each type of instrumentation installed for PVD-1. Table 4 summarizes the position of accelerometers, LVDTs, and string potentiometers. These locations are the same as for previous IPS1 testing to facilitate subsequent comparisons. Coordinates (x,y,z = 0,0,0) denote the center of the box at the top of ring 40 (x = positive in the East direction, y = positive in the North direction, and z = positive downward from the top of ring (laminate) 40). The top of laminate 40 is at an elevation of 6.10m or 20 ft.

Three vertical arrays of pore pressure transducers are located along Mesh 1, Mesh 2, and Mesh 3 as shown in Figure 30 to define the generation and dissipation of pore pressure versus

depth. One array was located 1 ft from the center of a drain, while the other two arrays were located at 2 ft from the center but at different positions relative to the surrounding drains. A distance of 2 ft from the drain represents the critical point where water has the furthest distance to travel to reach the drain. In addition, one pore pressure transducer is located at a depth of 7.5 ft within the center drain to monitor the pressure within the drain itself. Pore pressure transducer locations are summarized in Table 5. Figure 29 also shows the position of three surface settlement plates which are connected to string potentiometers fastened to a frame located above the box, as well as the slotted pipes for measuring permeability and Sondex settlement profilometers.

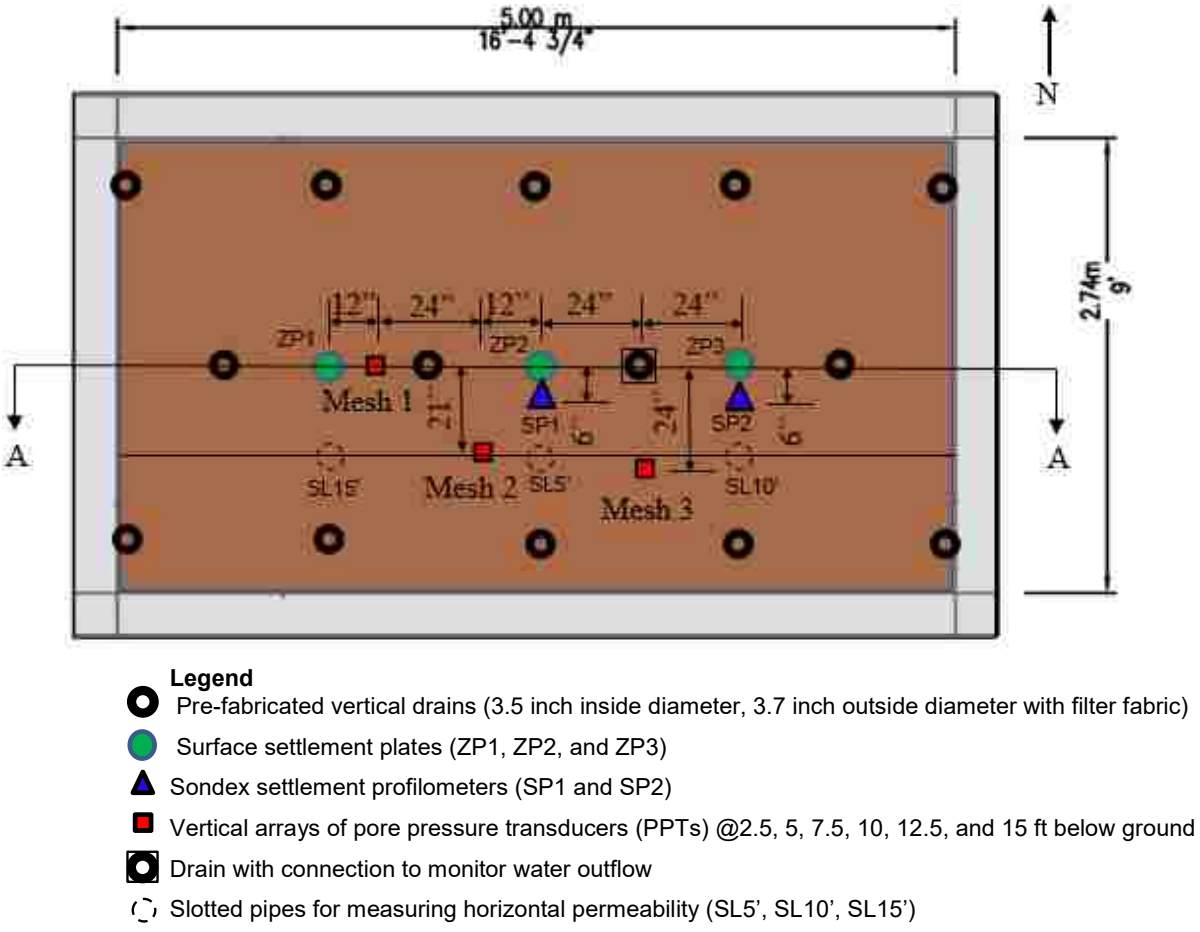

Figure 29 Plan View of Sensors for PVD-1

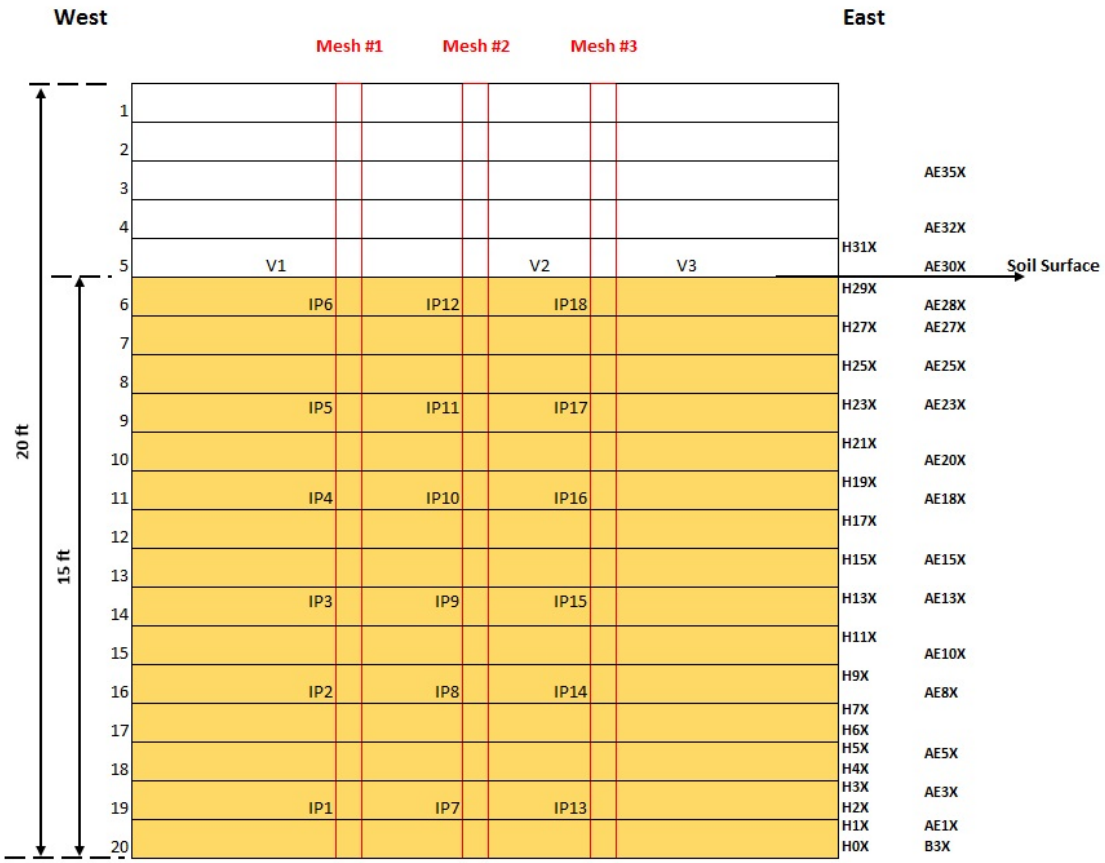

Figure 30 Profile View of Sensors Installed for PVD-1

Table 3 Instrumentation Summary for PVD-1

Instrument Sensors	Quantity PVD-1
P-Piezometers (PPT)	19
X-Acc (Ring and base) (AE, B)	19
Y-Acc (Ring and base (AE,B)	7
X-Potentiometers (H)	20
Z-Potentiometers (V)	3
Cameras (CA)	4

Table 4 Location of Accelerometers, LVDTs, and Potentiometers for PVD-1

Lanimate (Ring) #	Coor.	Direction	East				North								
			Soil	Ring			Soil		Ring		Ring			Ring	
	x (ft)		4	8.5			0	-4	-8.5		-8.5	-8.5		8.5	
	y (ft)		0	0			0	0	4.5		-0.25	-4.5		-4.5	
Top	z (ft)	Z(m)	ZP	X-Acc	Y-Acc	X-Pot	Z-Pot	Z-Pot	X-Acc	Y-Acc	X-Acc	X-Acc	Y-Acc	X-Acc	Y-Acc
	0.0	-1.37													
39	0.5	-1.22													
38	1.0	-1.07													
37	1.5	-0.91		**AE37X**											
36	2.0	-0.76													
35	2.5	-0.61		**AE35X**	**AE35Y**										
34	3.0	-0.46													
33	3.5	-0.30	**ZP3**				**ZP2**	**ZP1**							
32	4.0	-0.15		**AE32X**											
31	4.5	0.00				**H31X**									
30	5.0	0.15		**AE30X**	**AE30Y**										
29	5.5	0.30				**H29X**									
28	6.0	0.46		**AE28X**											
27	6.5	0.61		**AE27X**		**H27X**									
26	7.0	0.76													
25	7.5	0.91		**AE25X**		**H25X**									
24	8.0	1.07													
23	8.5	1.22		**AE23X**		**H23X**									
22	9.0	1.37													
21	9.5	1.52				**H21X**									
20	10.0	1.68		**AE20X**	**AE20Y**										
19	10.5	1.83				**H19X**									
18	11.0	1.98		**AE18X**											
17	11.5	2.13				**H17X**									
16	12.0	2.29													
15	12.5	2.44		**AE15X**		**H15X**									
14	13.0	2.59													
13	13.5	2.74		**AE13X**		**H13X**									
12	14.0	2.90													
11	14.5	3.05				**H11X**									
10	15.0	3.20		**AE10X**	**AE10Y**										
9	15.5	3.35				**H9X**									
8	16.0	3.51		**AE8X**											
7	16.5	3.66				**H7X**									
6	17.0	3.81				**H6X**									
5	17.5	3.96		**AE5X**	**AE5Y**	**H5X**									
4	18.0	4.11				**H4X**									
3	18.5	4.27		**AE3X**		**H3X**									
2	19.0	4.42		**AE2X**		**H2X**									
1	19.5	4.57		**AE1X**	**AE1Y**	**H1X**									
0 (fixed)	20.0	-3.35				**H0X**									
Base														**B3X**	**B3Y**

Soil Surface

Positive Direction:

H0X, H17X : West
Other H(No.)X: East
B1X, B2X, AW(No.)X: West
B3X, AE(No.)X: West
B1Y, B3Y, AE(no.)Y: South
B2Y : North

X Direction:
ASS-45704: East SAA-45886: East

Table 5 Location of Pore Pressure Transducers (PPTs) for PVD-1

Peizometer	Mesh	x (ft)	y (ft)	z (ft)	Depth to base (ft)	Depth from surface (ft)
PPT1	1	3	0	18.5	2	12.5
PPT2	1	3	0	16	4.5	10
PPT3	1	3	0	13.5	7	7.5
PPT4	1	3	0	11.25	9.25	5.25
PPT5	1	3	0	9	11.5	3
PPT6	1	3	0	6.75	13.75	0.75
PPT7	2	1	1.75	18.5	2	12.5
PPT8	2	1	1.75	16	4.5	10
PPT9	2	1	1.75	13.5	7	7.5
PPT10	2	1	1.75	11.25	9.25	5.25
PPT11	2	1	1.75	9	11.5	3
PPT12	2	1	1.75	6.75	13.75	0.75
PPT13	3	2	2	18.5	2	12.5
PPT14	3	2	2	16	4.5	10
PPT15	3	2	2	13.5	7	7.5
PPT16	3	2	2	11.25	9.25	5.25
PPT17	3	2	2	9	11.5	3
PPT18	3	2	2	6.75	13.75	0.75
PPT19	Drain	-2	0	13.5	7	7.5

Depth = Measured vertical distance from top of soil surface (downward positive)

Z = Distance from top of ring/laminate 40 (downward positive)

X = Measured horizontal distance from center of soil box (East Positive)

4.2 Characterization of Sand

The sand in the laminar shear box was deposited by water pluviation. The sand was pumped from containers in a saturated state and deposited into standing water at a height of about three feet using the spreader shown in the photograph in Figure 31. The spreader was moved longitudinally back and forth along the center of the box as the sand was deposited layer by layer. The sand was obtained commercially and was known as Ottawa F55 sand. The grain size distribution curve for the sand is provided in Figure 32 and basic properties of the sand are provided in Table 6. Small buckets were placed in the fill periodically during the deposition process to monitor the unit weight of the sand. Based on these measurements a plot of the average relative density versus depth was obtained as shown in Figure 33. The relative density was typically between 40% and 60%. The sand below 13' was left in the box from the previous test and was not removed. This sand was much denser than the sand deposited by pluviation. The CPT cone tip resistance was much higher in that zone during the Round 1 CPT. As in IPS1, and because the sand was not filled to 16 feet, the settlement for PVD-1 was scaled from 13' to a depth of 16' to better compare with other laminar shear box testing.

Figure 34 shows a schematic diagram of the layout of the slotted pipes used to perform horizontal borehole permeability tests. For each 5 ft segment, the water flow was increased until the head remained constant for steady-state conditions. The steady state parameters were then used to compute the horizontal permeability. The measured horizontal permeability was 0.07 cm/sec for the interval from 4.5 to 9.5 ft and 0.05 cm/sec for the interval from 9.5 to 14.5 ft.

Cone penetration (CPT) soundings were performed prior to the first set of three shaking tests and then at the beginning of each additional set of three shaking tests. After all tests were completed, a final CPT test was performed. The cone tip resistance, qc, versus depth profiles for

all four soundings are provided in Figure 35, as well as the sleeve friction for the first two tests. Based on the CPT resistance the sand was initially in a loose condition but the shaking process progressively increased the cone resistance and relative density state of the sand. Relative density based on correlations with CPT from Jamiolkowsky, et al. (1985) and Kulhawy and Mayne (1990) are shown in Figure 36.

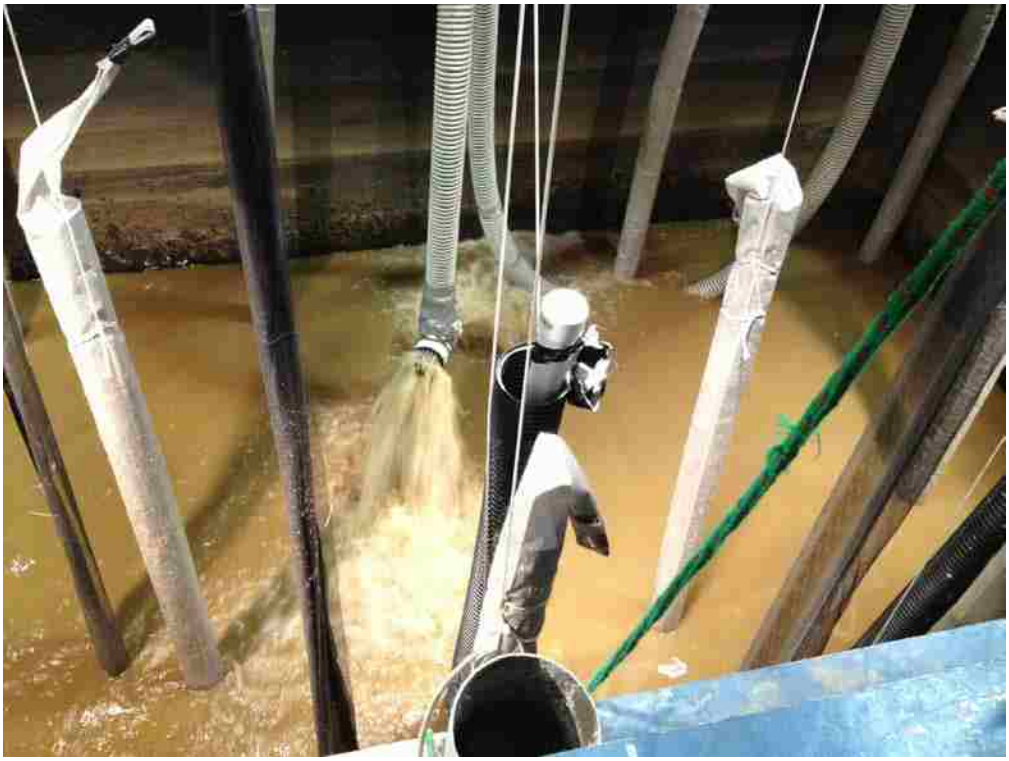

Figure 31 Photograph of Sand Being Deposited in Laminar Shear Box by Pluviation

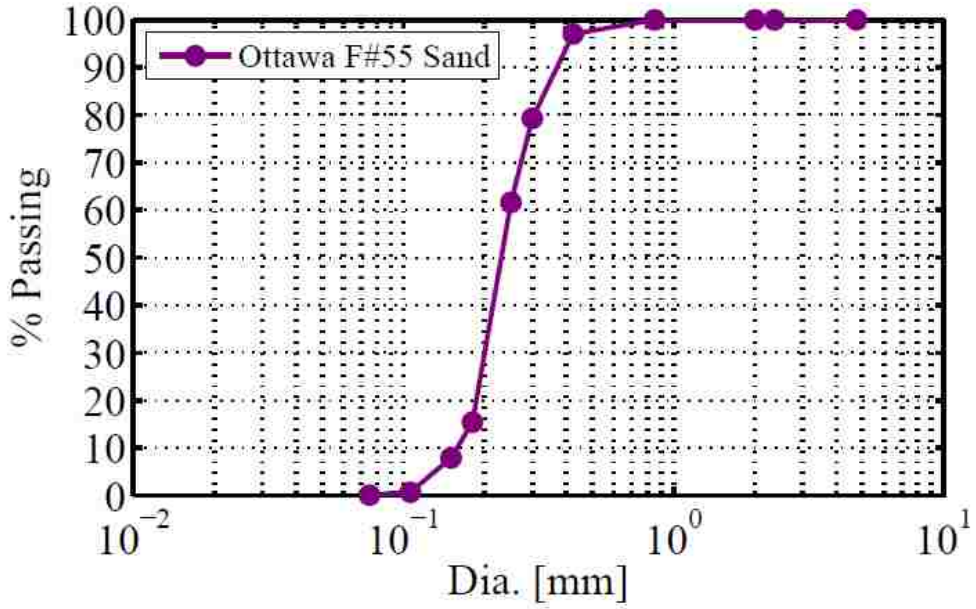

Figure 32 Grain Size Distribution for Ottawa F55 Sand

Table 6 Properties of Sand Used in the Laminar Shear Box

Parameters	Values
FC (%)	0
[1]e_{max}	0.800
[2]e_{min}	0.608
D_{10} (mm)	0.161
D_{30} (mm)	0.201
D_{50} (mm)	0.230
D_{60} (mm)	0.245
[3]C_u	1.522
[4]C_c	1.024

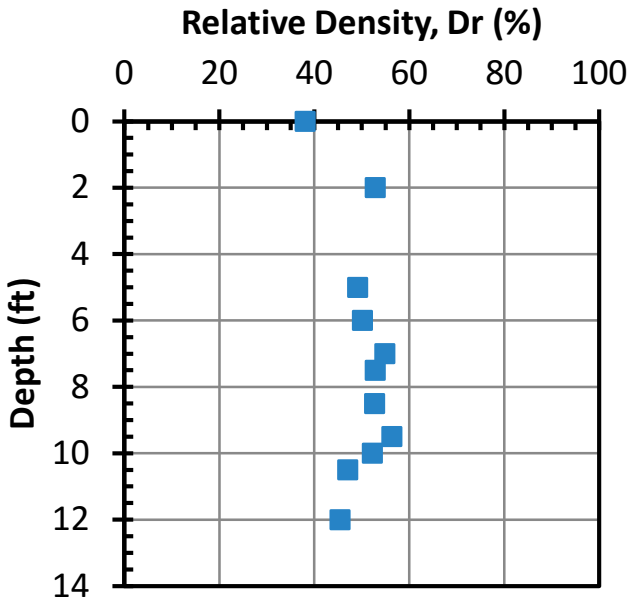

Figure 33 Density Measurements Taken During the Filling Process.

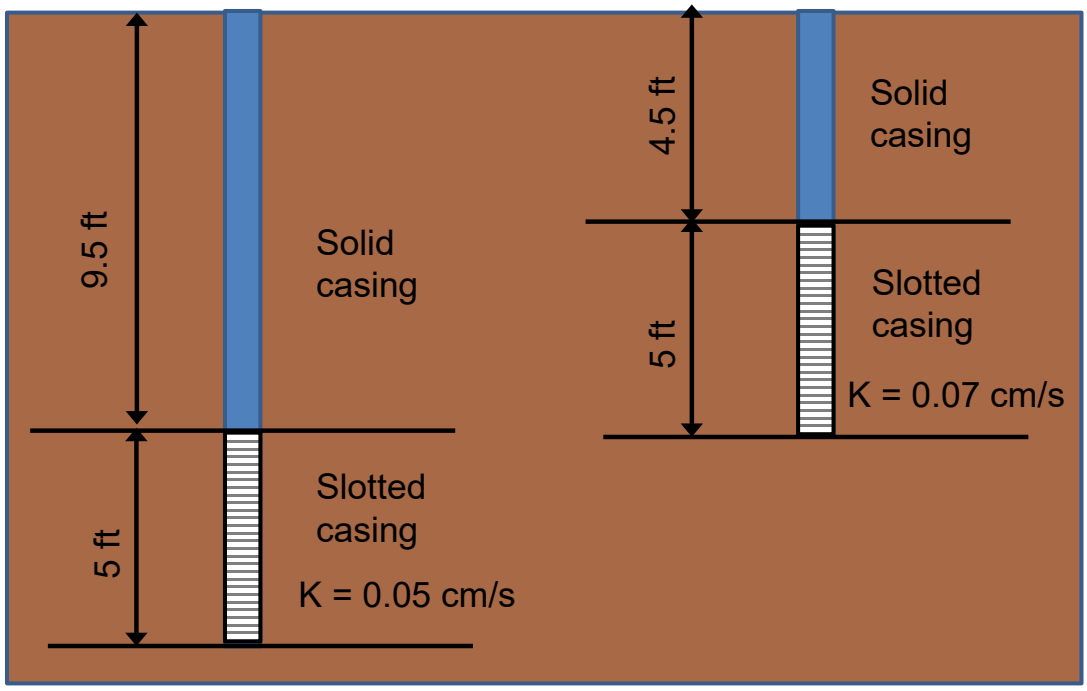

Figure 34 Schematic Drawing Showing Layout of Slotted Casing used to Measure Hydraulic Conductivity of Sand

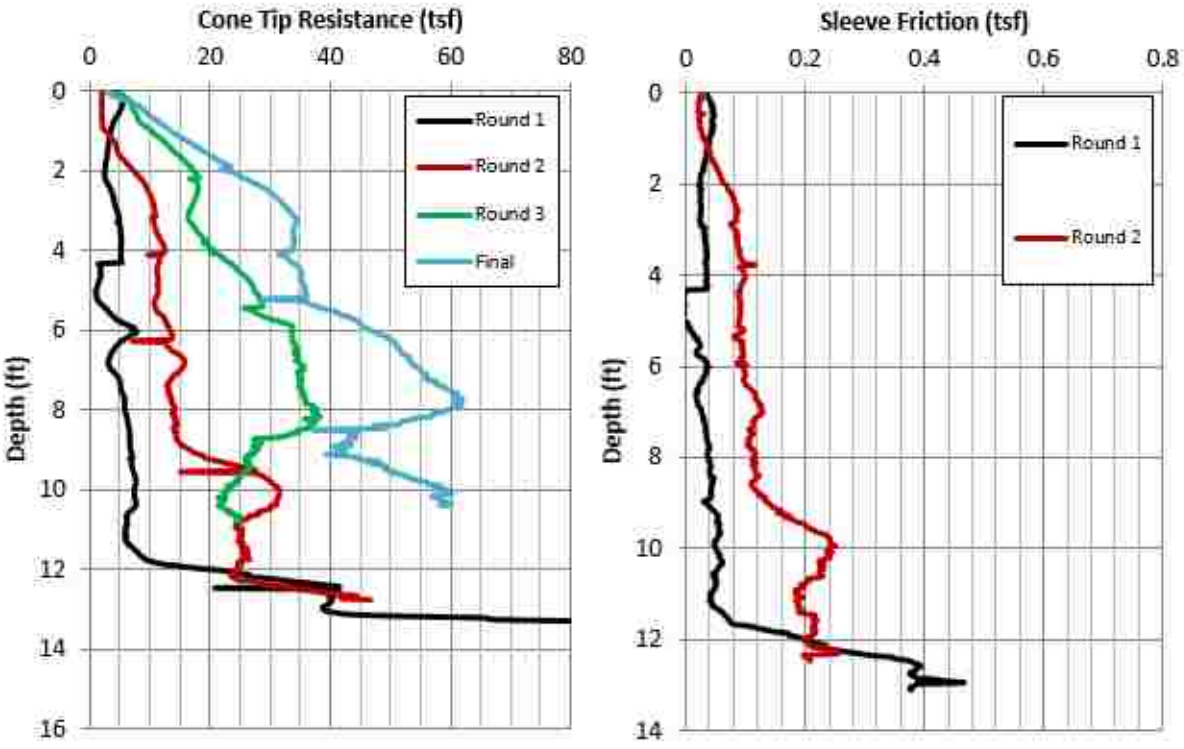

Figure 35 CPT Cone Tip Resistance Values for PVD-1.

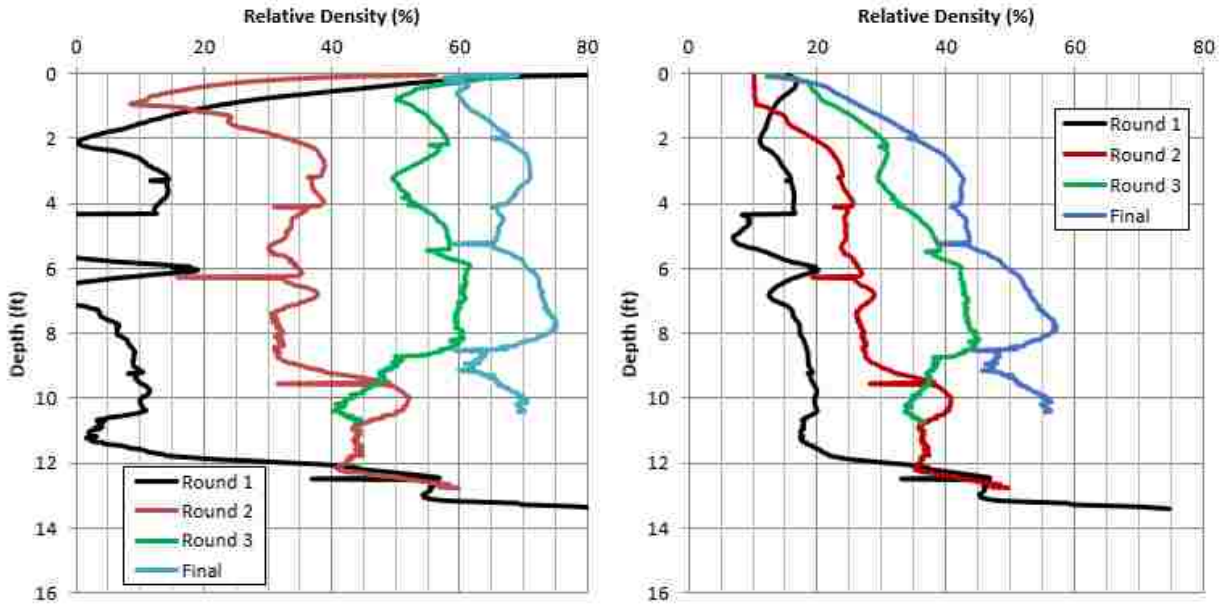

Figure 36 Relative Density from CPT Correlation, Jamiolkowsky, et al. (1985), Left, and Kulhawy and Mayne (1990), Right.

4.3 Test Pattern

Nine shaking tests were performed on the laminar shear box with 4 ft. drain spacing. Tests were performed in sets of three with peak accelerations of 0.05g, 0.10g, and 0.20g for each set. A peak acceleration of 0.20g was the highest acceleration permitted by the NEES@UB lab manager. A CPT sounding was performed prior to each set of three tests to provide an indication of the density state for the next set of tests. However, each test was performed independently and pore pressures were allowed to fully dissipate before the subsequent test was performed.

Figure 37 provides plots of the planned input base motions. All motions were intended to consist of 15 cycles of sinusoidal motion with a frequency of 2 Hz. Typically 15 cycles of motion are associated with a Magnitude 7.5 earthquake, which is often used as the base earthquake for liquefaction studies. A ramp-up and ramp-down period was used to be consistent with previous testing on untreated sand at the site. Actual motions applied and measured at the base differed slightly from the planned motions and will be presented with the results.

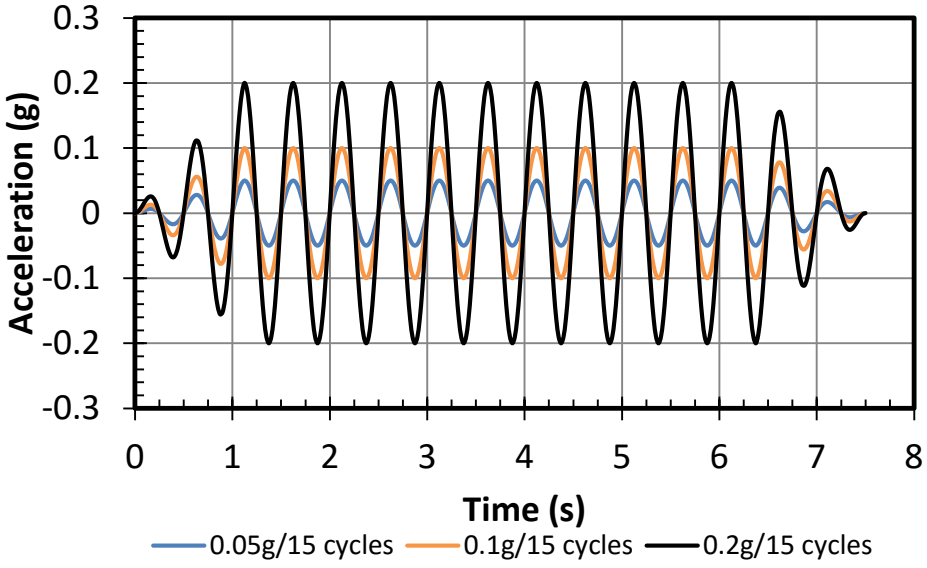

Figure 37 Input Motions for Each Set of Three Tests

4.4 Test Results and Discussion

4.4.1 Peak Excess Pore Pressure Versus depth

Excess pore pressure ratio profiles were provided by three vertical arrays of pore pressure transducers located at approximately 2.5 to 3 ft. depth intervals as described in section 4.1.2. The excess pore pressure ratio at a given depth was computed by taking the maximum excess pore pressure during the entire test at a given depth and dividing by the initial vertical effective stress at that depth. Liquefaction is defined as the condition when the excess pore pressure ratio (r_u) becomes equal to 1.0, meaning that the excess pore pressure is equal to the vertical effective stress. In most cases, the peak pore pressure ratio occurred during shaking; however, in some cases this occurred shortly after the shaking when upward flow of water produced higher excess pore pressures. In the figures below, the peak pore pressure ratio is an average of the three sensor meshes for each test. No pattern of behavior between the three sensor meshes suggests that there is a significant difference in the readings between meshes despite small variations in the distances from the pore pressure transducers and the adjacent drains. Profiles of peak excess pore pressure ratios during each round of testing are in Figure 38 through Figure 40.

Peak excess pore pressure ratio throughout the profile can be used to determine whether a section of the profile was liquefied (PPR=1), or if it reached above 0.5, which has been used as an indicator for settlement, as shown in Howell et. al. (2012). These plots are useful to quickly understand the effect of the shaking motions on the soil. More in depth discussion of excess pore pressures as they relate to settlement will be provided in subsequent sections.

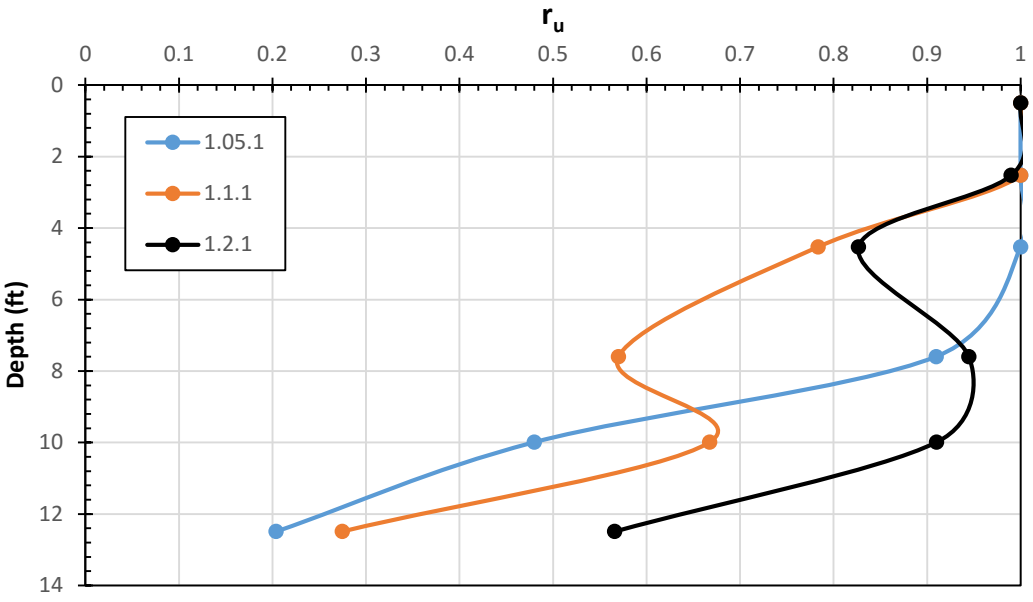

Figure 38 Profiles of Peak Excess Pore Pressure (r_u) Versus Depth (ft.) for Three Shaking Tests at 0.05g, 0.10g and 0.20g During Round 1

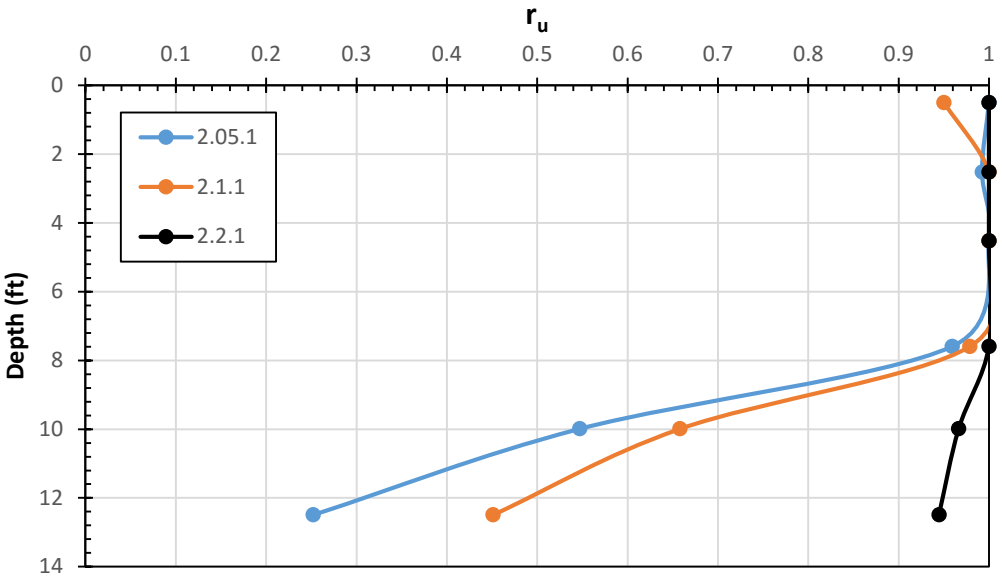

Figure 39 Profiles of Peak Excess Pore Pressure (r_u) Versus Depth (ft.) for Three Shaking Tests at 0.05g, 0.10g and 0.20g During Round 2

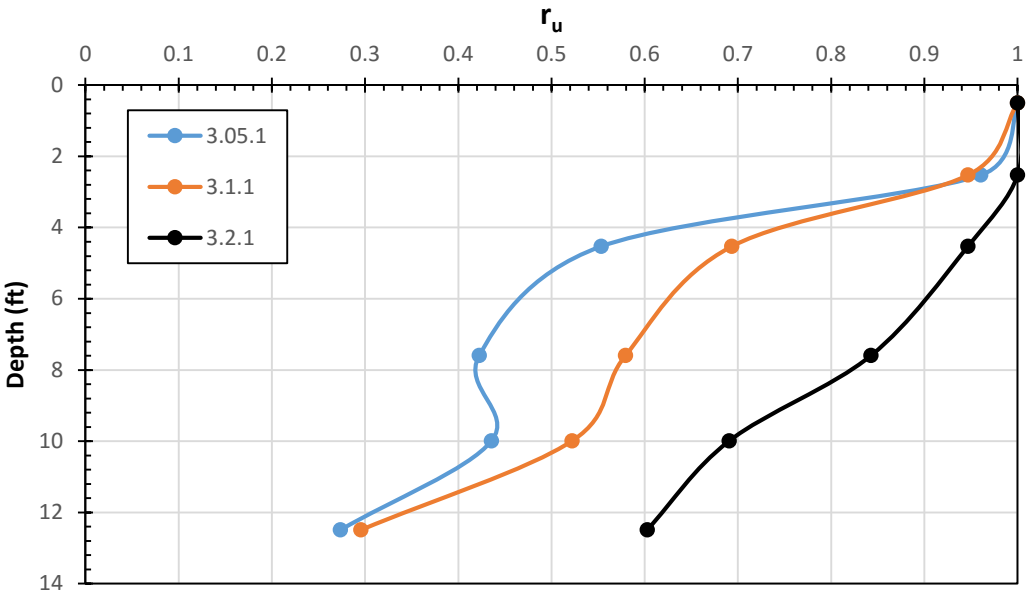

Figure 40 Profiles of Peak Excess Pore Pressure (r_u) Versus Depth (ft.) for Three Shaking Tests at 0.05g, 0.10g and 0.20g During Round 3

Peak excess pore pressure ratios generally decreased with depth in every case, and increased with increased acceleration. This is consistent with centrifuge test results (Marinucci et al. 2008) which showed that the drains were more effective in reducing excess pore pressure ratios deeper rather than at shallow depth. It also appears that the increasing density, owing to the settlement in each round of testing also reduced peak excess pore pressure ratios. This is not necessarily seen in the difference between round one and round two, but the peak excess pore pressures ratios in round three are much lower, and the completely liquefied zone (r_u=1.0) is much thinner as well.

4.4.2 Excess Pore Pressure Versus Time Paired with Acceleration Versus Time

Pore pressures were measured at multiple depths, as were accelerations. To understand the forces the soil was under during the tests, excess pore pressure ratio and acceleration at these

depths are included in Figure 41 through Figure 49. Acceleration versus time plots are on the left, with the 0 on the acceleration axis corresponding to the depth of the accelerometer on the far left axis for depth. The accelerometers used, in order from top to bottom, are: AE27X, AE23X, AE18X, AE13X, AE8X, and AE2X. Excess pore pressure versus time plots are located on the right with the 0 on the excess pore pressure axis corresponding to the depth of the pore pressure transducer on the far left axis for depth. The pore pressure transducers used, in order from top to bottom, are: PPT12, PPT 11, PPT 10, PPT 15, PPT 8, and PPT 7.

These plots are useful time histories for creating future models. The acceleration as an input is important, and understanding how the acceleration level is affected throughout the profile of the soil could be useful. Excess pore pressures throughout the profile are also very important because the excess pore pressures are what future computer models will be predicting based on the results of this study.

Pore pressure ratios build up rapidly during the shaking with liquefaction or peak excess pore pressure ratios typically developing in 1 to 2 seconds or 2 to 4 acceleration cycles. During shaking, some pore pressure transducers experienced large oscillations in excess pore pressure. For the first round of tests, the decreases in r_u from the mean were typically less than about r_u=10%; however, the magnitude of oscillations increased with each round of testing. For the third round of tests, the decreases in r_u were as much as r_u=100%. In addition, the oscillations decreased substantially for transducers located deeper in the box. These observations are consistent with dilation effects. As shear strains increase during cyclic loading, dilation would lead to a decrease in the excess pore pressure ratio. The potential for dilation increases as the sand becomes denser and the confining pressure decreases. Therefore dilation would be expected to increase as the sand became denser with each progressive round of testing. In addition, dilation would be expected to

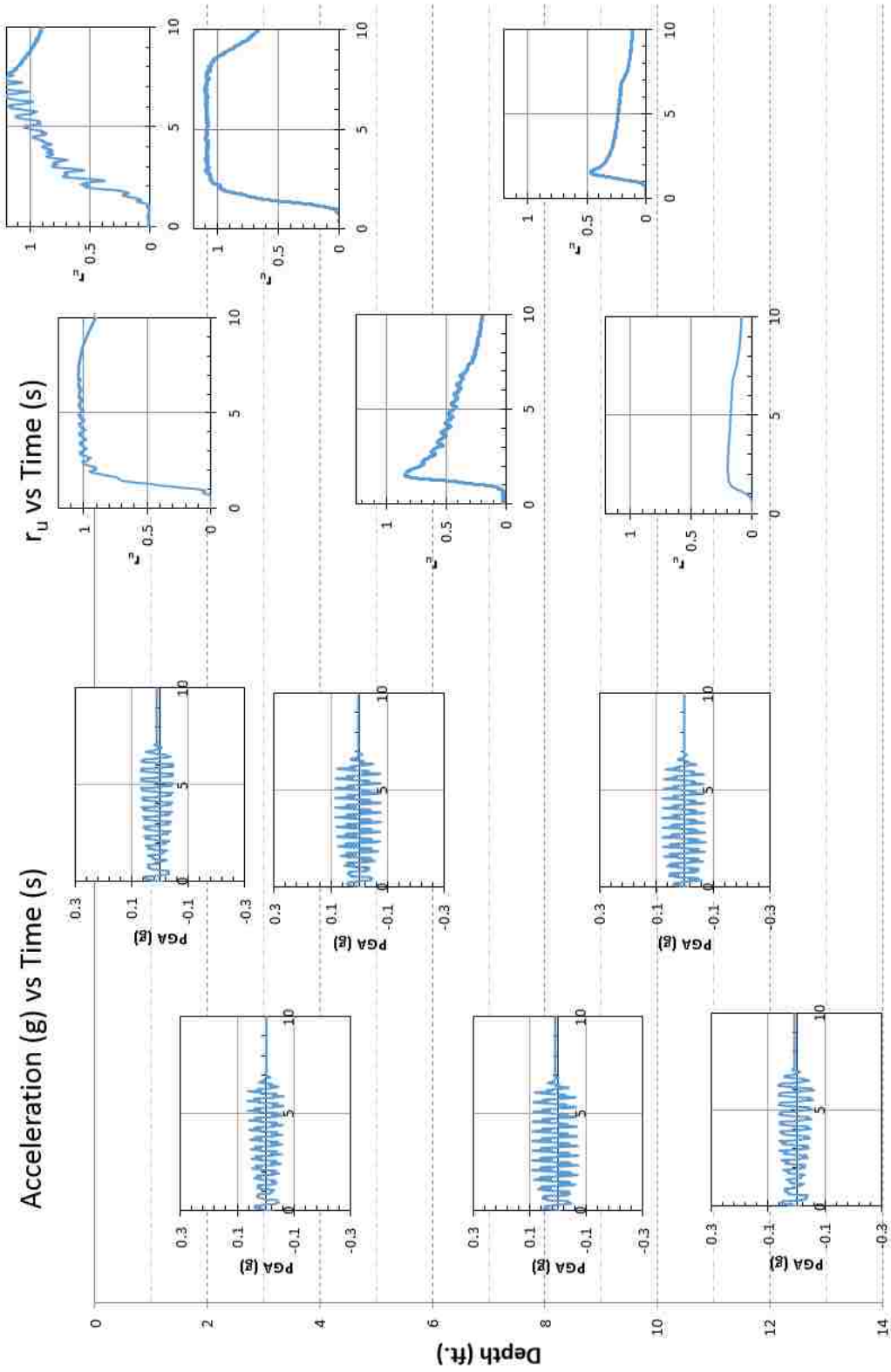

Figure 41 Acceleration Versus Time Paired with Excess Pore Pressure Ratio Versus Time for Round 1, a_{max} = 0.05

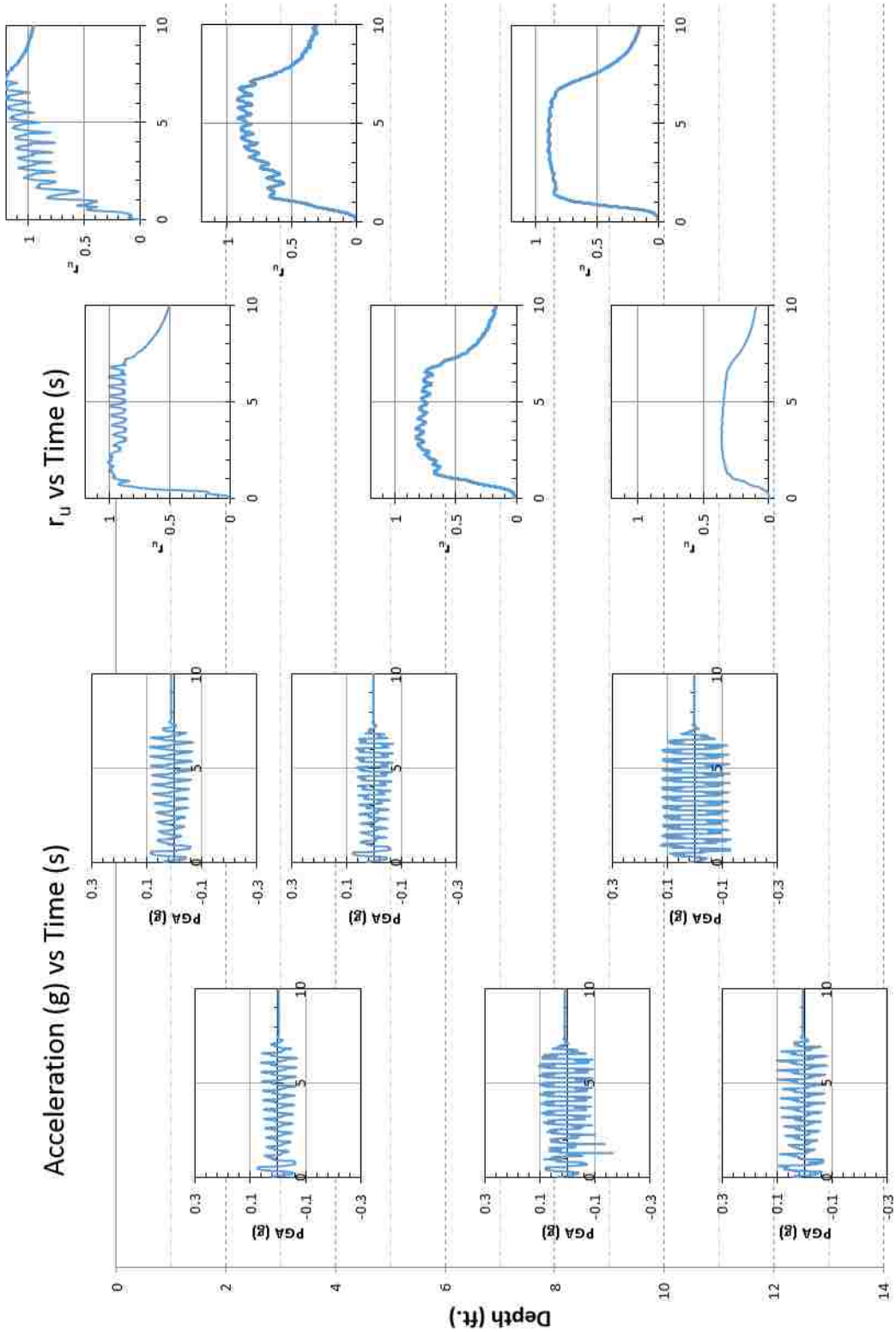

Figure 42 Acceleration Versus Time Paired with Excess Pore Pressure Ratio Versus Time for Round 1, a_{max} = 0.1g

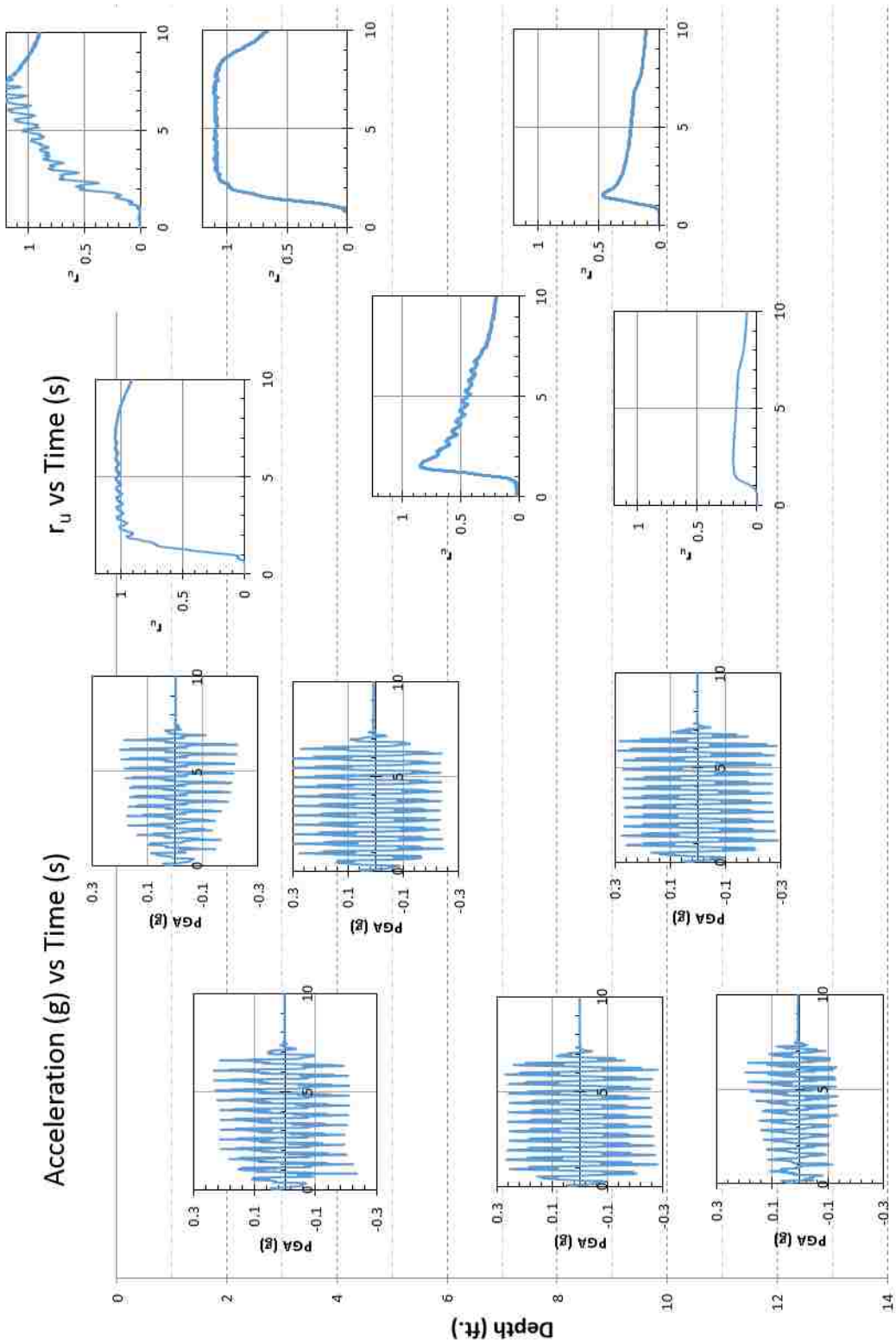

Figure 43 Acceleration Versus Time Paired with Excess Pore Pressure Ratio Versus Time for Round 1, a_{max} = 0.2g

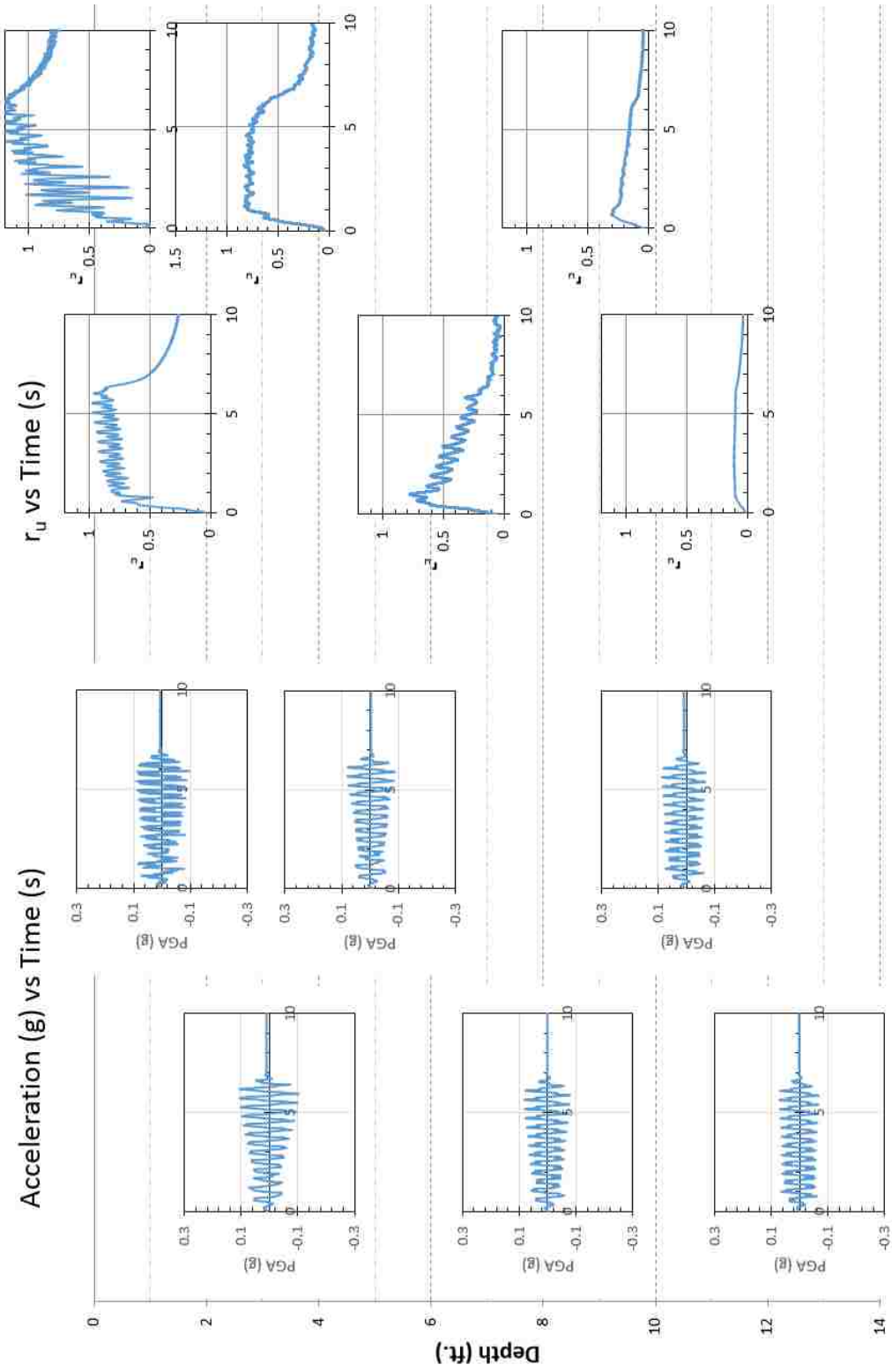

Figure 44 Acceleration Versus Time Paired with Excess Pore Pressure Ratio Versus Time for Round 2, a_{max} = 0.05g

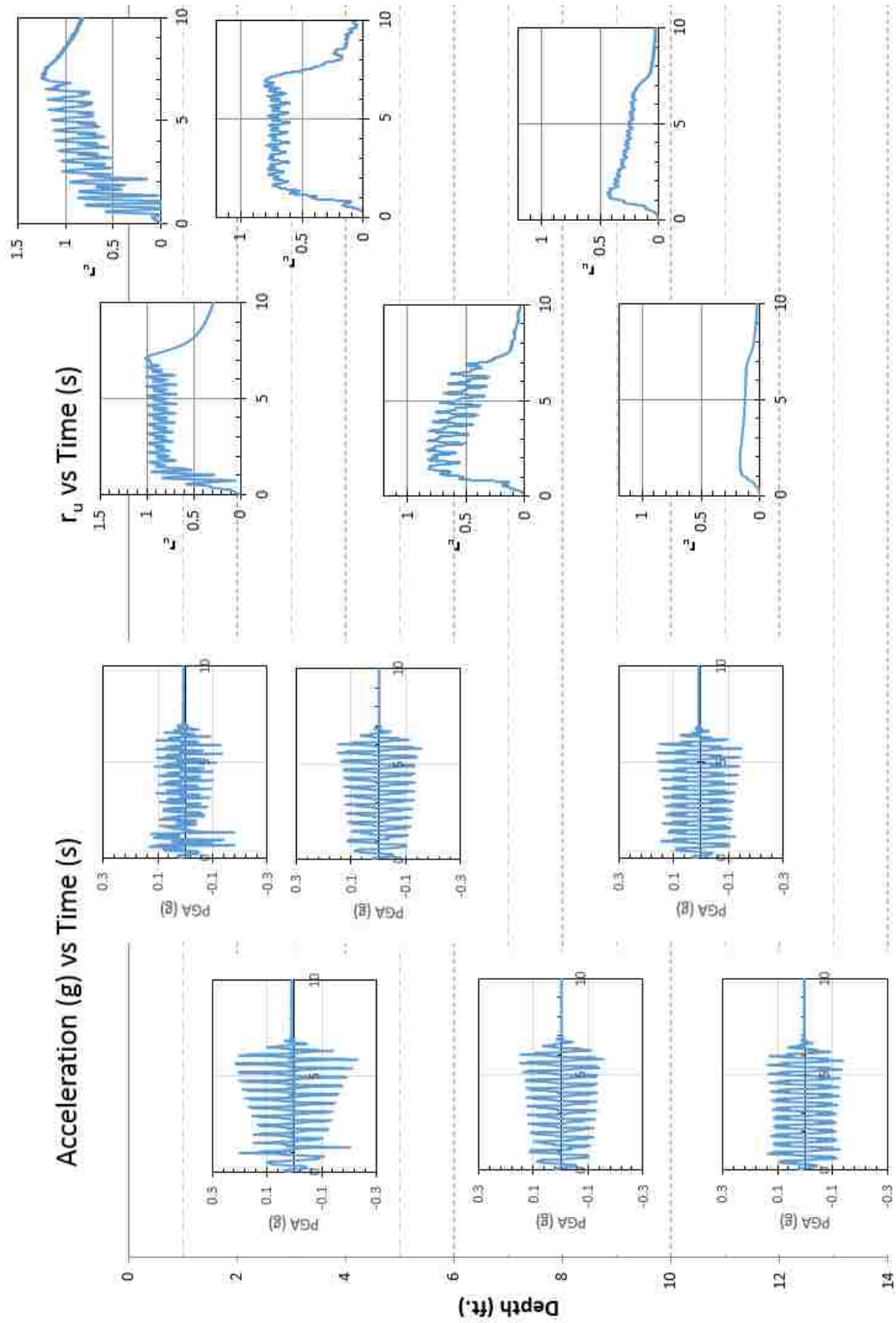

Figure 45 Acceleration Versus Time Paired with Excess Pore Pressure Ratio Versus Time for Round 2, a_{max} = 0.1g

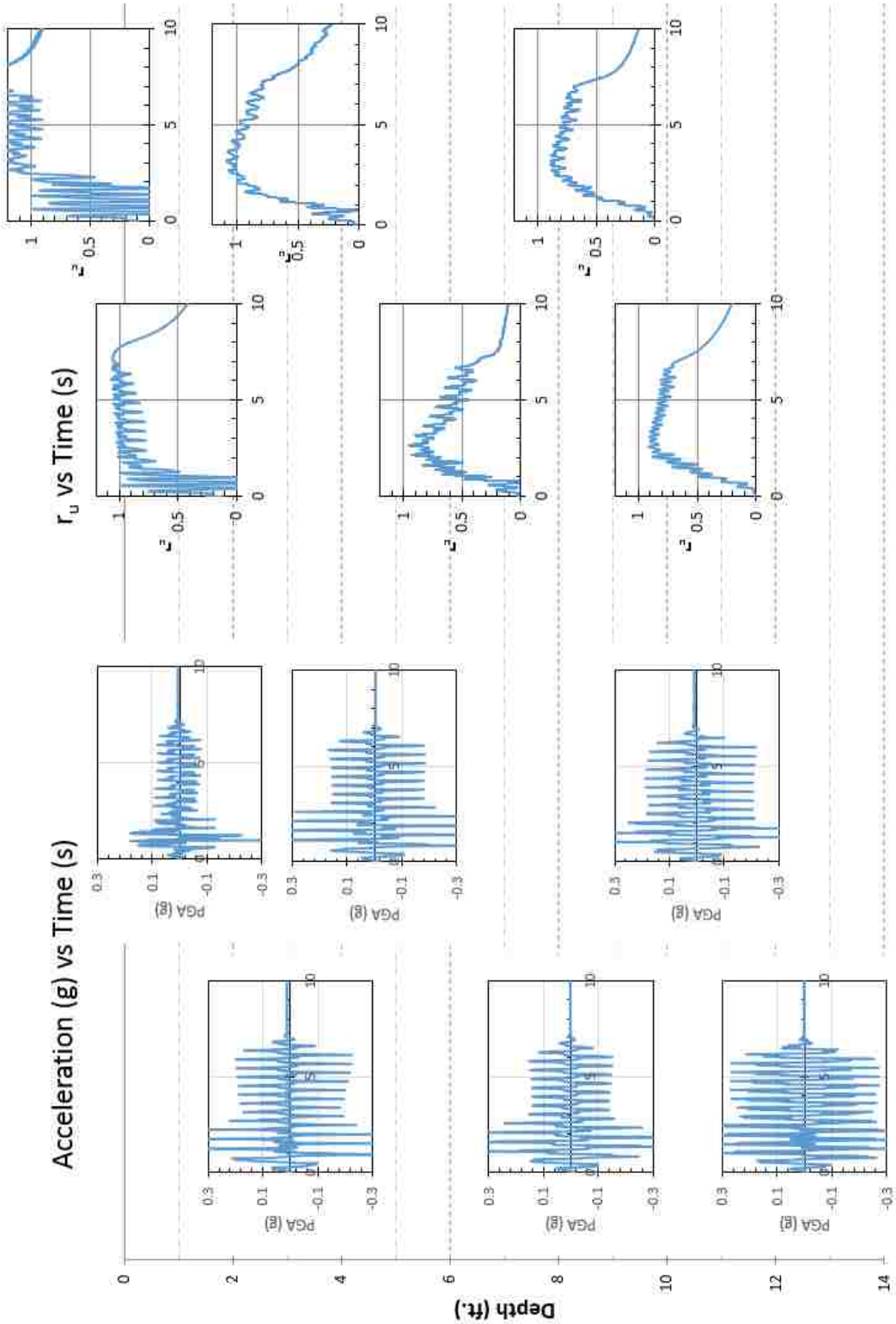

Figure 46 Acceleration Versus Time Paired with Excess Pore Pressure Ratio Versus Time for Round 2, a_{max} = 0.2g

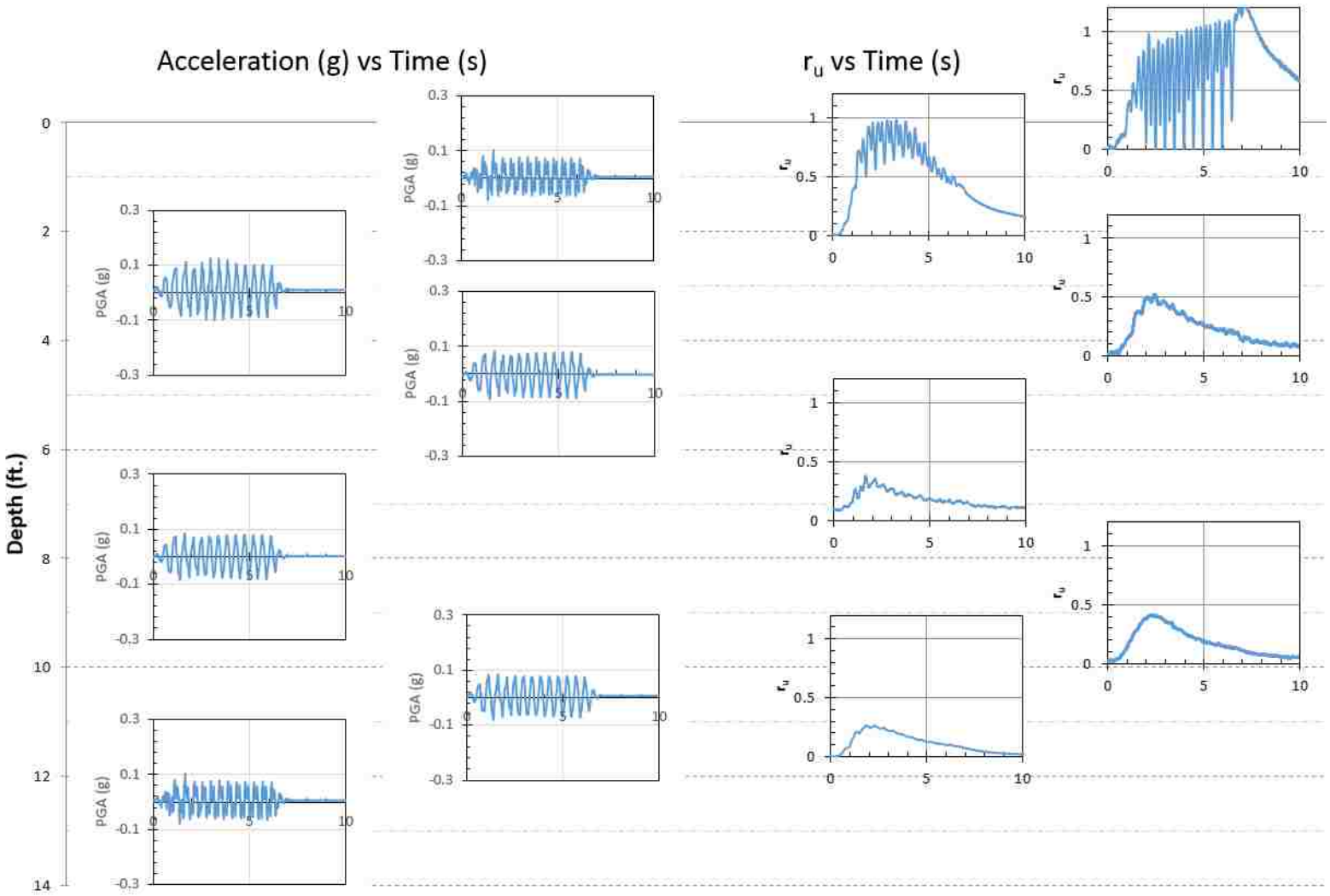

Figure 47 Acceleration Versus Time Paired with Excess Pore Pressure Ratio Versus Time for Round 3, a_{max} = 0.05

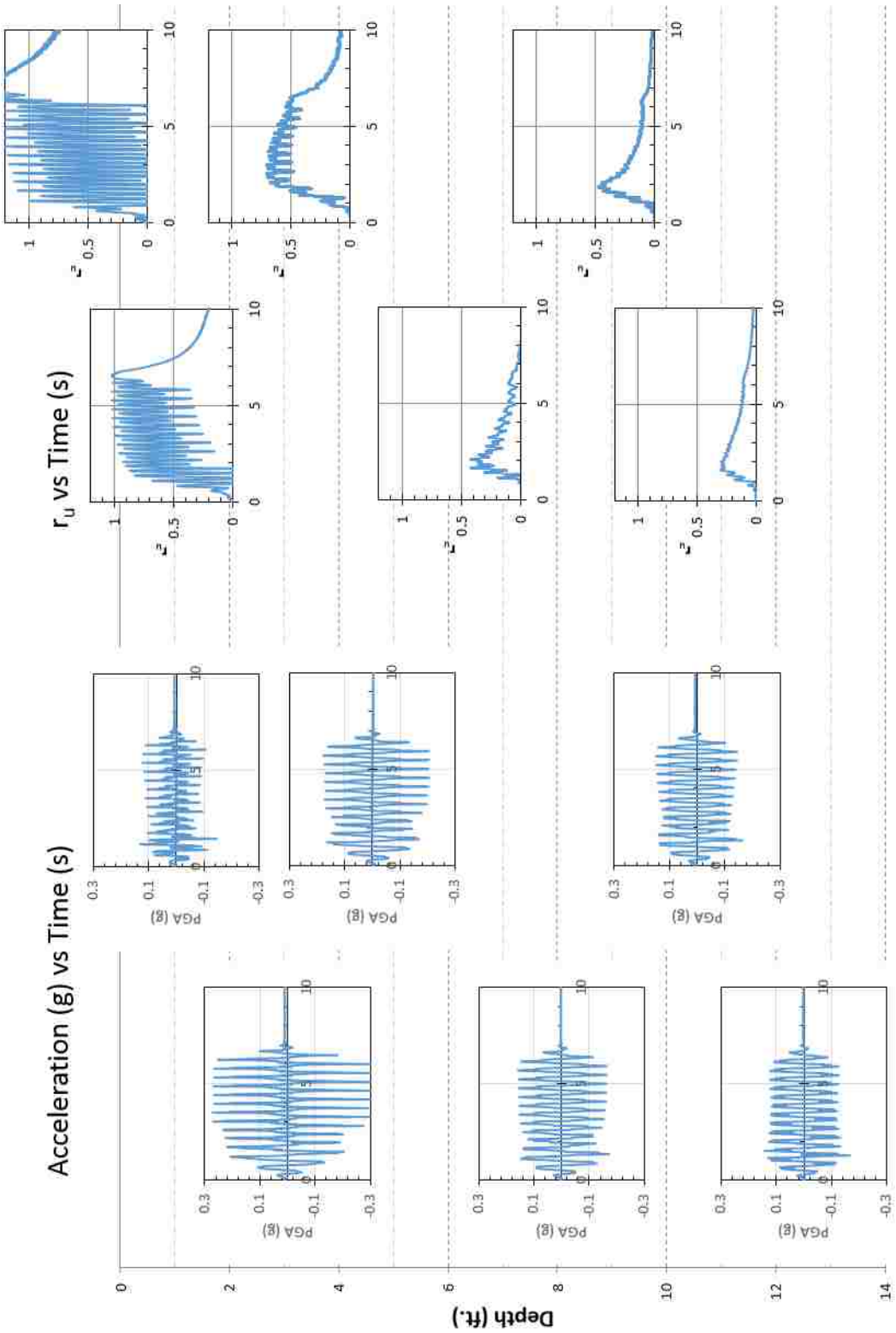

Figure 48 Acceleration Versus Time Paired with Excess Pore Pressure Ratio Versus Time for Round 3, a_{max} = 0.1g

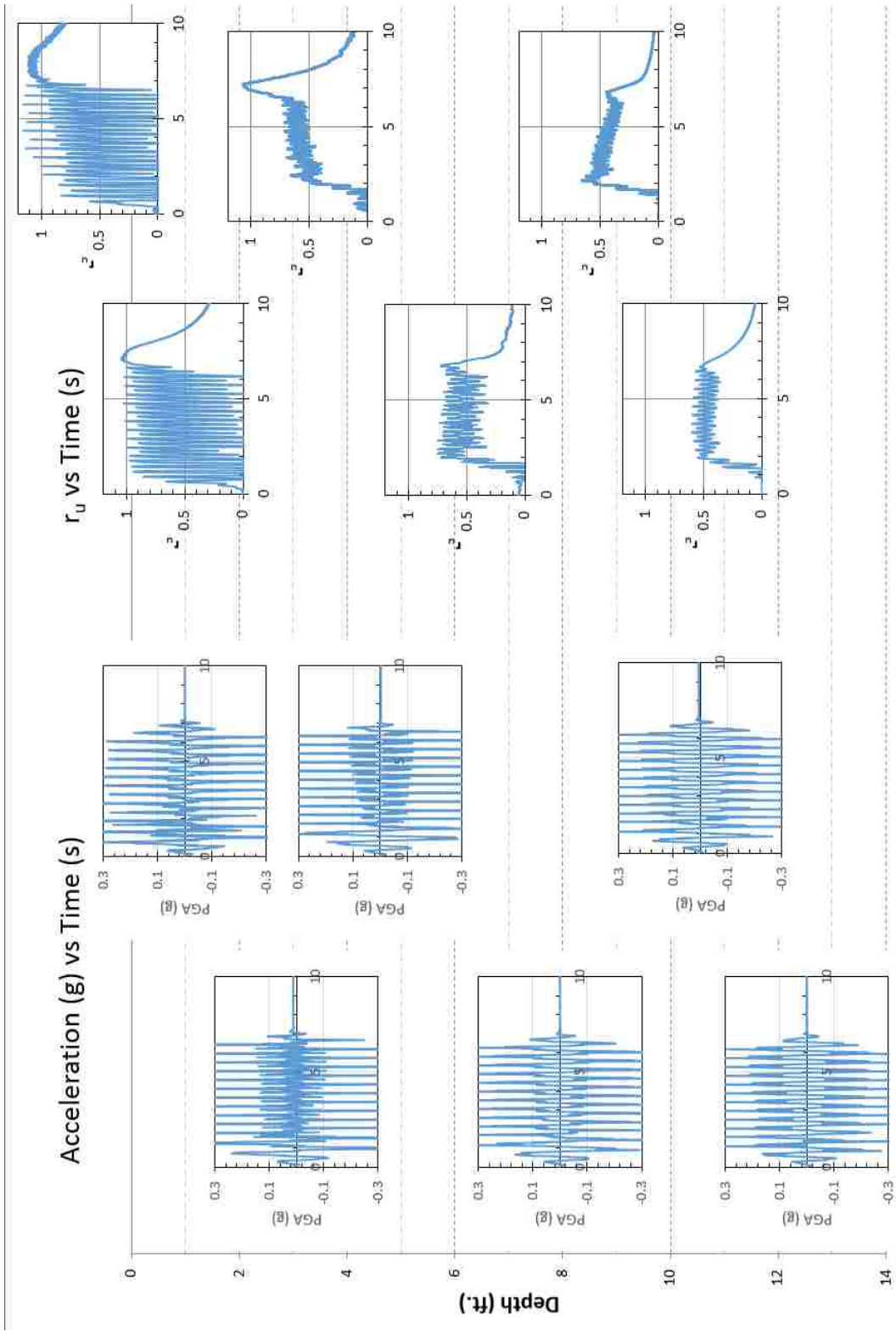

Figure 49 Acceleration Versus Time Paired with Excess Pore Pressure Ratio Versus Time for Round 3, a_{max} = 0.2g

decrease as the confining pressure increased with depth in the box. Similar results were obtained by Howell et al (2012) when using sinusoidal acceleration inputs with drains in centrifuge tests. For example, the line representing the soil with drains (SIN01 in Figure 14) looks very similar to the r_u curve measured near the surface in Figure 47 through Figure 49.

Generally, liquefaction occurs near the surface, but deeper in the sand layer pore pressures were somewhat less than 50%. The deepest that r_u remains above 0.5 after shaking occurs is at 12 feet during the second round test at 0.2g (see Figure 46). This corresponds with the highest amount of settlement between 10 and 12 feet for PVD-1 (see Figure 55). This shows that r_u reaching 0.5 does impact the settlement of the sand.

Pore pressure ratios decrease rapidly immediately after shaking, especially as depth increases. The time to reach a pore pressure ratio of 0.2 after shaking reduced by half for every two feet more of depth in the profile. For example, in the third round of testing with an acceleration level of 0.2g, the first pore pressure transducers, less than one foot below the surface, took an average of 15 seconds to reach 0.2. The next set of transducers, approximately 2.5 feet below the surface, took only 8 seconds to reach 0.2. The next set of transducers at 4.5 feet below the surface took an average of 2.5 seconds to reach 0.2. At depths below 4.5 feet the pore pressure ratio was reduced to 0.2 in one second or less. Pore pressure ratios appear to reduce faster in the later rounds than in the first round, which is most likely due to the denser soil in the later rounds. Although the reduction in void space would be expected to reduce permeability and thus reduce the dissipation rate, the compressibility of the soil also decreases with densification. According to Seed and Booker (1977), the rate of dissipation is proportional to the permeability but inversely proportional to the compressibility and the reduction in compressibility more than compensate for the reduced

permeability. This is consistent with previous findings that densification of liquefiable soils can be used as a mitigation technique.

Acceleration appears to be mostly uniform throughout the profile. However in some cases the measured acceleration was higher than the input acceleration level, such as reading 0.3g when performing a test at 0.2g in round 3, or the second accelerometer in the round 3 test at 0.1g reading acceleration above 0.2g. In the case of the round 3 test at 0.2g, the input motion appears to be closer to 0.3 than 0.2, causing higher accelerations throughout the profile. In the case of the 0.1g test in round 3, the input motion appears to be correct, but something occurred near the top of the box causing higher accelerations at that depth, but then decreasing acceleration at the surface. Higher peak acceleration tests have more variation in acceleration throughout the profile. In Figure 42, Figure 46, and Figure 48, the acceleration nearest the surface does appear to be lower than the rest of the profile, which may be due to prolonged liquefaction near the surface as observed in field cases by Youd and Carter, (2005) along with Zeghal and Elgamal (1994). However, there does not appear to be a decrease in frequency of the motions after liquefaction as observed in the field. In most cases the acceleration cycles are fairly uniform after the first two or three cycles.

4.4.3 Settlement and Peak Excess Pore Pressure Ratio Versus Depth

Figure 50 through Figure 58 provide plots of settlement versus depth profiles and peak excess pore pressure ratios ($r_{u,max}$) versus depth for each of the nine shaking tests. Settlement data is shown from three sources. First, two Sondex settlement profilometers provided settlement data for each test with data at two foot depth intervals. Secondly, three string potentiometers provided settlement for each test at the ground surface. The string "pots" were attached to a plate sitting on the ground surface. Finally, the amount of water which flowed to the surface was measured to give

a volume, which when averaged over the surface of the box gives an average settlement for the box. This calculation assumes that the water volume expelled is equal to the settlement of the sand. Excess pore pressure ratio profiles were provided by three vertical arrays of pore pressure transducers located at approximately 2.5 ft. depth intervals.

Note that in some cases in the settlement versus depth, a settlement reading is less than that both above and below the reading. This may be due to incorrect reading of a measurement, an artifact of reading at increments of 0.01 feet, or due to the Sondex tube slipping through the soil in one layer. This does not reflect the true settlement, and was corrected by creating a "smoothed" settlement curve. The smoothed curve represents a combination of both Sondex profilometers in a way that removes negative settlement from any zone. Surface settlement from the string pots and volume measurement are factored into the smoothed curve to include the best value for settlement near the surface. This smoothed curve is used to calculate the strain in the next section.

The first plot is missing a volume reading because it was not until after that test that we began measuring the volume of water (Figure 50). Some of the tests are missing certain string pots due to malfunctions of the string pot or excessive settlement of the plate into the surface of the sand during the test.

In round one for the 0.05g test (Figure 50), the zone of liquefaction extends to about 6 to 8 feet, only 40 to 50 percent of the thickness of the loose sand layer. In contrast, tests conducted on sand in the box without drains experienced liquefaction throughout the entire depth after only a few cycles of loading (Bethapudi, 2008). This result indicates that the drains are producing increased liquefaction resistance which is more effective at depth. The settlement profile also indicates that most of the settlement is occurring within the upper part of the profile and extends to a depth where $r_{u,max}$ is above 0.5. The 0.1g test created approximately 2 inches of settlement in

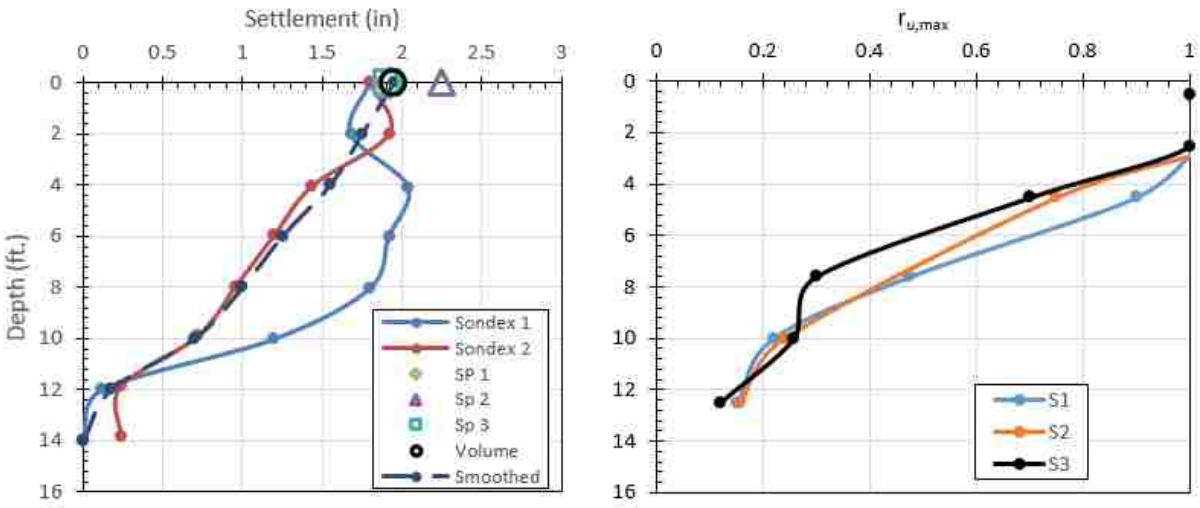

Figure 50 Profiles of Liquefaction Induced Settlement and Maximum Excess Pore Pressure Ratio ($r_{u,max}$) for Round 1 Test with a_{max}=0.05 g

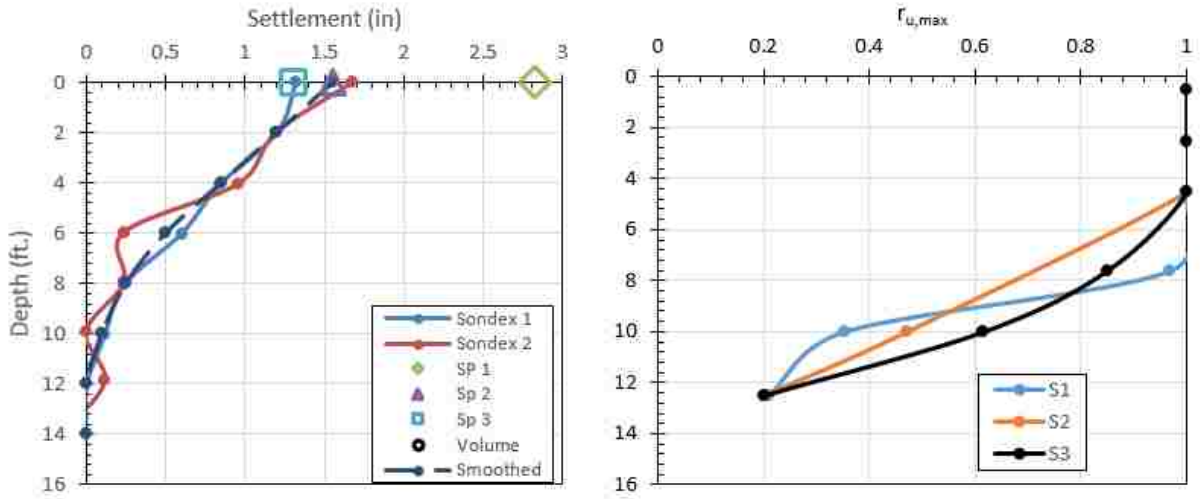

Figure 51 Profiles of Liquefaction Induced Settlement and Maximum Excess Pore Pressure Ratio ($r_{u,max}$) for Round 1 Test with a_{max}=0.10 g.

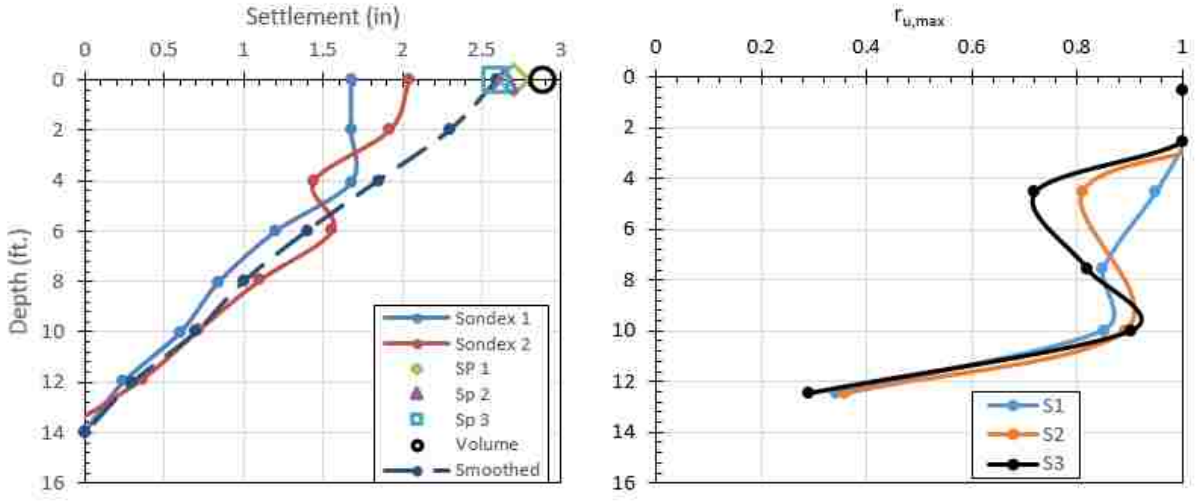

Figure 52 Profiles of Liquefaction Induced Settlement and Maximum Excess Pore Pressure Ratio ($r_{u,max}$) for Round 1 Test with a_{max}=0.20 g.

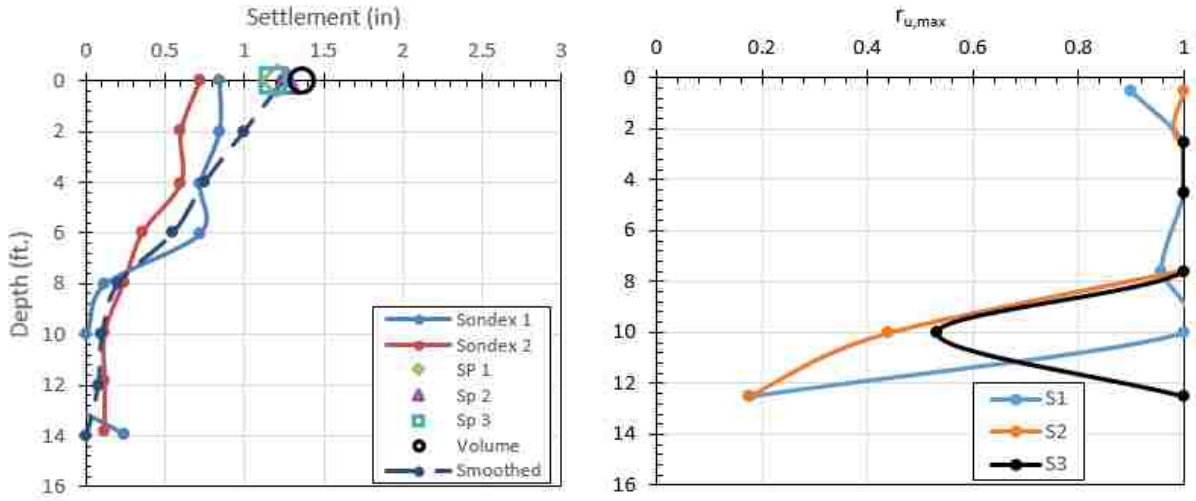

Figure 53 Profiles of Liquefaction Induced Settlement and Maximum Excess Pore Pressure Ratio ($r_{u,max}$) for Round 2 Test with a_{max}=0.05 g.

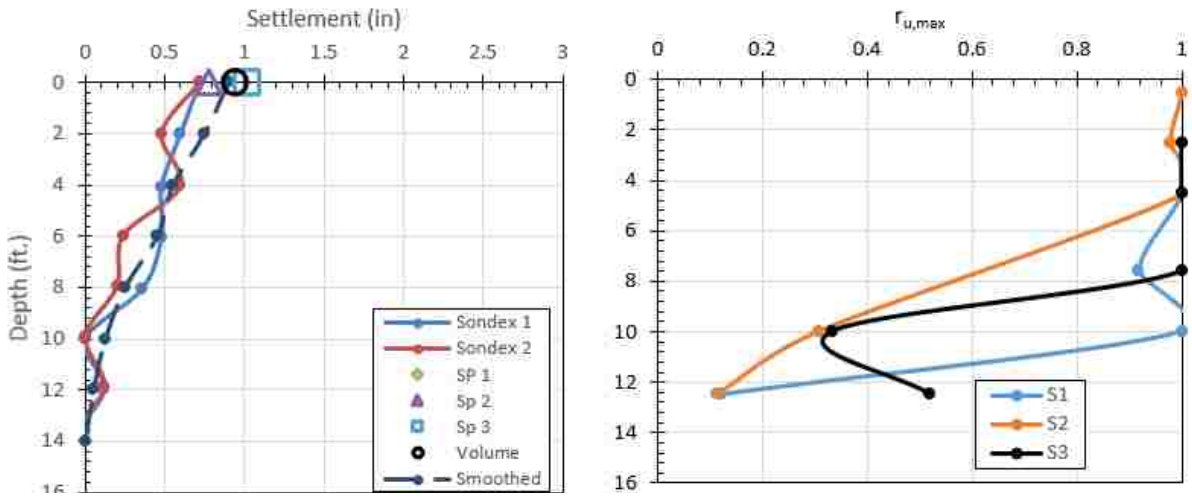

Figure 54 Profiles of Liquefaction Induced Settlement and Maximum Excess Pore Pressure Ratio ($r_{u,max}$) for Round 2 Test with a_{max}=0.10 g.

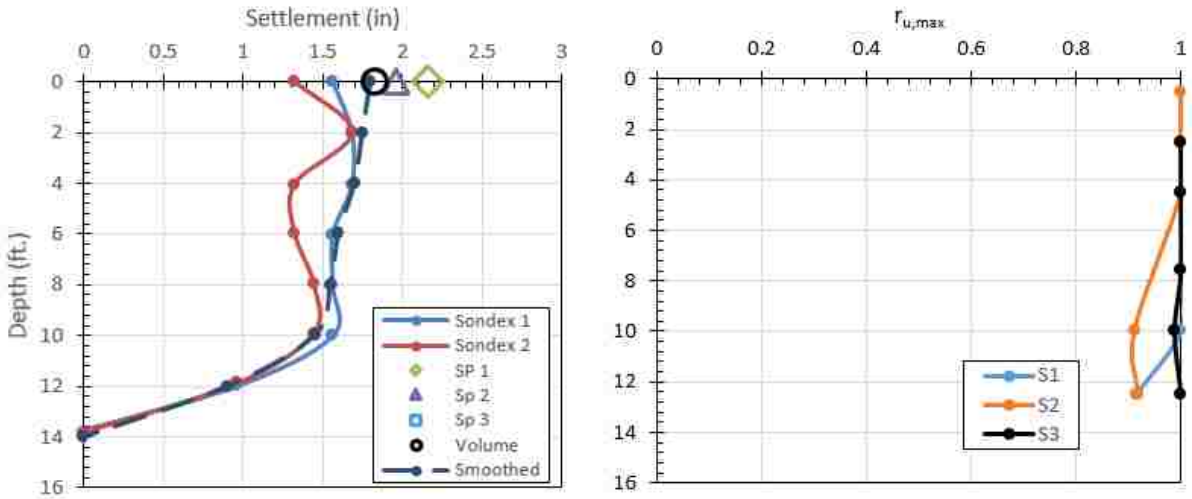

Figure 55 Profiles of Liquefaction Induced Settlement and Maximum Excess Pore Pressure Ratio ($r_{u,max}$) for Round 2 Test with a_{max}=0.20 g.

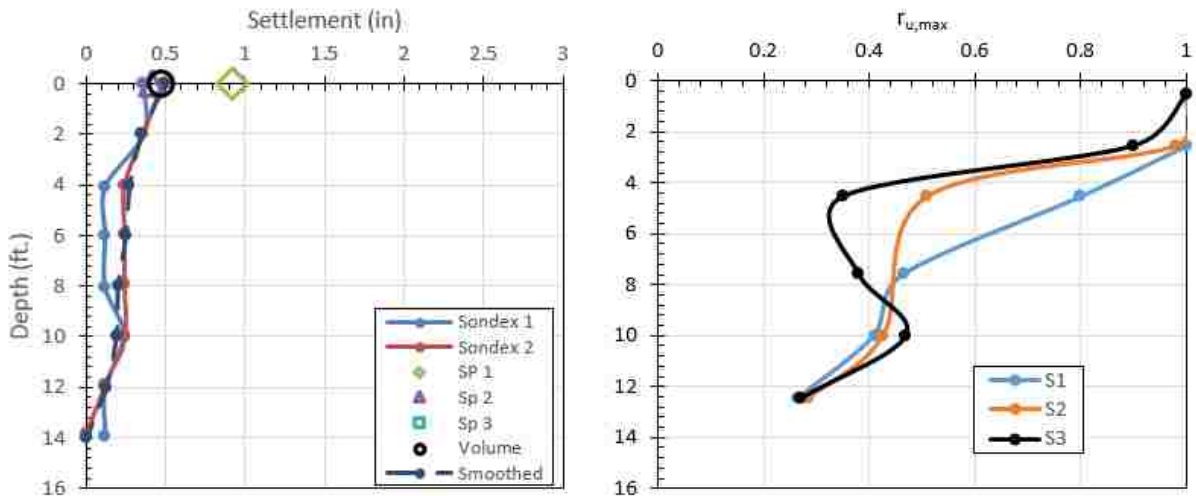

Figure 56 Profiles of Liquefaction Induced Settlement and Maximum Excess Pore Pressure Ratio ($r_{u,max}$) for Round 3 Test with a_{max}=0.05 g.

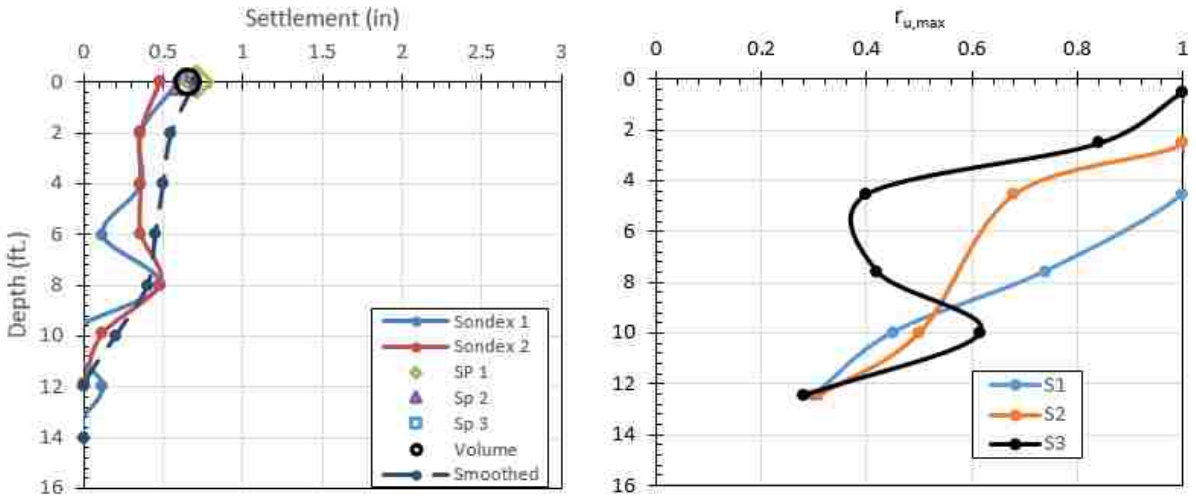

Figure 57 Profiles of Liquefaction Induced Settlement and Maximum Excess Pore Pressure Ratio ($r_{u,max}$) for Round 3 Test with a_{max}=0.10 g.

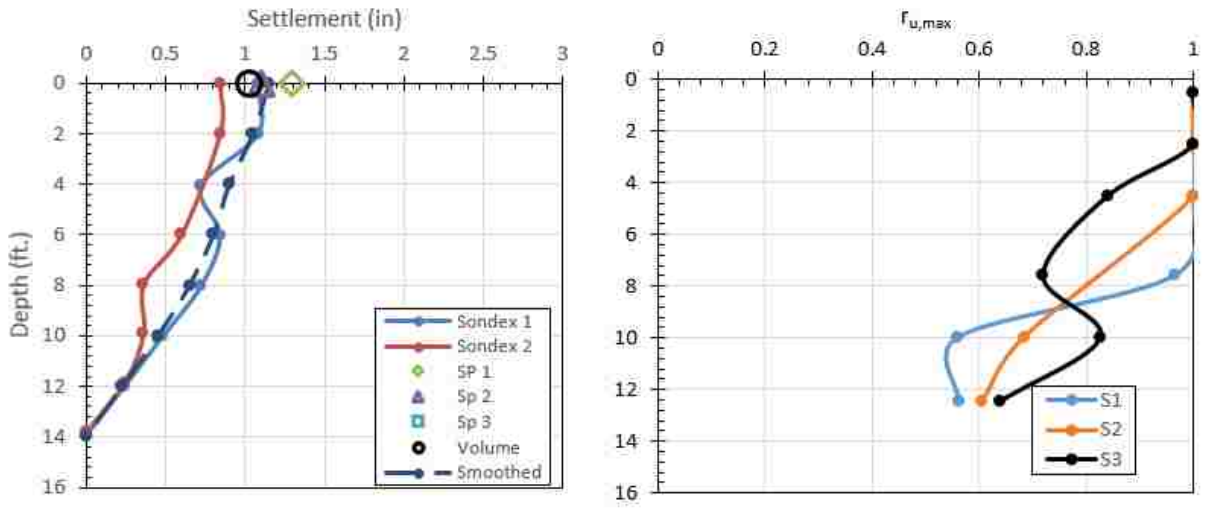

Figure 58 Profiles of Liquefaction Induced Settlement and Maximum Excess Pore Pressure Ratio ($r_{u,max}$) for Round 3 Test with a_{max}=0.20 g.

12 feet of soil which represents a strain of about 1.4%. The first 0.1g test in the Dobry and Thevanayagam series of tests had about 3.5 inches of settlement over 16 feet of soil, which is equivalent to a strain of about 1.8%. This result suggests that even in the liquefied zones, the drains have reduced the liquefaction induced settlement to some extent.

Round 2 (Figure 53 through Figure 55) had high values of $r_{u,max}$, but lower settlement, about 30% less than in round 1. The high values of $r_{u,max}$ with reduced settlement may indicated that $r_{u,max}$ is more related to the acceleration level than the amount of settlement, and that time above r_u of 0.5 is a better indicator of settlement, as was found by Howell et. al. (2012). Settlement does appear to occur mainly in zones where $r_{u,max}$ is above 0.5.

The settlement profiles appear to have more flat sections, with more settlement occurring near the surface and the bottom than in the middle section. This is especially noticeable in the 0.2g test (Figure 55), where the settlement curve is nearly flat until a depth of 10 feet, below which nearly all of the settlement for the test occurred. This trend is continued in the 0.05g and 0.1g tests

of round 3 (see Figure 56 and Figure 57). The settlement from the previous tests in the upper zone may prevent subsequent settlement in that zone.

The various settlement measurement techniques were relatively consistent in determining the ground surface settlement for each test; however, there are certainly variations. The Sondex measurements at the surface were either similar or smaller than the other methods. The Sondex measurements were particularly low when the settlement was more than 1.5 inches, which may be the maximum settlement that the corrugated pipe could accommodate without some slippage during such a short time period. Generally, water pumped from the box after the shaking seems to give a settlement very similar to the measurement obtained from the string pots. The water volume is a better measure of the average volume lost across the entire box, whereas the string pots occasionally measured extreme values, possibly due to the non-uniformity soil profile or due to the plate sinking into the softened ground at the surface.

4.4.4 Volumetric Strain Versus Depth from Settlement

Volumetric strain was calculated using settlement data obtained from the Sondex profilometers. Data was collected at intervals of approximately 2 feet. To reduce scatter in the strain plots, the settlement data used to calculate the volumetric strain versus depth was taken from the smoothed settlement curves. This removed any negative strain from settlement readings that are lower than the readings both above and below it which do not reflect the true conditions. Strain was calculated between each Sondex measurement by dividing the difference in the settlement between the two readings above and below, and dividing by the distance between the two readings. Because the length and width of the box at all points remains the same, the strain is equal to the

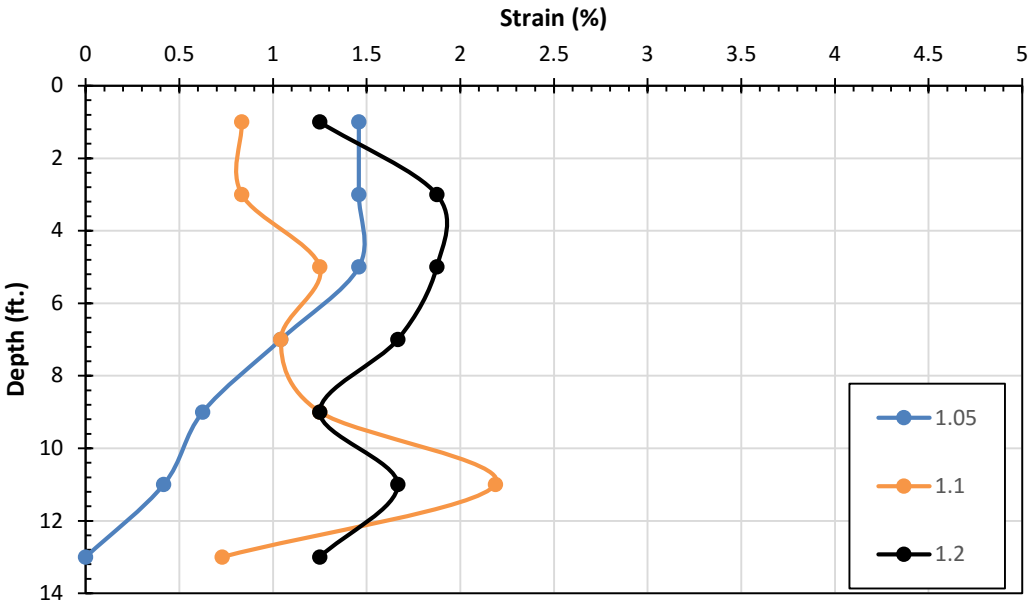

Figure 59 Profiles of Strain Versus Depth Using Smoothed Sondex Measurements for Round 1

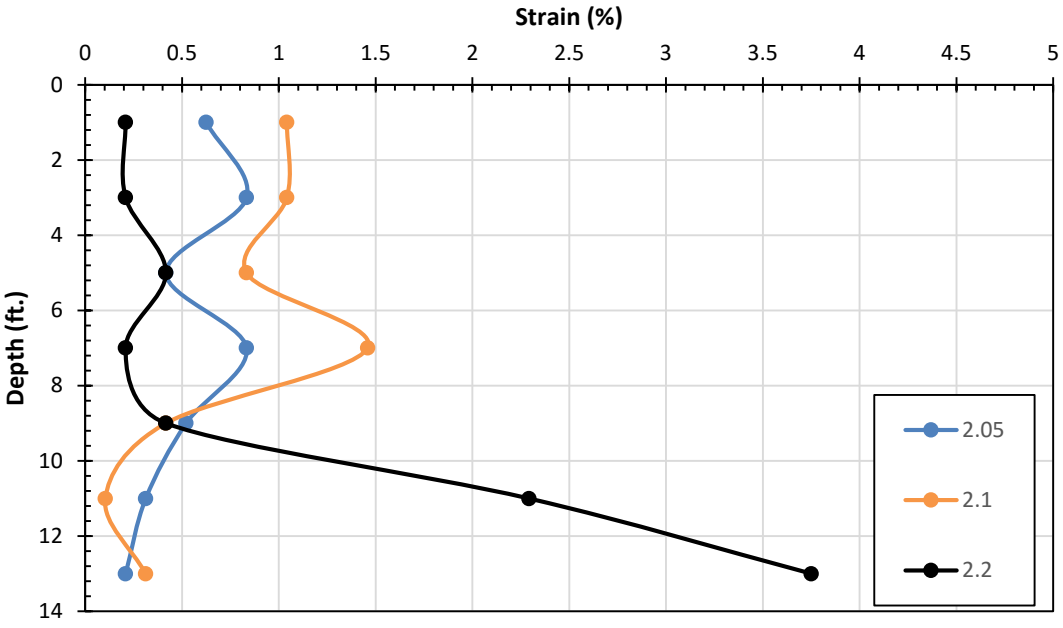

Figure 60 Profiles of Strain Versus Depth Using Smoothed Sondex Measurements for Round 2

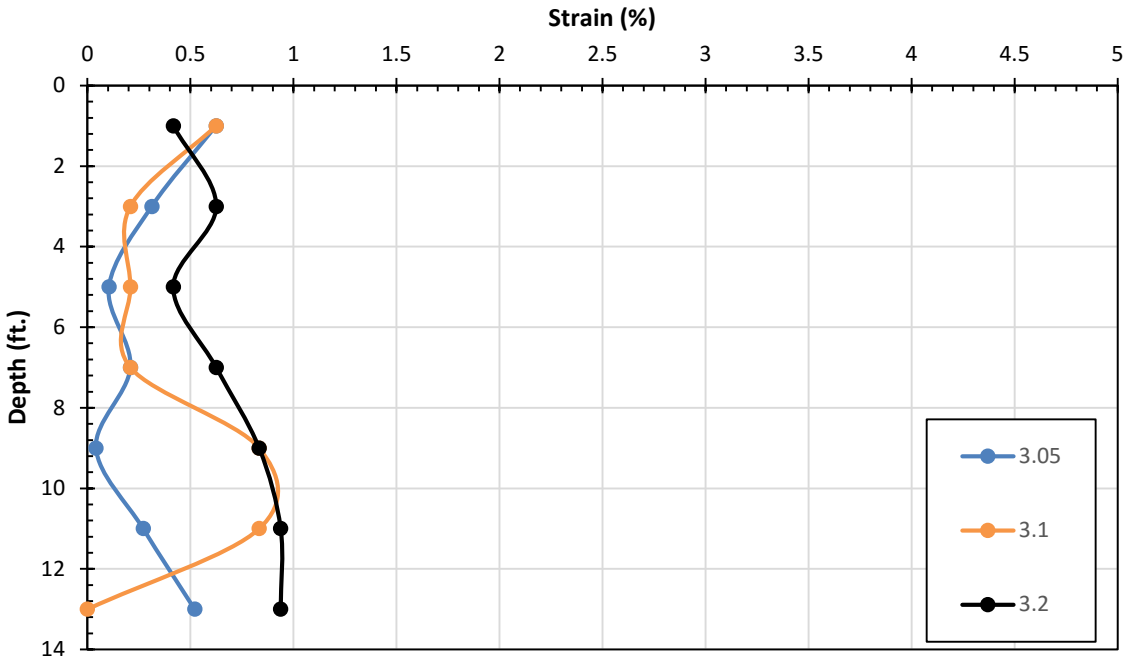

Figure 61 Profiles of Strain Versus Depth Using Smoothed Sondex Measurements for Round 3

volumetric strain. Figure 59 through Figure 61 show the volumetric strain profiles for each round of testing.

Strain appears to be higher with higher acceleration, especially deeper in the soil profile. The strain at the lowest acceleration level has the least variation through the depth profile. While the strain in round 3 appears to be more uniform, it does have some variation. Generally, strain levels tend to decrease with each round. For the first round of tests, strain was commonly between 1 and 2%. In contrast, for the third round test, volumetric strain was typically between 0.2 and 1%. It is interesting to note that the majority of the strain in the second round test at 0.2g acceleration had a significant amount of strain at or below 10 feet, with very low strain above that depth (see Figure 60). This suggests that the settlement from previous rounds in the upper region was

precluding further settlement in that zone during that test. The final test at 0.2g during round 3 also had higher strain at depths below 10 feet, but not as extreme as in round 2.

In general, the lower acceleration tests had peak strain at shallower depths, from 0 to 8 feet. It is interesting to note that in many cases the strain in the 0.05g and 0.1g tests was higher than the 0.2g tests at these shallow depths, which may indicate that the settlement in this area densified the shallower soil such that less settlement occurred in the shallow soil during the 0.2g tests. The 0.2 g tests had peak strain occurring at a depth below 8 feet in most cases, and had higher strain than the lower acceleration tests below 8 feet as well, meaning that the higher acceleration was required to liquefy the soil at that depth.

A relative density of 40% would correspond to an $(N1)_{60}$ value of 10 based on correlations developed by Kulhawy and Mayne (1990). For $(N1)_{60}$ of 10, using the Tokimatsu and Seed curve for predicting liquefaction induced settlement gives a volumetric strain of about 2.5%. The volumetric strain from the first 0.lg test, using an average settlement of 2 inches, would have a volumetric strain of 1.15%. In comparison, the first two LG1 tests at 0.1g had approximately 4 inches of settlement, which is a strain of 2%. The sand without drains developed strain close to the expected strain based on the Tokimatsu and Seed method, while the sand with drains had nearly half the strain of the untreated soil. This result is most likely due to reducing excess pore pressures near the surface, where the drains are most effective.

4.4.5 Surface Settlement Versus Time with Excess Pore Pressure Ratios Surrounding the Liquefied Layer

As indicated previously, surface settlement was measured using string pots connected to plates sitting on the surface of the sand at three locations (see Figure 29 for locations of surface

string pots). Settlement versus time plots are in Figure 62 through Figure 64. The settlement plots are in groups of three for each round. The left plot represents the settlement from the 0.05 g test, the center plot is the 0.1 g test, and the right plot is the 0.2 g test. Beneath each settlement plot are two plots of excess pore pressure ratio versus time. The upper plot is located near the surface and the lower plot is near the bottom of the liquefied layer. In some of the tests the one of the string pots malfunctioned or became disconnected, giving a zero reading for the test. The malfunctioning readings have been removed. V1 from the 0.05g test during round 2 has been removed, as well as V3 from the 0.2g test during round 2 and all tests during round 3.

Settlement increases with increasing acceleration, which is to be expected, as more energy is being introduced into the soil. In addition, settlement decreases with each progressive round of testing. Each round of testing has densified the sand from the settlement of the previous rounds, also evidenced by the increased cone tip resistance in the CPT soundings (see Figure 35). The settlement from the final round is much less than the settlement from the first round, and even the second round.

Most of the settlement occurs during shaking (0 to 7.5 seconds), and the remainder occurs mainly within the next 15 seconds as pore pressures dissipate. Very little settlement occurs after r_u decreases below 0.5. The test in round 2 and especially round 3 have a very flat curve after the shaking is finished because the time for r_u to go below 0.5 is decreasing with increasing rounds of testing. For example, in Figure 62, about 0.5 inch (20%) of the 2.5 inches of total settlement occurred after the shaking had stopped for the 0.2g test for round 1, whereas in Figure 64, only about 0.1 inch(10%) of the 1.0 inch of total settlement or less occur after the shaking has stopped in the 0.2g test for round 3. The time for r_u to dissipate to 0.5 after shaking stopped in Figure 64

for the round 3 0.2g test is about 6 seconds. In contrast, Figure 62, it takes 11 seconds for r_u to reach 0.5 again in the 0.2g test, almost twice as long as in round 3.

Table 7 and Table 8 summarize the amount of time for excess pore pressures to dissipate to 0.2 and 0.5, respectively, after shaking stops. The values in the table are averages of the three sensor arrays.

The time for r_u to dissipate to 0.2 after shaking includes values for every depth represented by the sensor arrays, while only the top two sensor locations are used for dissipation to 0.5. This is because many of the lower sensor locations finish shaking below 0.5 or take less than one second to reach 0.5. The time for r_u to reach 0.5 at a depth of 1 foot from Table 8 are used to determine the amount of settlement that occurred while r_u was greater than 0.5. The total amount of settlement for each test taken from string pots, water volume, and Sondex measurements is given in Table 9. The percentage of settlement that occur during shaking is summarized in Table 10. The percentage of settlement that occurs while r_u is greater than 0.5 is summarized in Table 11.

The amount of time for excess pore pressures to dissipate reduces significantly between rounds of testing. The time to reach r_u=0.5 at the surface is much less impacted by acceleration level than time to reach r_u=0.2 at the same depths, especially in rounds 2 and 3. The higher acceleration tests cause higher pore pressures deeper in the soil profile, as found in previous sections. The time for r_u to dissipate to 0.5 does not seem to have a direct correlation to total settlement for each test as was observed in the centrifuge tests reported by Howell et. al. (2006), but this may be because the depth of the liquefied layer is different in each test in PVD-1. For example in round 1, the higher acceleration tests which had more total settlement took less time to reach 0.5. Also, the settlement from round 2 with 0.2g acceleration and round 1 with 0.1g

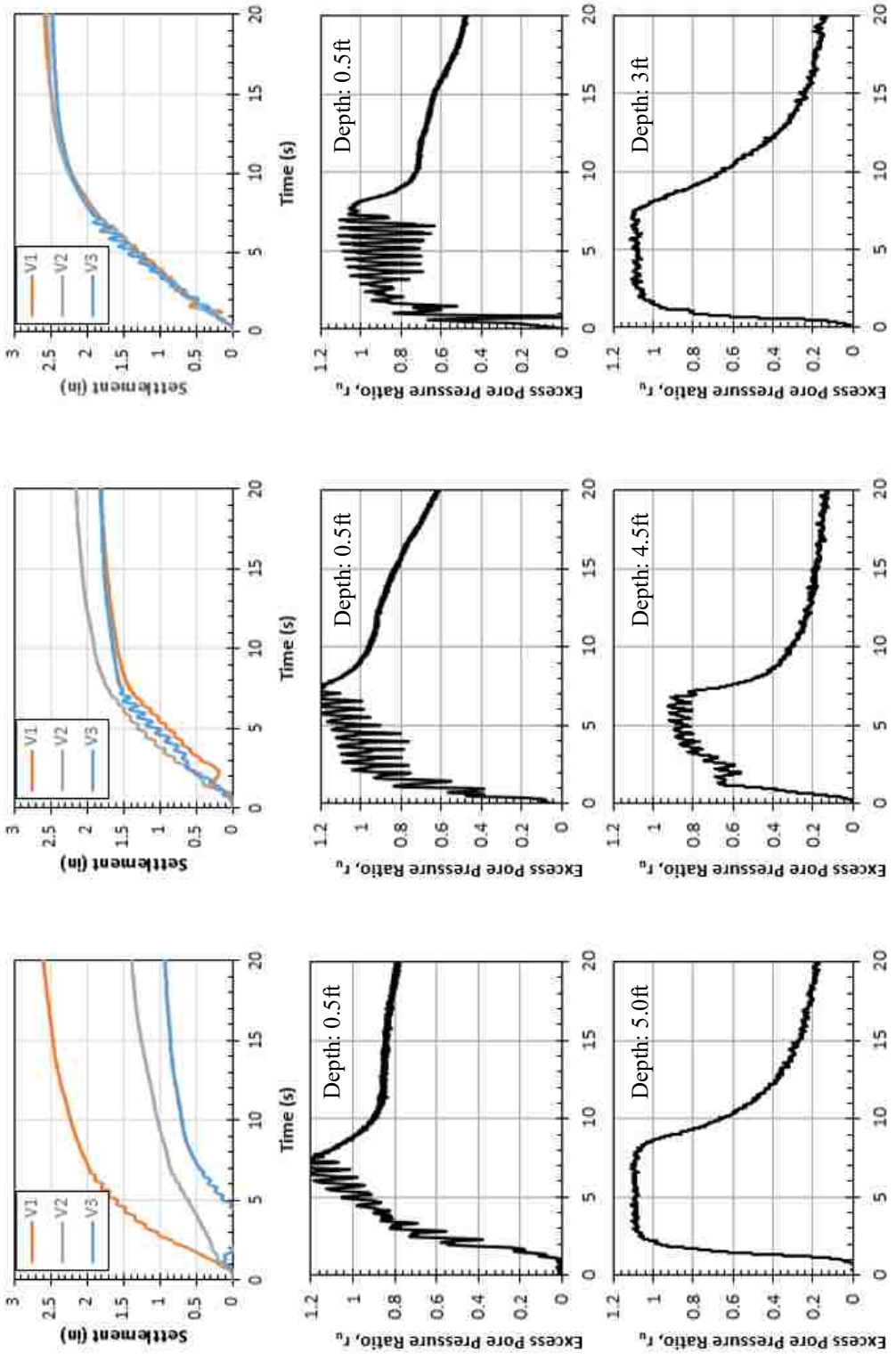

Figure 62 Surface Settlement Versus Time Paired with Excess Pore Pressure Ratio (r_u) Versus Time for Round 1, Left a_{max}=0.05 g, Middle a_{max}=0.10 g, Right a_{max}=0.20 g

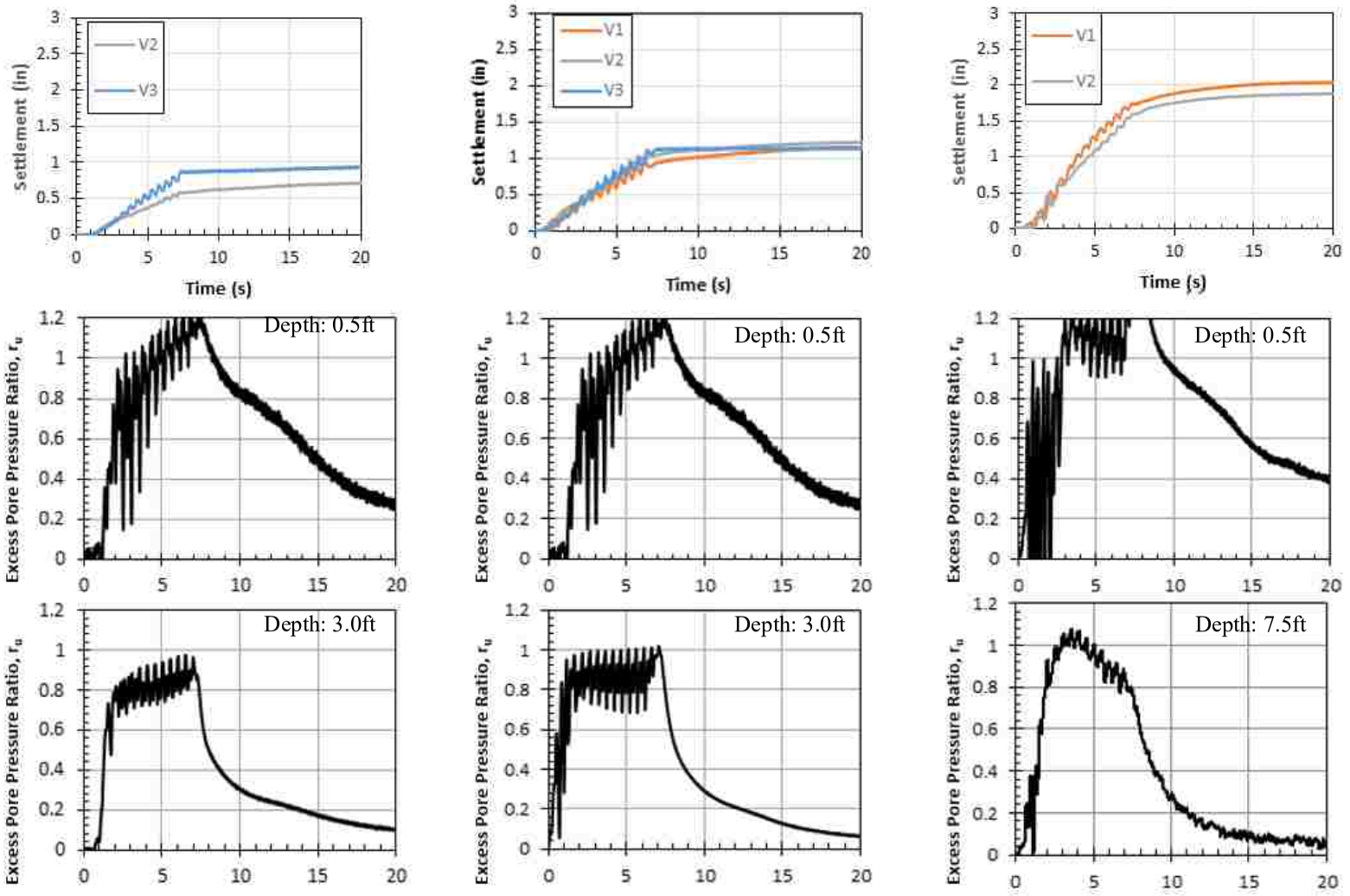

Figure 63 Surface Settlement Versus Time Paired with Excess Pore Pressure Ratio (r_u) Versus Time for Round 2, Left a_{max}=0.05 g, Middle a_{max}=0.10 g, Right a_{max}=0.20 g

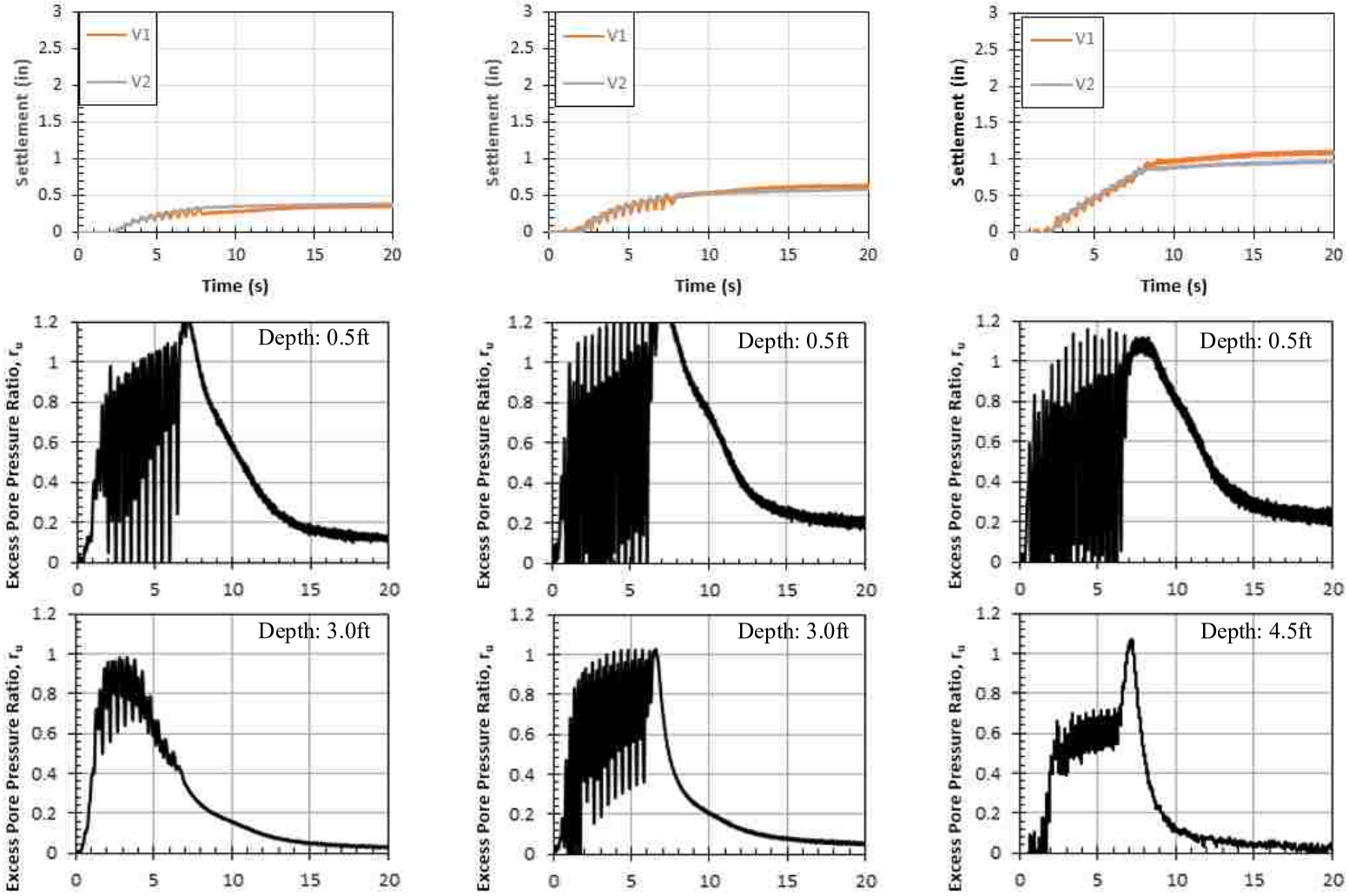

Figure 64 Surface Settlement Versus Time Paired with Excess Pore Pressure Ratio (r_u) Versus Time for Round 3, Left a_{max}=0.05 g, Middle a_{max}=0.10 g, Right a_{max}=0.20 g

Table 7 Time in Seconds for r_u to Dissipate to 0.2 After Shaking.

depth (ft)	Round 1			Round 2			Round 3		
	Acceleration (g)			Acceleration (g)			Acceleration (g)		
	0.05	0.1	0.2	0.05	0.1	0.2	0.05	0.1	0.2
0.5	30	30	30	17	13	22	4	7	15
2.5	24.33	18	22.33	5.33	6.33	6.67	2.3	3	8
5	10.33	9.67	10.67	3.67	1.33	4	0	1.33	2.33
7.5	4	3	7	0	1	1	0	0	1
10	0	2.33	4	0	0	1.67	0	0	1
12.5	0	1	2.33	0	0	2.67	0	0	1

Table 8 Time in Seconds for r_u to Dissipate to 0.5 After Shaking.

Round 1				Round 2				Round 3			
depth (ft)	Acceleration (g)			depth (ft)	Acceleration (g)			depth (ft)	Acceleration (g)		
	0.05	0.1	0.2		0.05	0.1	0.2		0.05	0.1	0.2
1	25	19	11	1	7	7	6	1	2	5	6
3	7	7	5	3	2	2	3	3	0	1	2

Table 9 Settlement for Each Test from Sondex, String Pots, and Water Volume

		Average Sondex (in)	Average string pot (in)	Water volume (in)
Round 1	0.05	1.32	1.89	#N/A
	0.1	1.80	2.03	1.94
	0.2	1.68	2.64	2.88
Round 2	0.05	0.72	0.90	0.94
	0.1	0.84	1.22	1.36
	0.2	1.56	1.39	1.83
Round 3	0.05	0.36	0.46	0.47
	0.1	0.60	0.67	0.65
	0.2	1.08	1.19	1.02

Table 10 Percentage of Settlement that Occurs During Shaking.

Acceleration (g)	Settlement (%)		
	Round 1	Round 2	Round 3
0.05	58.1	85.4	80.0
0.1	74.6	84.9	80.6
0.2	70.1	84.8	79.4

Table 11 Percentage of Settlement that Occurs While r_u>0.5.

Acceleration (g)	Settlement (%)		
	Round 1	Round 2	Round 3
0.05	98.2	92.4	86.3
0.1	99.0	96.1	91.2
0.2	97.2	96.3	95.7

acceleration had nearly the same settlement, but the time that r_u exceeded 0.5 was much less. In round 3, where the density does not change as drastically because there was little settlement in each test, longer time to dissipate does correlate to more settlement, which may be because the depth of the liquefied layer is more consistent.

While it appears that round 1 has a significant amount of settlement that occurs with excess pore pressures above 0.5 (see Table 11), this is partly attributable to the fact that the time that the excess pore pressures were elevated was longer in round one than in other rounds. For example, r_u was greater than 0.5 for 25 seconds in the round 1 0.05g test, but only 5 seconds for the round 3 0.05g test. More significant is that over 95% of settlement occurred while r_u was above 0.5 in round 3 with an acceleration level of 0.2g only 6 seconds after shaking had stopped. The lowest value in Table 9 occurs in round 3 with an acceleration level of 0.05, but 86% of the settlement occurred during and within 2 seconds after the shaking stopped in this case, which is a significant amount. For comparison, 80% of the settlement in round three test at 0.05g occurred during shaking, while in the first round rest at 0.05g only 60% of settlement occurred during

shaking. Time with ru greater than 0.5 does seem to be a good indicator or settlement based on density, such as the difference in settlement between round 1 and round 3, but it is not necessarily a good indicator of total settlement.

4.4.6 Settlement Comparisons

The cumulative settlement from PVD-1 for all tests is shown in Figure 65. The tests are in order by date of the test. The 0.2g tests in each round produced more settlement than the lower acceleration levels, and round 2 and round 3 each have less total settlement than the rounds preceding them.

Figure 66 shows settlement of the sand versus acceleration level normalized by the settlement for the 0.05g test from each round. Round 1 had lower normalized settlement with higher acceleration, but in rounds 2 and 3, an increase from 0.05g to 0.1g gives a 40% increase in settlement. Increasing from 0.1g to 0.2 g gives an additional increase of 70% increase or a total increase of 2.4 times. Figure 67 plots the incremental settlement of the sand for each test by round and acceleration level. For all acceleration levels the settlement decreases significantly from the first round of tests to the final round. Increased density should account for some of this decrease; however, the drainage function also appears to be more effective as the density of the sand increases. Figure 68 plots settlement of the sand at a given peak acceleration after normalization by settlement for the first test. This normalization shows that the second round tests had 20 to 50% less settlement than the first round, and the third round tests had 60 to 75% less settlement than the first round of tests.

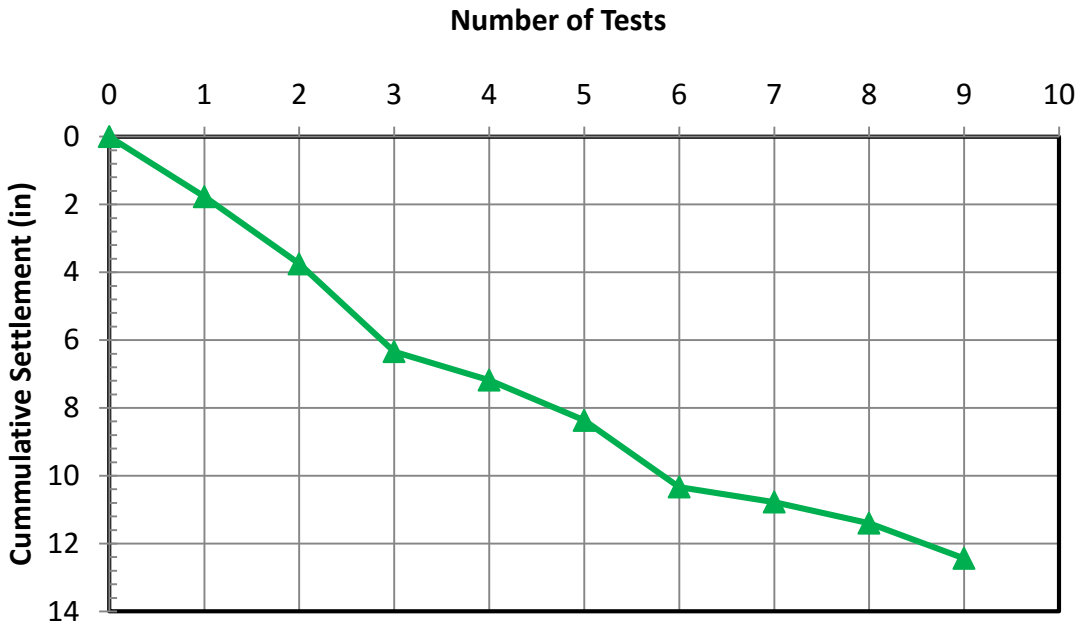

Figure 65 Cumulative Settlement for all Tests During PVD-1

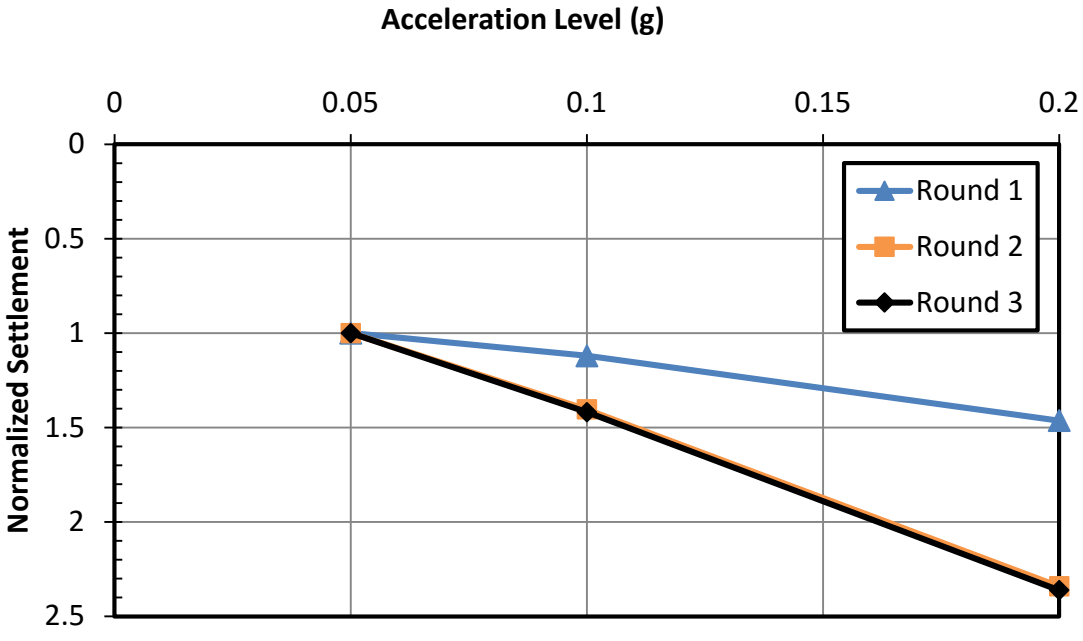

Figure 66 Settlement of Sand Versus Acceleration Level by Round After Normalizing by Settlement for the 0.05g Test for Each Round

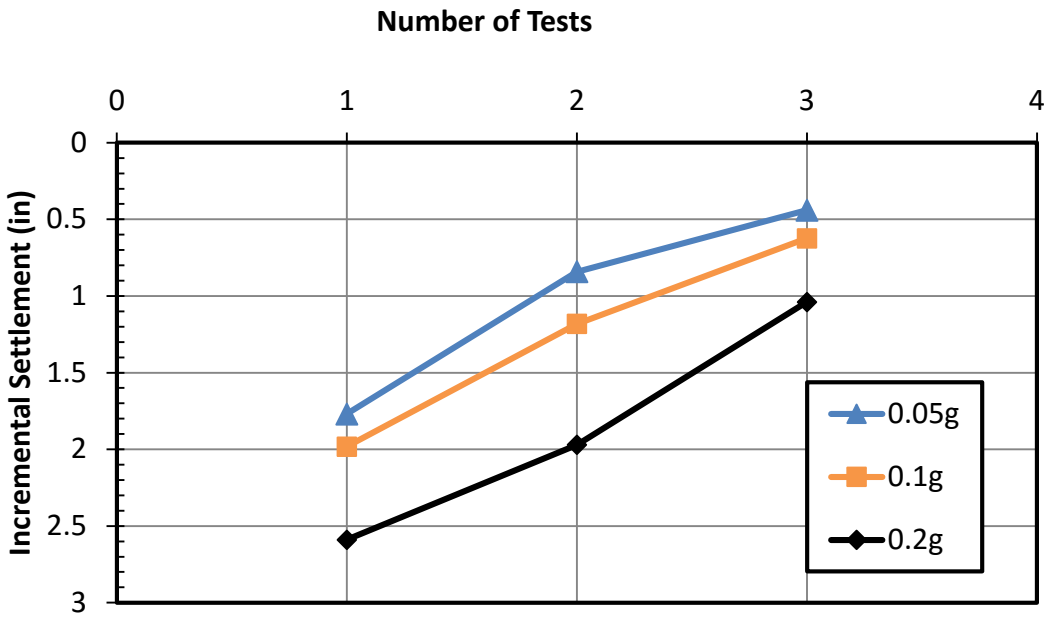

Figure 67 Incremental Settlement at a Given Peak Acceleration

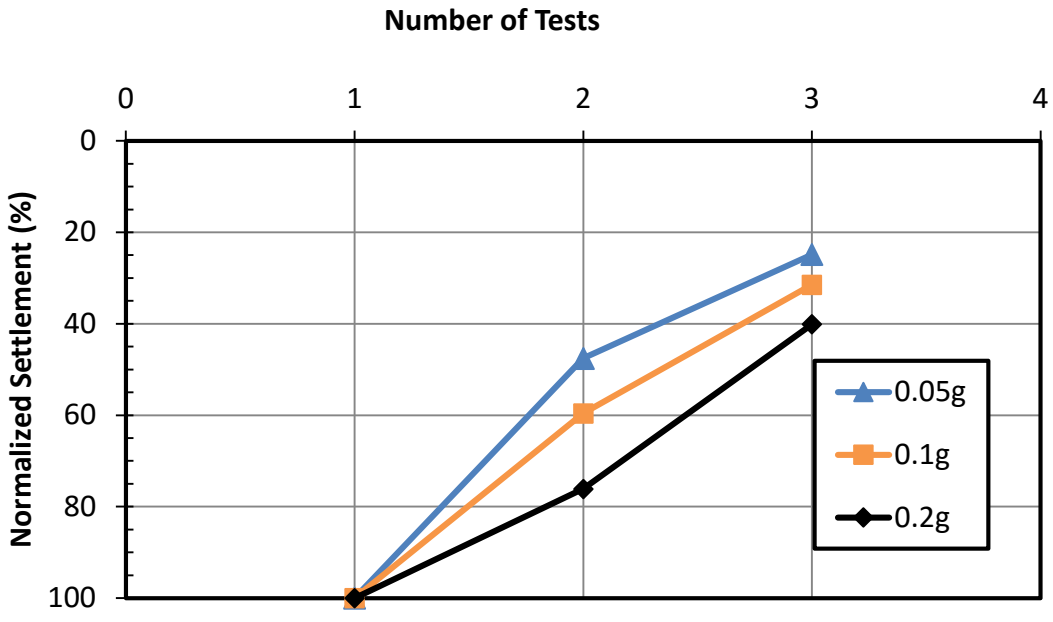

Figure 68 Settlement of Sand with Number of Tests at a Given Acceleration Level After Normalization by Settlement for the First Round

4.5 Comparisons with Other Tests

4.5.1 Laminar Box Tests

Figure 69 provides a comparison of the cumulative settlement as a function of the number of tests for the first set of nine tests with drains spaced at four feet intervals, PVD-1 Test, in comparison with previous studies without drains. All settlement has been scaled to match a soil depth of 16 feet. PVD-1 settlement was scaled up by the ratio from 13 feet to 16 feet, adjusting for the 1.5 feet of dense sand left over from the previous test. The LG1 test involves repeated tests with a peak acceleration of 0.1g with an untreated sand layer 16 feet deep. The IPS1 test result involved testing with induced partial saturation treatment in a 10 foot layer of the total 16 foot thickness, with a dense layer of sand 1.5 feet deep at the bottom that is not considered part of the liquefiable soil profile. Settlement has been scaled up proportionally assuming that the untreated sand was responsible essentially all majority of the settlement. In the IPS1 testing the sand was subjected to 0.1g acceleration for six tests and 0.2g acceleration for two tests. Significantly more settlement was observed for tests where 0.2g accelerations were applied. While the comparisons are not perfect nor completely direct because of differing acceleration levels, using 0.05g, 0.1g, and 0.2g accelerations in PVD-1, it is clear that the cumulative settlement curve for the profile with vertical drains is significantly lower than without. In many cases the settlement is only 50 to 60 percent of the settlement for the untreated sand. Considering that the untreated test curves are generally for 0.1g, while the treated sand experienced three 0.2g cycles, the reduction produced by the drains may be even greater than represented in Figure 69.

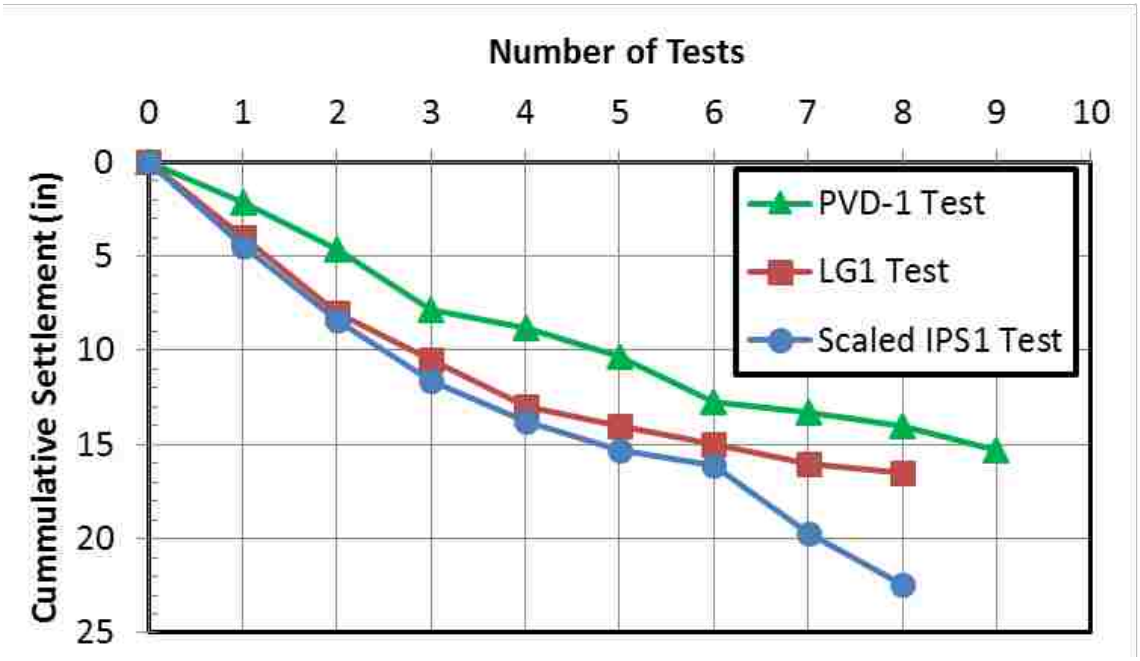

Figure 69 Comparison of Cumulative Settlement from PVD-1 with Other Tests

Figure 70 shows the normalized settlement for PVD-1 by acceleration level compared to the normalized settlement from LG1 and IPS1 testing. The LG1 curve uses the assumption that all settlement from the lower acceleration tests can be attributed to the next 0.1g test, and is normalized based on the 0.1g tests. The IPS1 curve consists of normalizing the six 0.1g tests based on the first 0.1g test.

Figure 70 shows that the drains are more effective in compacting the soil as a result of pore pressure generation, such that settlement after repeated shaking is substantially reduced in comparison to sand without drains. The subsequent tests in PVD-1 had much lower settlement compared to the first test at the same magnitude than subsequent tests performed without drains, such as LG1 and IPS1.

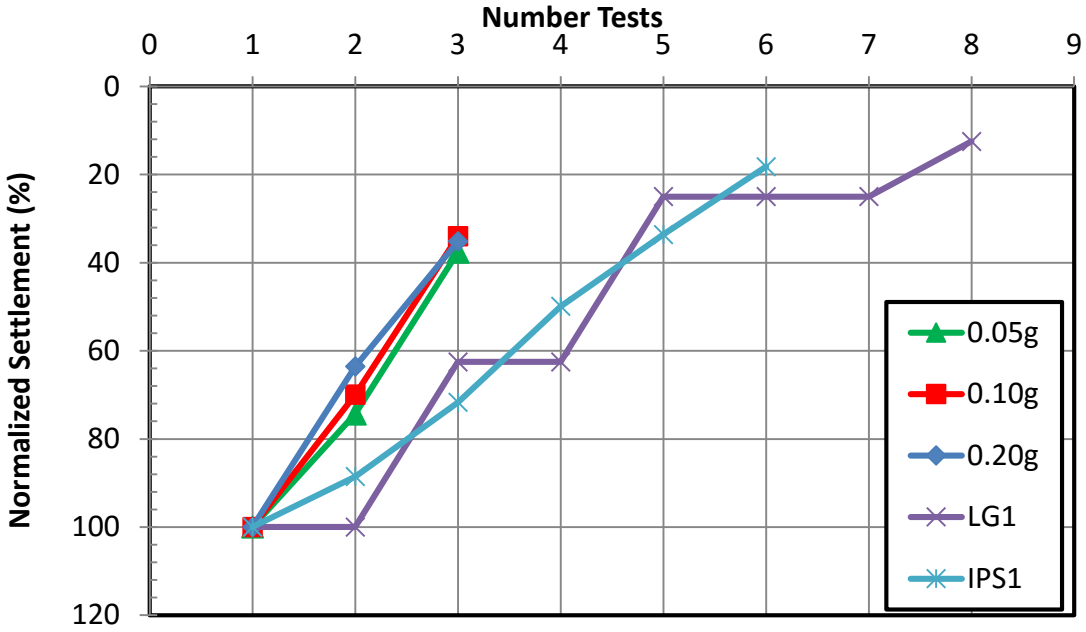

Figure 70 Normalized Settlement Comparisons with Other Tests.

LG0 had acceleration levels and shaking time much longer than in PVD-1, making comparisons with settlement difficult, but LG0 does have records of excess pore pressure dissipation without drains which are useful for comparison. The side-by-side excess pore pressure dissipation for LG0 (left) and PVD-1 (right) is shown in Figure 71. Note that LG0 shows excess pore pressure, while PVD-1 shows excess pore pressure ratios. The scales are such that r_u=1 is equal to o'_{v0}. The excess pore pressure ratios are taken from round 1 at 0.2g to compare with LG0, which had a maximum acceleration of 0.3g. The shaking lasts 35 seconds in LG0, and 7 seconds in PVD-1.

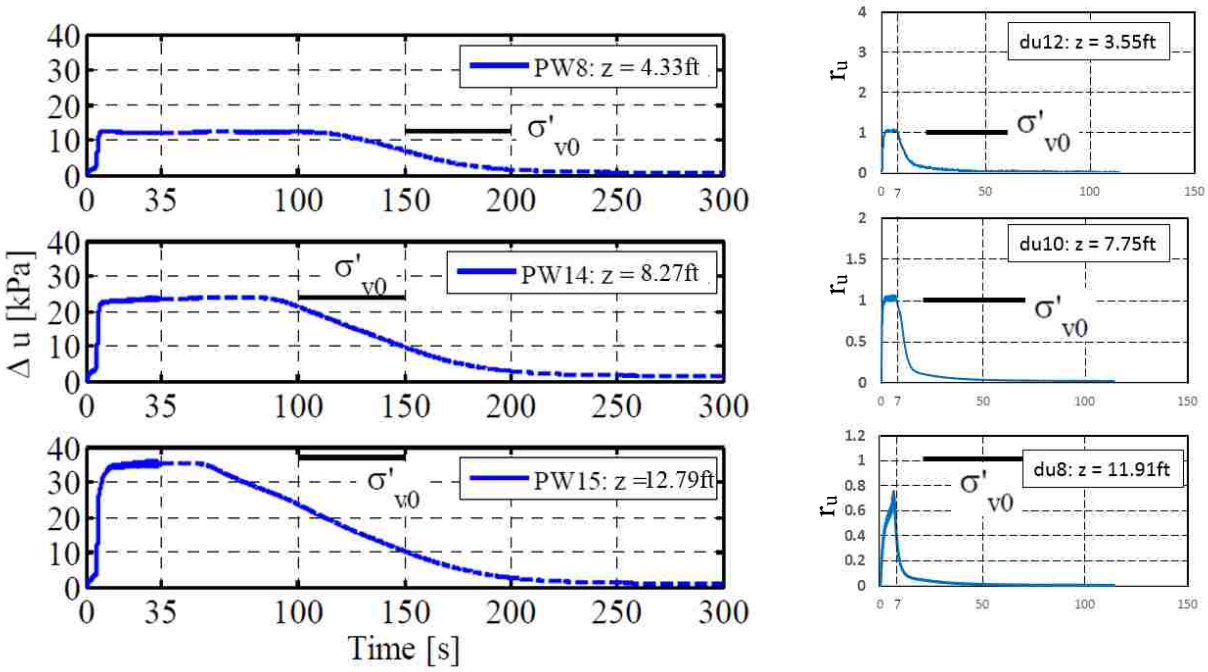

Figure 71 Comparison of Excess Pore Pressures from LG0 (left) and PVD-1 (right).

The pore pressures remain at r_u=1 in LG0 for up to one minute at 4.33 feet, or about 20 seconds at 12.41 feet. The excess pore pressures are not reduced to r_u=0.5 in LG0 until approximately 125 to 160 seconds, depending on depth. In comparison, the excess pore pressure ratios from PVD-1 immediately begin to dissipate, and are completely dissipated within 30 seconds after shaking. At greater depths the excess pore pressure ratio does not even reach r_u=1.0.

Figure 18 shows pore pressure generation during shaking for LG0. After 10 seconds of shaking, with only 5 seconds of shaking at 0.05g, the excess pore pressure ratio had reached r_u=1.0 down to 11.5 feet. In the first test at 0.05g in PVD-1 (see Figure 41), r_u at 11.5 never reached above 0.5, and after 5 seconds of shaking, r_u at 7.5 feet depth was reduced to 0.5 after peaking at 0.9 after a couple cycles of shaking.

4.5.2 Centrifuge Tests

Vertical drains used during centrifuge testing were successful at reducing vertical settlement as much as 50% (see Figure 12). After 8 tests, the reduction in cumulative settlement versus LG1 is 25%. Comparing with the scaled IPS1 test, the reduction in cumulative settlement is 45%, which matches very well the previous centrifuge testing. Individual comparisons are difficult because there is not an exact match with acceleration levels between the tests, but drains do appear to provide decreased settlement in agreement with previous centrifuge testing.

Howell attributes the large variation in PPR for SIN01 to be dilation spikes (2012). The results for r_u versus time from SIN01 in Figure 14 match those of Figure 47 through Figure 49. All four had sinusoidal inputs with drains, and dilation spikes occurred. This confirms the results of the centrifuge testing, as well as the relatively fast reduction of r_u after shaking in the same figures.

As noted in centrifuge testing (Marinucci et al, 2008), drains seem to be more effective at reducing pore pressures deep in the soil profile, rather than at the surface. In Figure 38 through Figure 40, $r_{u,max}$ for each test shows a trend of high $r_{u,max}$ near the surface which drops off at depth.

5 PVD-2

5.1 Layout of Drains and Instrumentation

5.1.1 Vertical Drain Plan

The layout of the prefabricated vertical drains in plan and profile view is shown in Figure 72 and the positions are detailed in Table 12 with coordinates relative to the center of the box. The drains are 3 inch diameter corrugated plastic pipes with an outside diameter of approximately 3.7 inches which are surrounded by a filter fabric sock to prevent infiltration of the sand. The fabric sock was sealed closed at the bottom. These drains are identical to those used for PVD-1 tests.

Prior to sand placement, the drains were hung from a framework above the top of the box and tied to the bottom PVC grid with wire to prevent uplift in the event of liquefaction. After the sand fill was placed, the drains were cut off about 2 to 3 inches above the ground surface. After movement of the drains occurred in PVD-1, 2” PVC pipe was placed inside the vertical drains during installation and were tied at the top to the framework to reduce movement while filling. This was in response to the filling of PVD-1, in which the upper portions of some of the drains were moved from their original locations during filling. This did not occur during PVD-2 because of the PVC pipes.

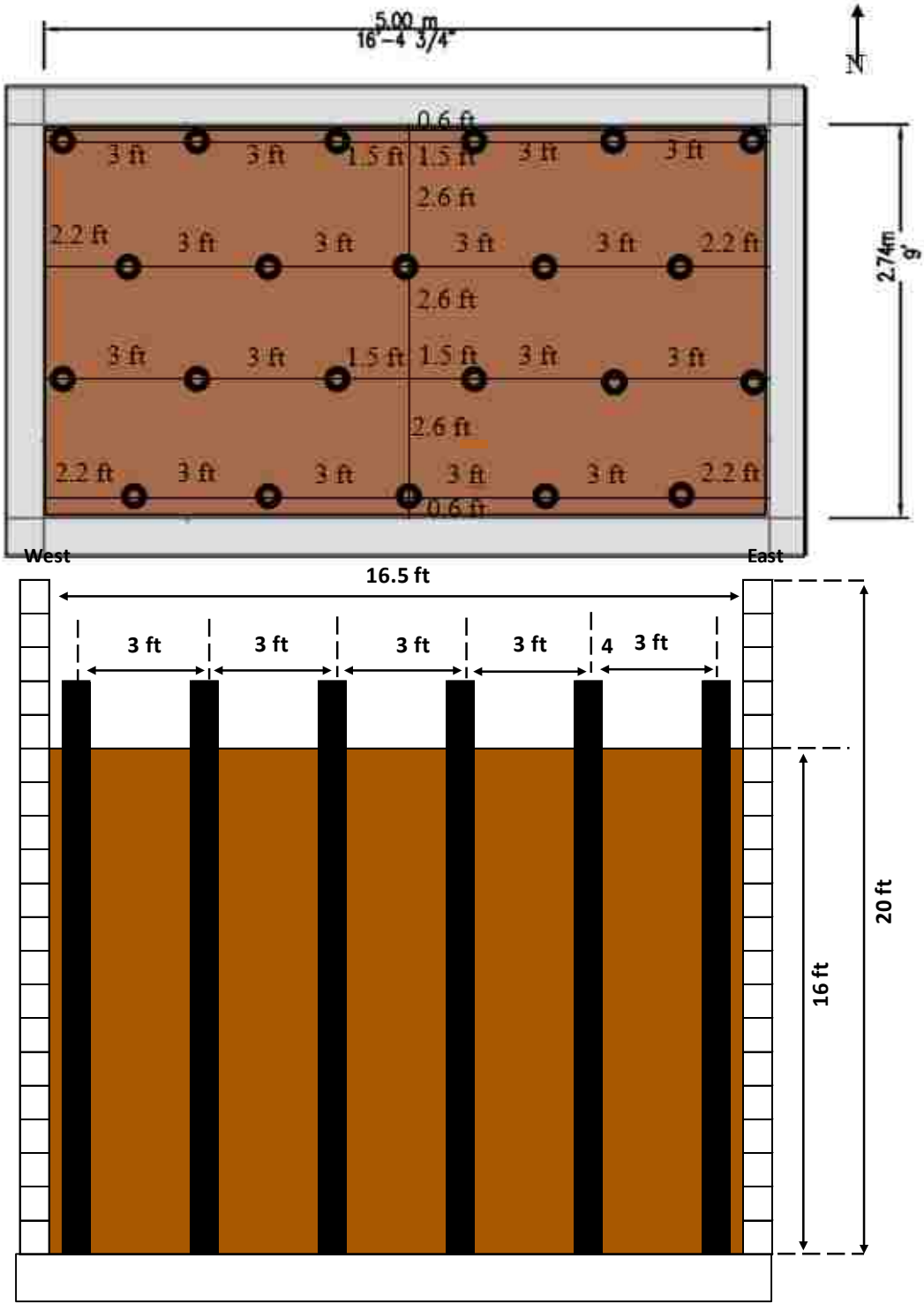

Figure 72 Plan and Elevation Views of the Laminar Shear Box with Prefabricated Vertical Drains

Table 12 Location of Prefabricated Vertical Drains (PVDs) for PVD-2

Drain	x (in)	y (in)	Drain	x (in)	y (in)
1	-90	47	12	-72	-16
2	-54	47	13	-36	-16
3	-18	47	14	0	-16
4	18	47	15	36	-16
5	54	47	16	72	-16
6	90	47	17	-90	-47
7	-72	16	18	-54	-47
8	-36	16	19	-18	-47
9	0	16	20	18	-47
10	36	16	21	54	-47
11	72	16	22	90	-47

5.1.2 Instrumentation Plan

Table 3Table 3 shows a summary of the number of each type of instrumentation used in PVD-2, which is consistent with PVD-1. Figure 73 and Figure 74 show plan and profile views, respectively, of the locations of the various sensors. Table 4 summarizes the position of accelerometers, LVDTs, and string potentiometers, which is the same as PVD-1. These locations are the same as for previous IPS1 testing to facilitate subsequent comparison. Coordinates (x,y,z = 0,0,0) denote the center of the box at the top of ring 40 (x = positive in the East direction, y = positive in the North direction ,and z = positive downward from the top of ring (laminate) 40). The top of laminate 40 is at an elevation of 6.10 m or 20 ft.

Three vertical arrays of pore pressure transducers are located along Mesh 1, Mesh 2, and Mesh 3 as shown in Figure 74 to define the generation and dissipation of pore pressure versus depth. Note that these arrays are located at different locations from PVD-1 to fit the different spacing arrangement in the laminar box. Mesh 1 and Mesh 3 were located halfway between two

drains, 1.5 feet away, while Mesh 2 was located between three drains, 1.5 feet away from each drain. In addition, one pore pressure transducer is located at a depth of 7.5 ft within the center drain to monitor the pressure within the drain itself. Pore pressure transducer locations are summarized in Table 13. The locations of three surface settlement plates named ZP1, ZP2, and ZP3 are also found in Figure 73. The plates are connected to string potentiometers fastened to a frame located above the box. SL5', SL10' and SL15' mark the location of the three slotted pipes for measuring permeability. For SL5' slots are located in the first 5 feet, for SL10' slots are located from 5 to 10 feet, and for SL15' slots are located from 10 to 15 feet deep.

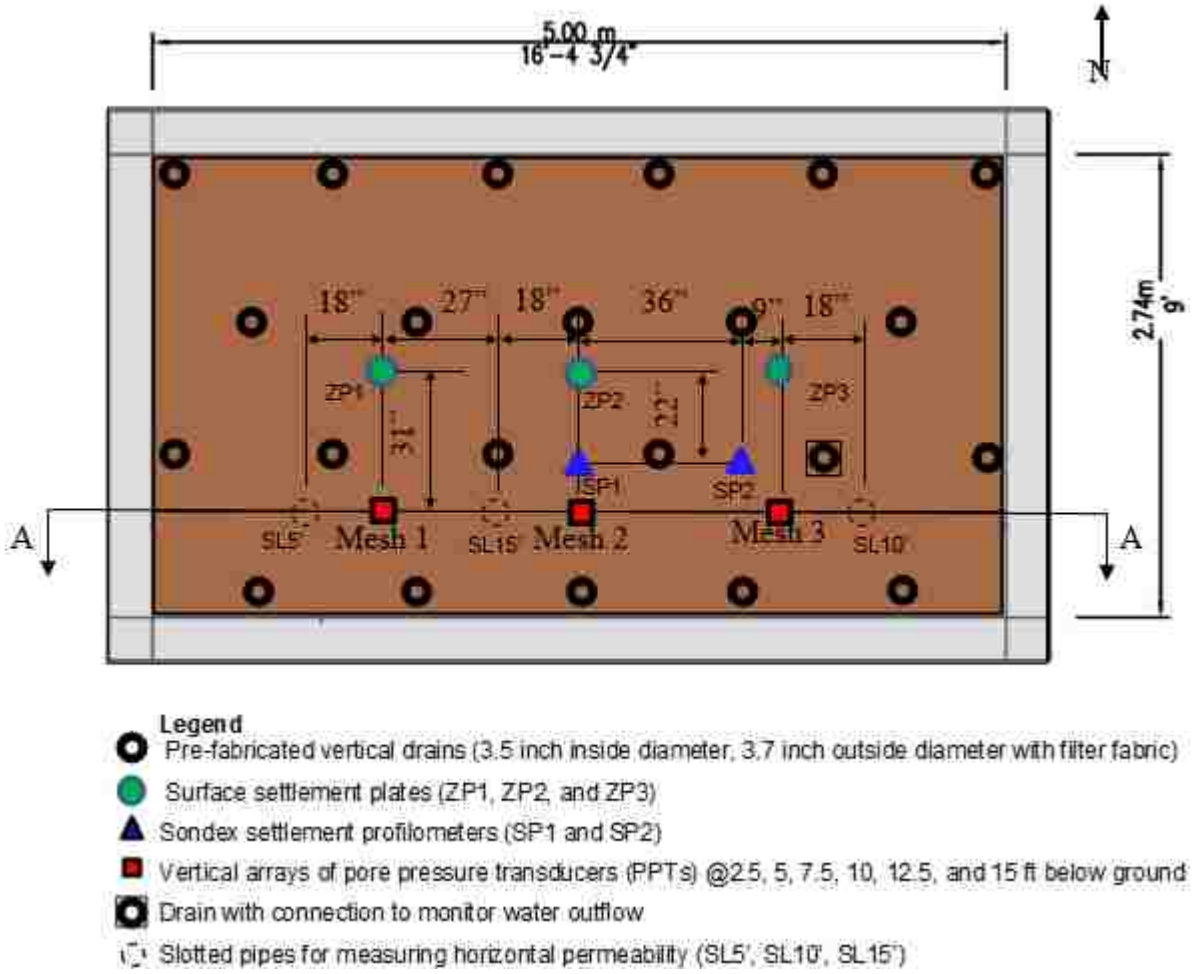

Figure 73 Plan View of Sensors for PVD-2

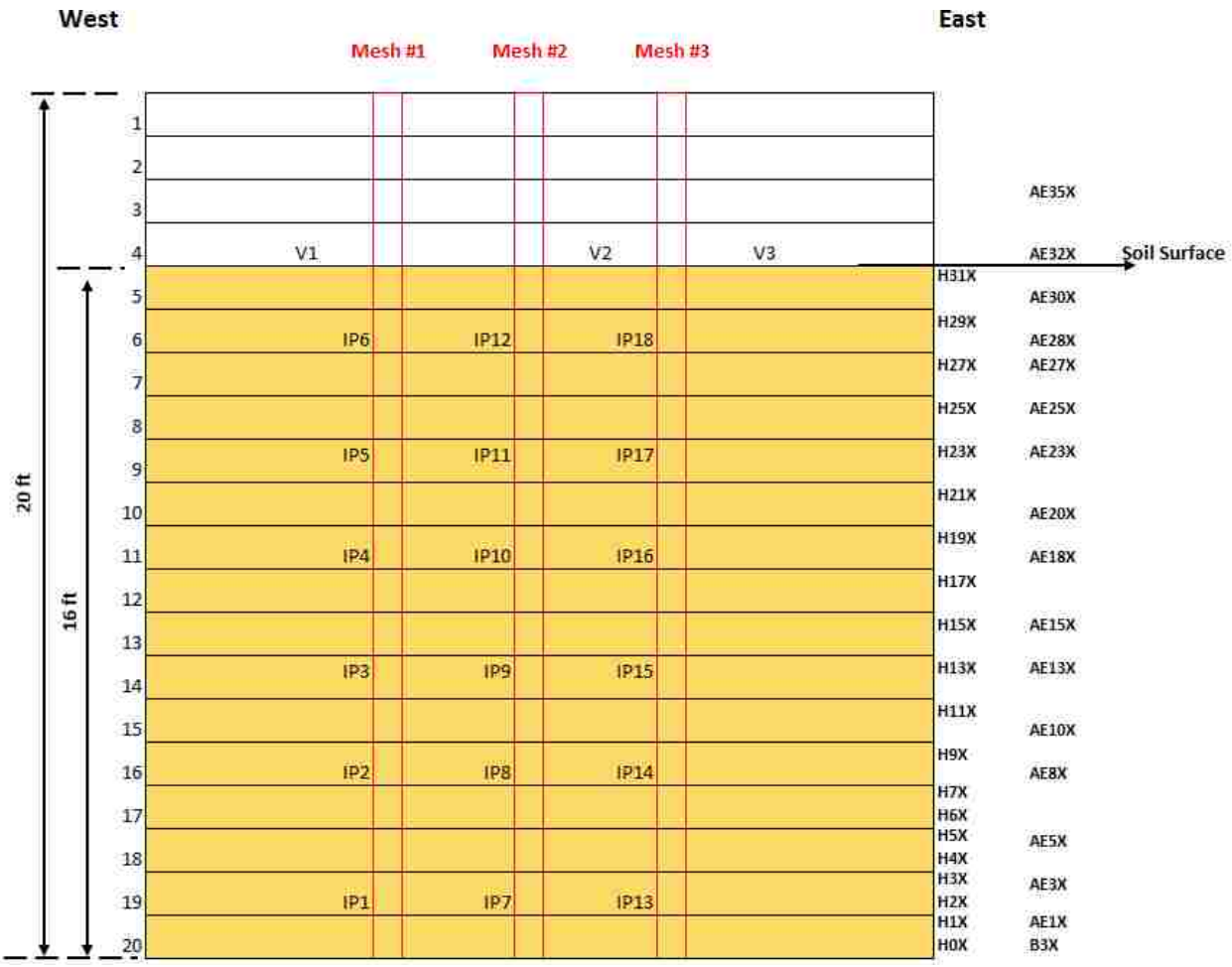

Figure 74 Profile View of Sensors Installed for PVD-2

Table 13 Location of Pore Pressure Transducers (PPTs) for PVD-2

Peizometer	Mesh	x (ft)	y (ft)	z (ft)	Depth to base (ft)	Depth from surface (ft)
PPT1	1	-3.75	-2.59	18.5	1.5	14.5
PPT2	1	-3.75	-2.59	16	4	12
PPT3	1	-3.75	-2.59	13.5	6.5	9.5
PPT4	1	-3.75	-2.59	11.25	8.75	7.25
PPT5	1	-3.75	-2.59	8.75	11.25	4.75
PPT6	1	-3.75	-2.59	6.5	13.5	2.5
PPT7	2	0	-2.59	19	1	15
PPT8	2	0	-2.59	16.5	3.5	12.5
PPT9	2	0	-2.59	14	6	10
PPT10	2	0	-2.59	11.5	8.5	7.5
PPT11	2	0	-2.59	9.25	10.75	5.25
PPT12	2	0	-2.59	6.75	13.25	2.75
PPT13	3	3.75	-2.59	19.5	0.5	15.5
PPT14	3	3.75	-2.59	17	3	13
PPT15	3	3.75	-2.59	14.5	5.5	10.5
PPT16	3	3.75	-2.59	12	8	8
PPT17	3	3.75	-2.59	9.75	10.25	5.75
PPT18	3	3.75	-2.59	7	13	3
PPT19	Drain	-1.5	-1.33	11.5	8.5	7.5

Depth = Measured vertical distance from top of soil surface (downward positive)

Z = Distance from top of ring/laminate 40 (downward positive)

X = Measured horizontal distance from center of soil box (East Positive)

Y = Measured horizontal distance from center of soil box (North Positive)

5.2 Characterization of Sand

The sand used in this test is the same as in PVD-1. For a detailed description of the sand, see section 0. In summary, the sand used is Ottawa F55 sand, with a grain size distribution curve shown in Figure 32. The sand was deposited by pluviation. The density was monitored using density buckets and with CPTs taken before and after each test. See Figure 75 for a plot of the relative density based on soil buckets during filling. The cone tip resistance, q_c, versus depth and sleeve friction profiles for all four soundings are provided in Figure 77. Some of the later soundings have discontinuities with much lower cone tip resistance. This may be due to stopping the cone to do shear wave velocity tests before continuing the sounding. Based on the CPT resistance the sand was initially in a loose condition but the shaking process progressively increased the cone resistance and relative density state of the sand. The results of the CPT are similar to those in PVD-1, with minor differences at a depth of 10 feet for the 2nd and 3rd soundings. All sand to the bottom of the box was removed after PVD-1 so that no dense layer of sand was left in the box. This means that no scaling of settlement was required for PVD-2.

Figure 76 shows a schematic of the layout of the slotted pipes used to perform horizontal borehole permeability tests. For each 5 foot segment, the water flow was increased until the head remained constant for steady-state conditions. The steady state parameters were then used to compute the horizontal permeability using borehole permeability test procedures developed by the US Bureau of Reclamation. The hydraulic conductivity was recorded before and after each test, and the results are summarized in Table 14.

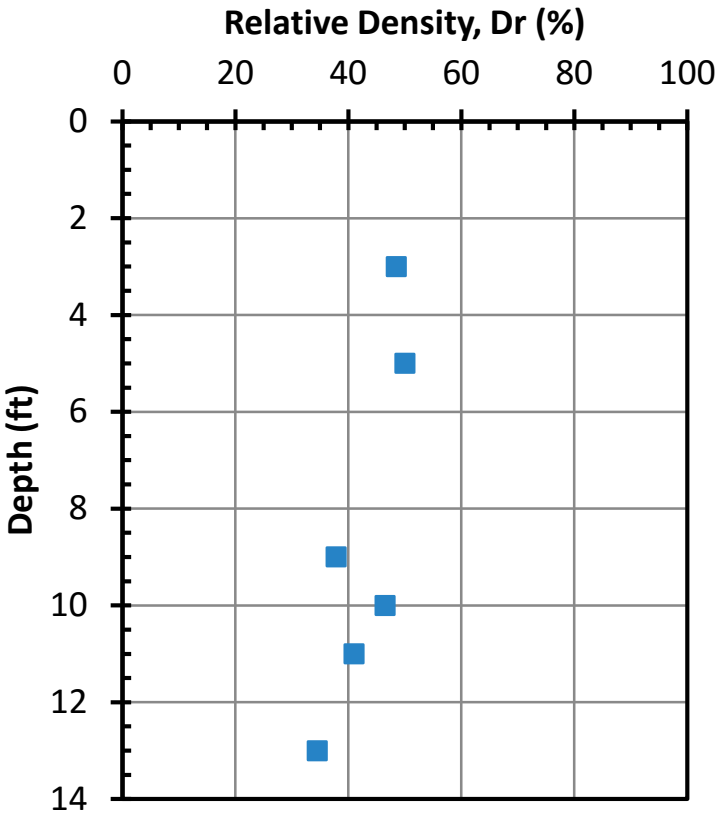

Figure 75 Density Measurements Taken During Filling

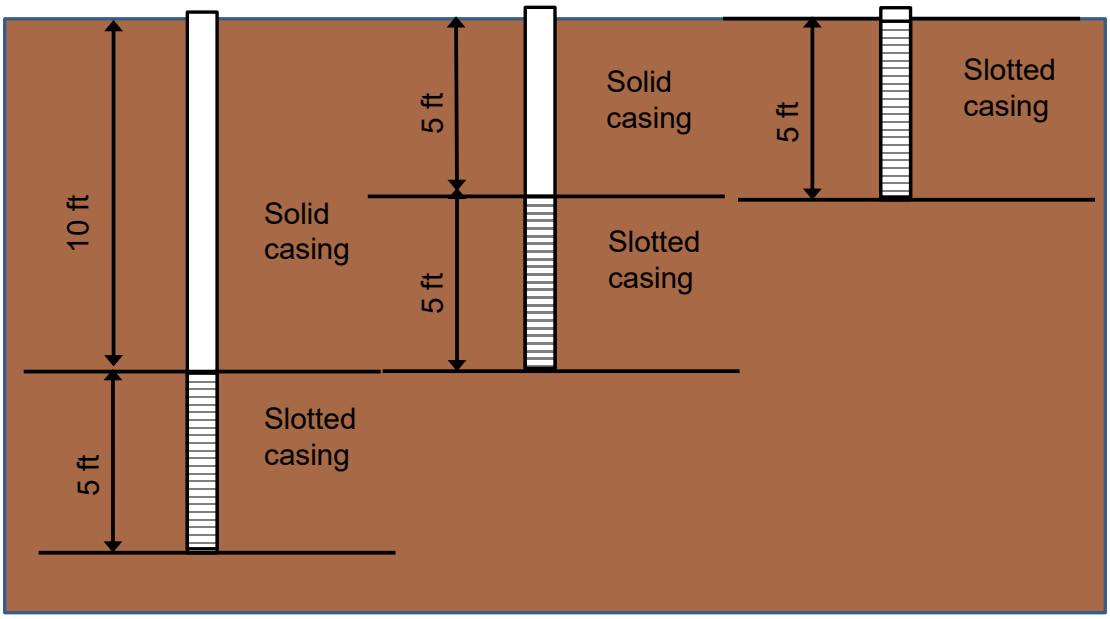

Figure 76 Schematic Drawing Showing Layout of Slotted Casing Used to Measure Hydraulic Conductivity of Sand

Table 14 Hydraulic Conductivity Measurements During PVD-2

	Horizontal Hydraulic Conductivity (cm/sec)			
Depth Interval (ft)	Round 1	Round 2	Round 3	Average
0-5	0.064	0.043	0.036	0.0477
5-10	0.045	0.032	0.029	0.0353
10-15	0.039	0.032	0.028	0.0330
Average	0.049	0.036	0.031	0.0387

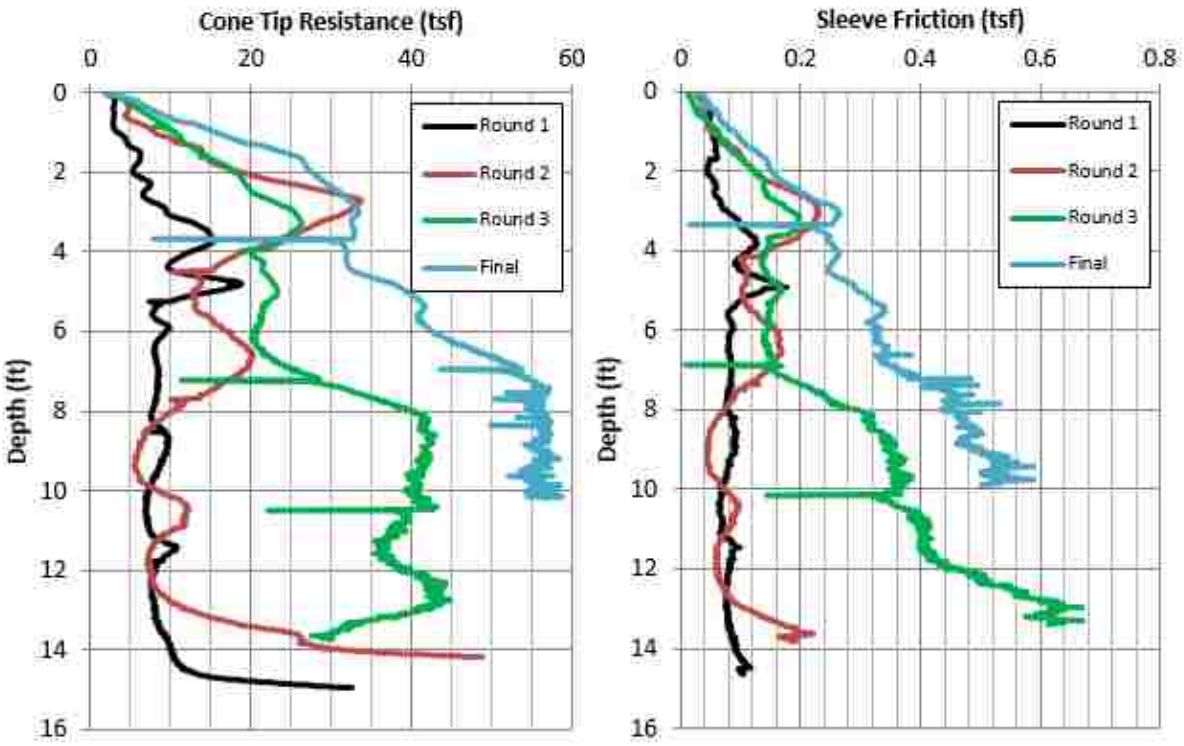

Figure 77 CPT Cone Tip Resistance Values Throughout PVD-2

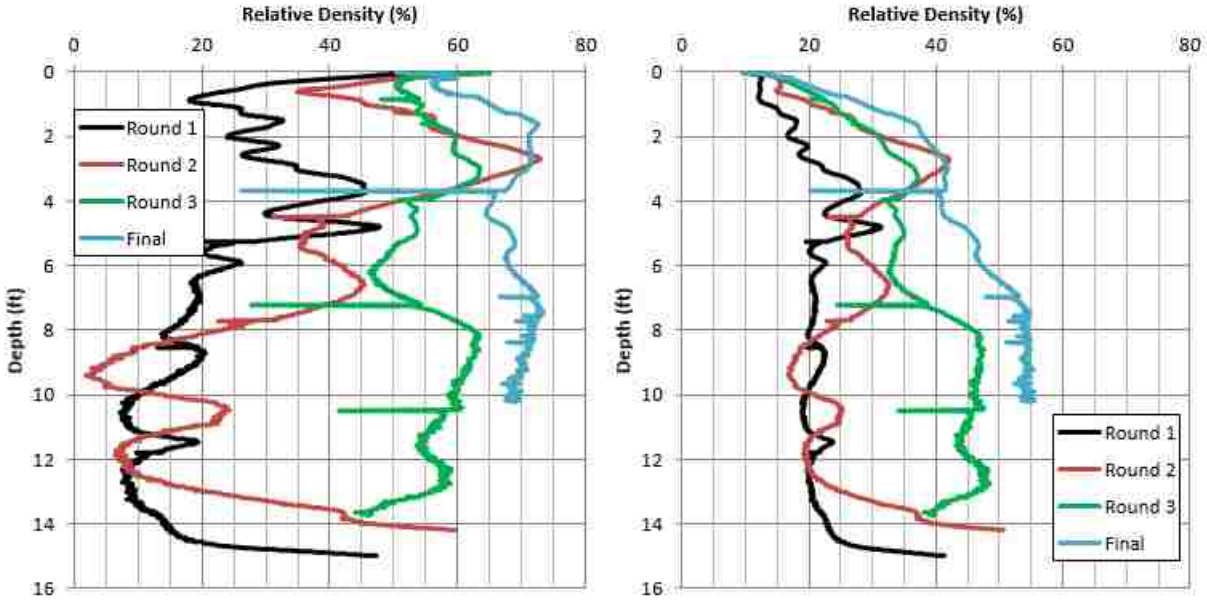

Figure 78 Relative Density from CPT Correlation, Jamiolkowsky, et al. (1985), Left, and Kulhawy and Mayne (1990), Right.

5.3 Test Pattern

Nine shaking tests were performed on the laminar shear box with 3 ft. drain spacing. Tests were performed in sets of three with peak accelerations of 0.05g, 0.10g, and 0.20g for each set. A peak acceleration of 0.20g was the highest acceleration permitted by the NEES@UB lab manager. A CPT sounding was performed prior to each set of three tests to provide an indication of the density state for the next set of tests. However, each test was performed independently and pore pressures were allowed to fully dissipate before the subsequent test was performed.

Figure 79 provides plots of the planned input base motions. All motions were intended to consist of 15 cycles of sinusoidal motions with a frequency of 2 Hz. Typically 15 cycles of motion are associated with a Magnitude 7.5 earthquake, which is often used as the base earthquake for liquefaction studies. A ramp-up and ramp-down period was used to be consistent with previous

testing at the site. Actual motions applied and measured at the base differed slightly from the planned motions and will be presented with the results. The test pattern is the same as in PVD-1.

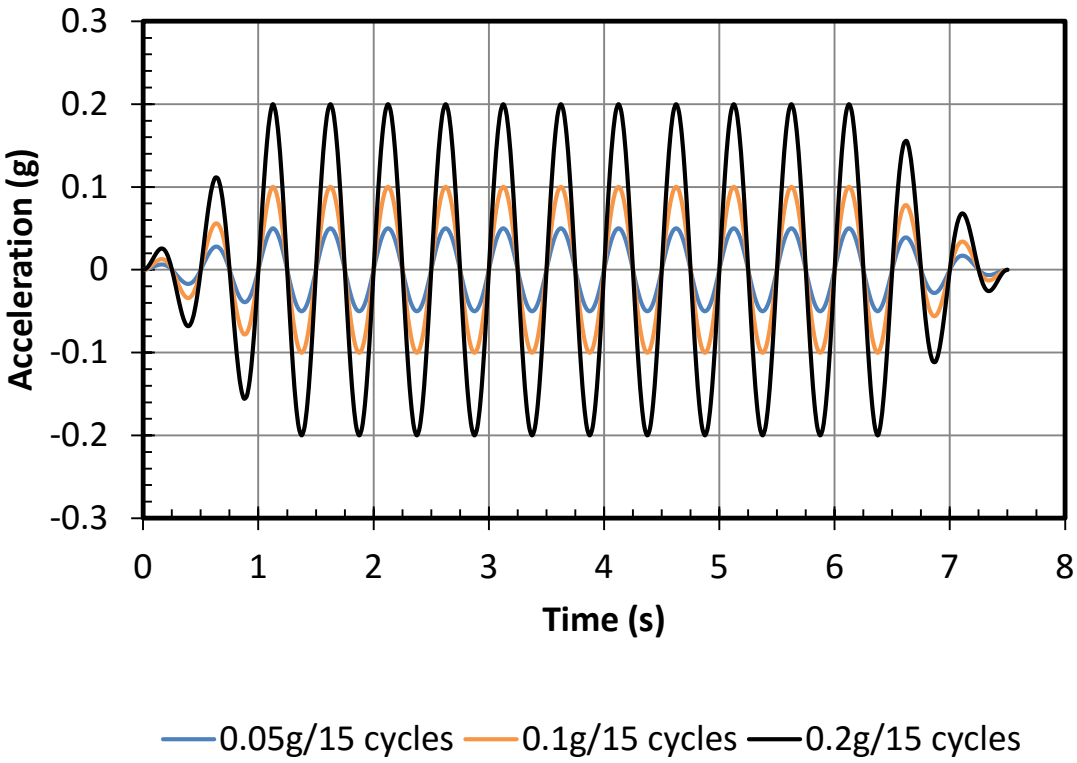

Figure 79 Input Motions for Each Set of Three Tests

5.4 Test Results and Discussion

5.4.1 Peak Excess Pore Pressure Versus Depth

Excess pore pressure ratio profiles were provided by three vertical arrays of pore pressure transducers located at approximately 2.5 to 3 ft. depth intervals, as described in section 5.1.2. The locations of the arrays were in different positions than in PVD-1 to fit the different configuration of drains in PVD-2. The excess pore pressure ratio at a given depth was computed by taking the maximum excess pore pressure ratio during the entire test at a given depth and dividing by the

initial vertical effective stress at that depth. Liquefaction is defined as the condition when the excess pore pressure ratio (r_u) becomes equal to 1.0, meaning that the excess pore pressure is equal to the vertical effective stress. In most cases, the peak pore pressure ratio occurred during shaking; however, in some cases this occurred after the shaking when upward flow of water produced higher excess pore pressures. In the figures below, the peak pore pressure ratio is an average of the three sensor meshes for each test. No pattern of behavior between the three sensor meshes suggests that there is a significant difference in the readings between meshes despite small variations in the distances from the pore pressure transducers and the adjacent drains. Peak excess pore pressures for each round of testing are shown in Figure 80 through Figure 82.

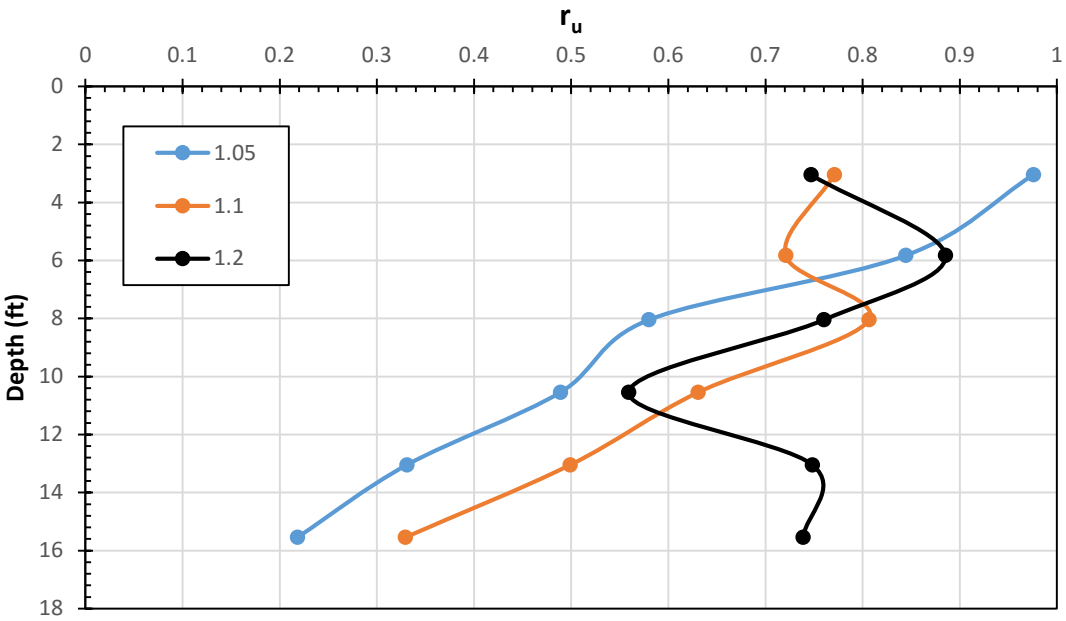

Figure 80 Profiles of Peak Excess Pore Pressure ($r_{u,max}$) Versus Depth (ft.) for Three Shaking Tests at 0.05g, 0.10g, and 0.20g During Round 1.

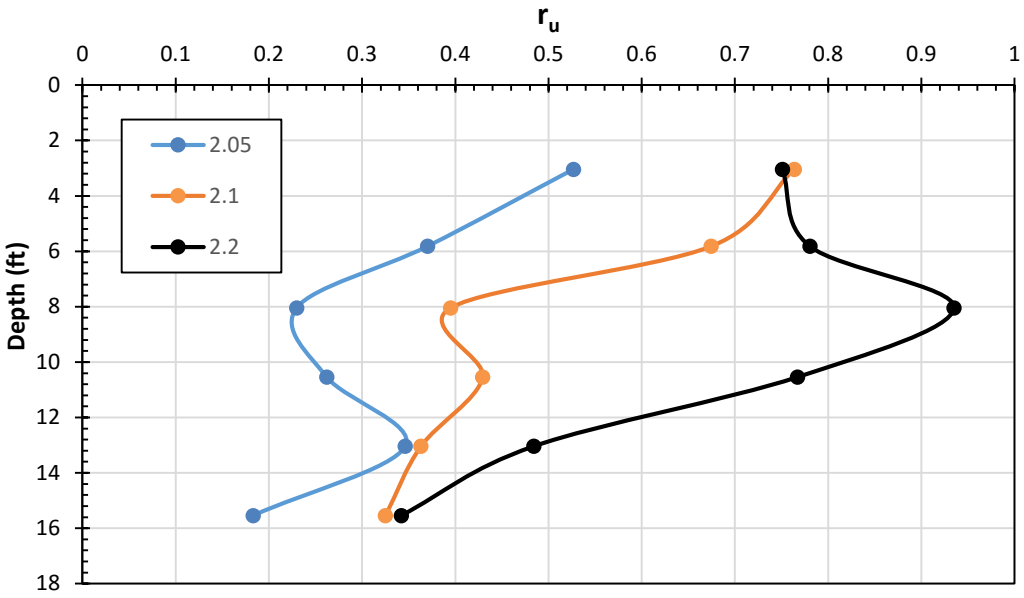

Figure 81 Profiles of Peak Excess Pore Pressure ($r_{u,max}$) Versus Depth (ft.) for Three Shaking Tests at 0.05g, 0.10g, and 0.20g During Round 2.

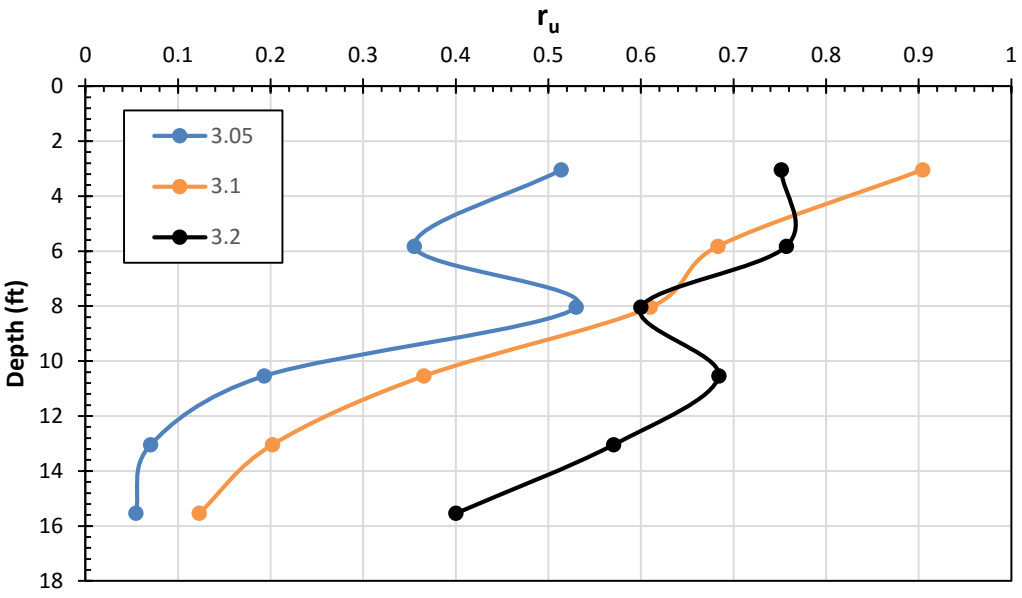

Figure 82 Profiles of Peak Excess Pore Pressure ($r_{u,max}$) Versus Depth (ft.) for Three Shaking Tests at 0.05g, 0.10g, and 0.20g During Round 3

Peak excess pore pressure ratio throughout the profile can be used to determine whether a section of the profile was liquefied (r_u=1), or if it reached above 0.5, which has been used as an indicator for settlement, as shown in Howell et. al. (2012). These plots are useful to quickly understand the effect of the shaking motions on the soil. More in depth discussion of excess pore pressures as they relate to settlement will be provided in subsequent sections.

Peak excess pore pressure ratios generally remain below 0.5 at a depth of 12 feet except for the first round with an acceleration level of 0.2g. The $r_{u,max}$ increases with increased acceleration, especially at depth, and $r_{u,max}$ also decreases with depth. Subsequent rounds of testing have lower excess pore pressures, especially at depths below 8 feet. The increasing density due to settlement from each round appears to reduce excess pore pressure ratios.

5.4.2 Excess Pore Pressure Versus Time Paired with Acceleration Versus Time

Pore pressures and accelerations were measured at multiple depths in the profile. To understand the forces the soil was under during the tests, excess pore pressure ratio and acceleration at depth are included in Figure 83 through Figure 91. Acceleration versus time plots are located on the left, with the horizontal axis located at the depth of the accelerometer. The accelerometers used, in order from top to bottom, are: AE27X, AE23X, AE18X, AE13X, AE8X, and AE2X. R_u versus time plots are located on the right with the horizontal axis also located at the depth of the pore pressure transducer. The pore pressure transducers used, in order from top to bottom, are: PPT12, PPT 11, PPT 16, PPT 9, PPT 8, and PPT 7.

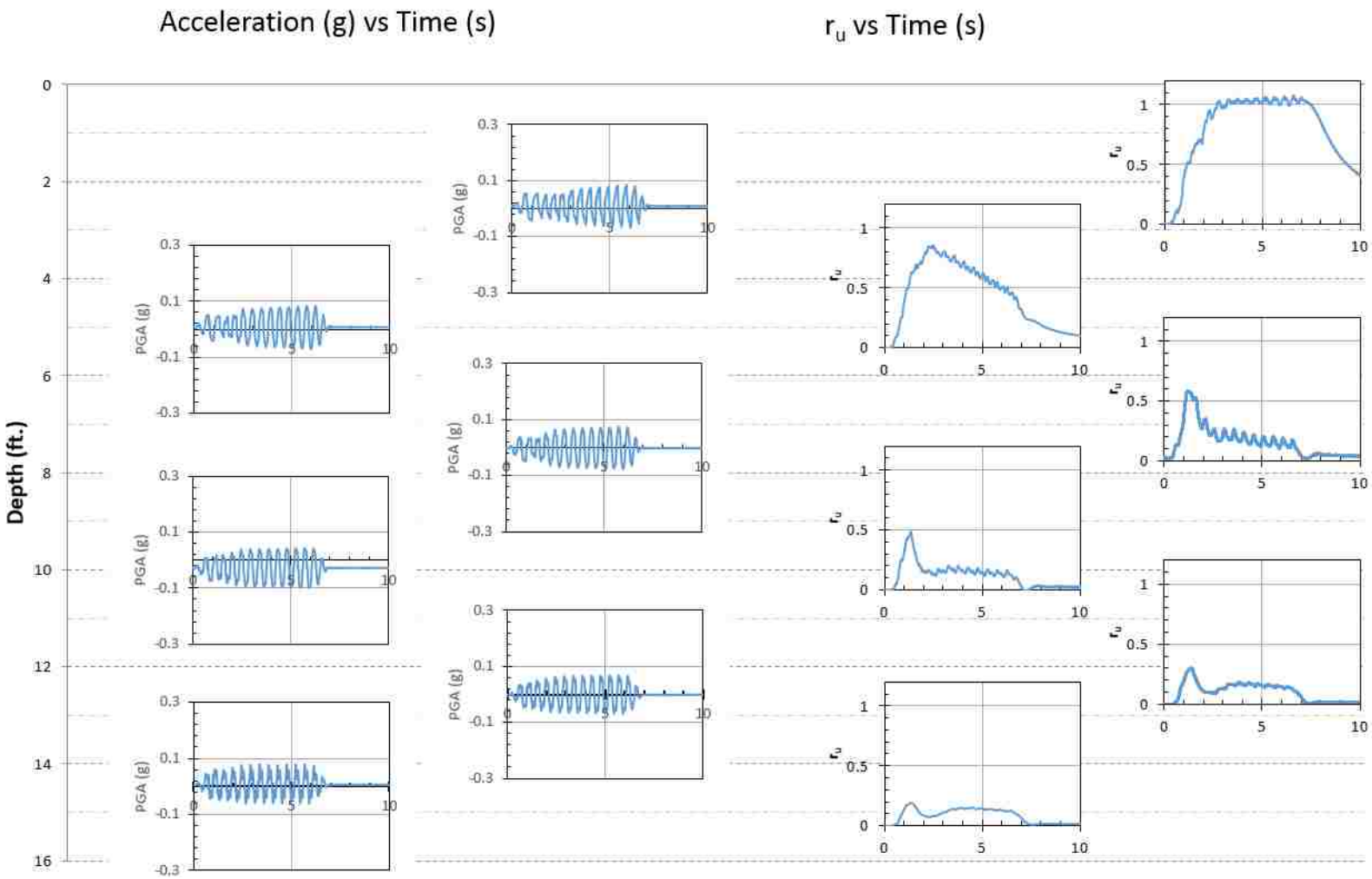

Figure 83 Acceleration Versus Time Paired with Excess Pore Pressure Ratio Versus Time for Round 1, a_{max} = 0.05g

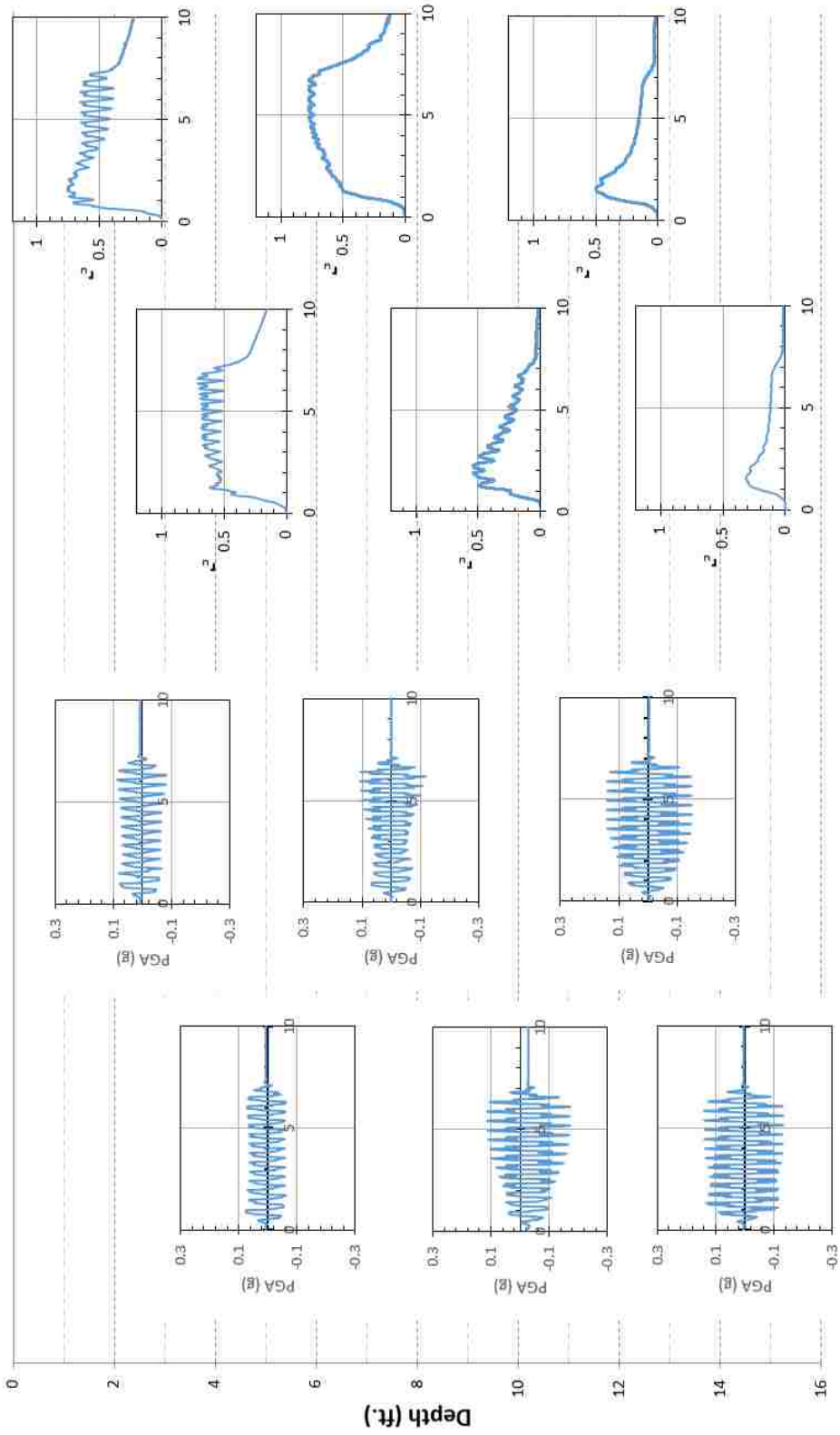

Figure 84 Acceleration Versus Time Paired with Excess Pore Pressure Ratio Versus Time for Round 1, a_{max} = 0.1g

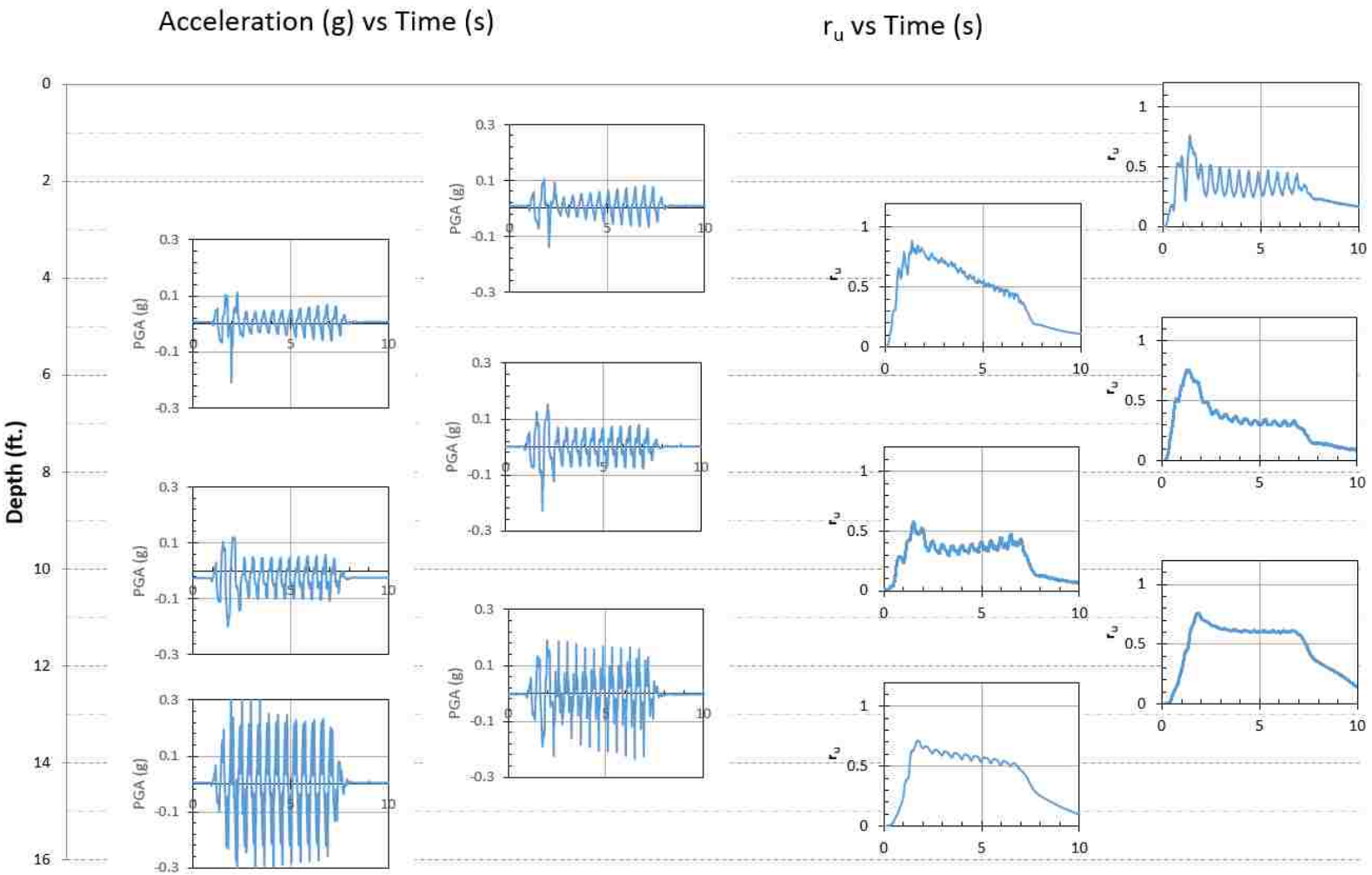

Figure 85 Acceleration Versus Time Paired with Excess Pore Pressure Ratio Versus Time for Round 1, a_{max} = 0.2g

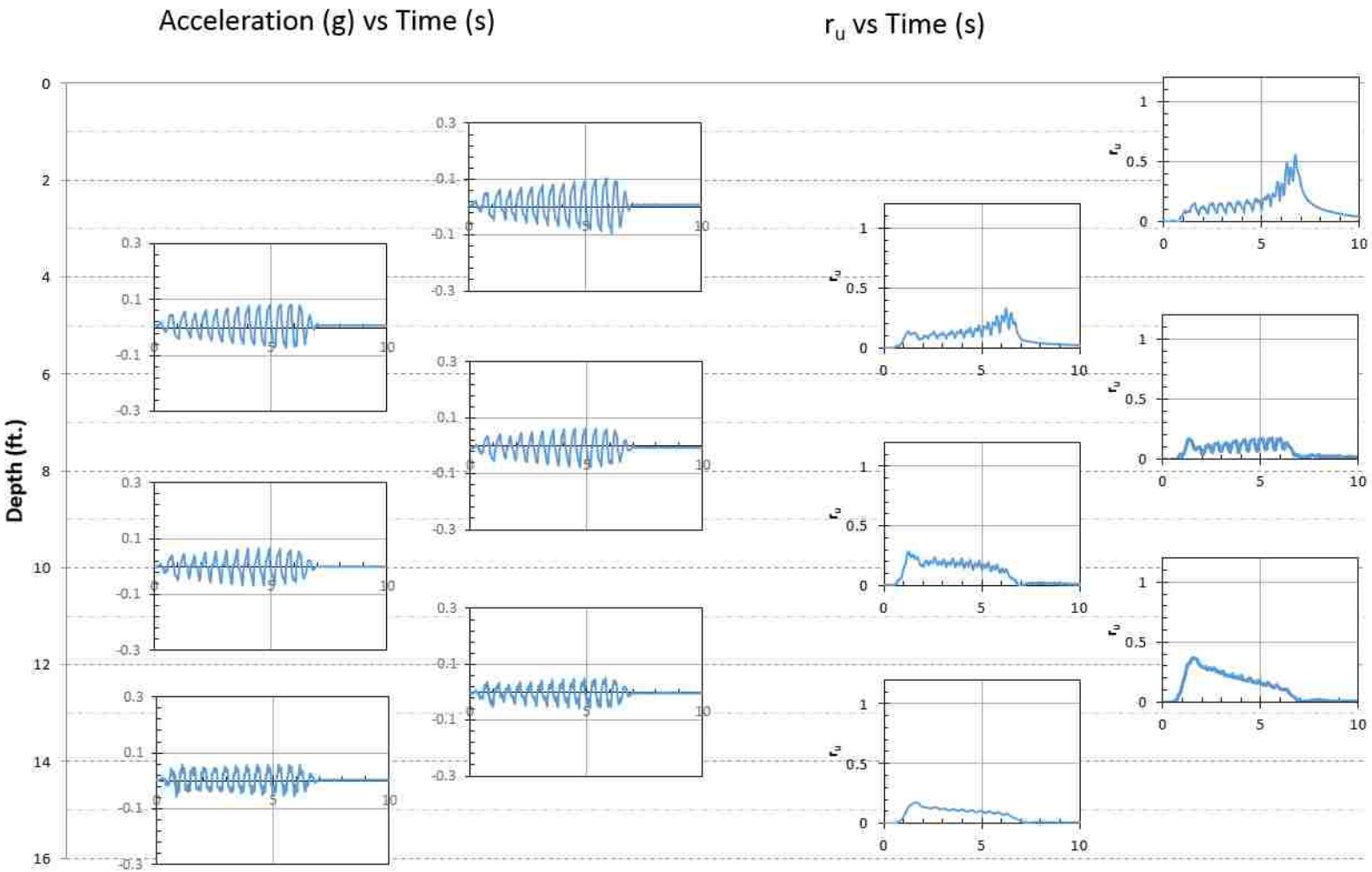

Figure 86 Acceleration Versus Time Paired with Excess Pore Pressure Ratio Versus Time for Round 2, a_{max} = 0.05g

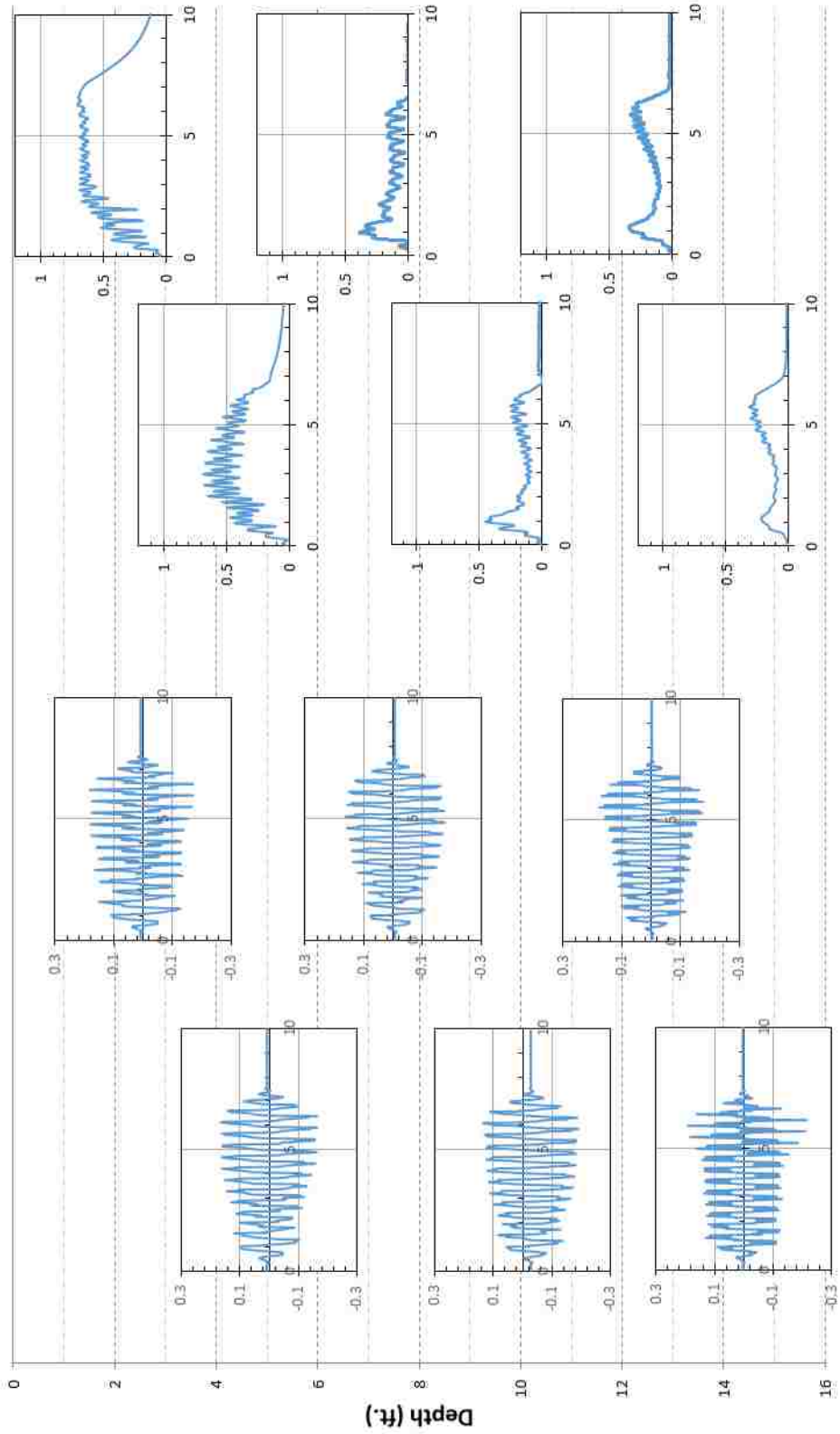

Figure 87 Acceleration Versus Time Paired with Excess Pore Pressure Ratio Versus Time for Round 2, a_{max} = 0.1g

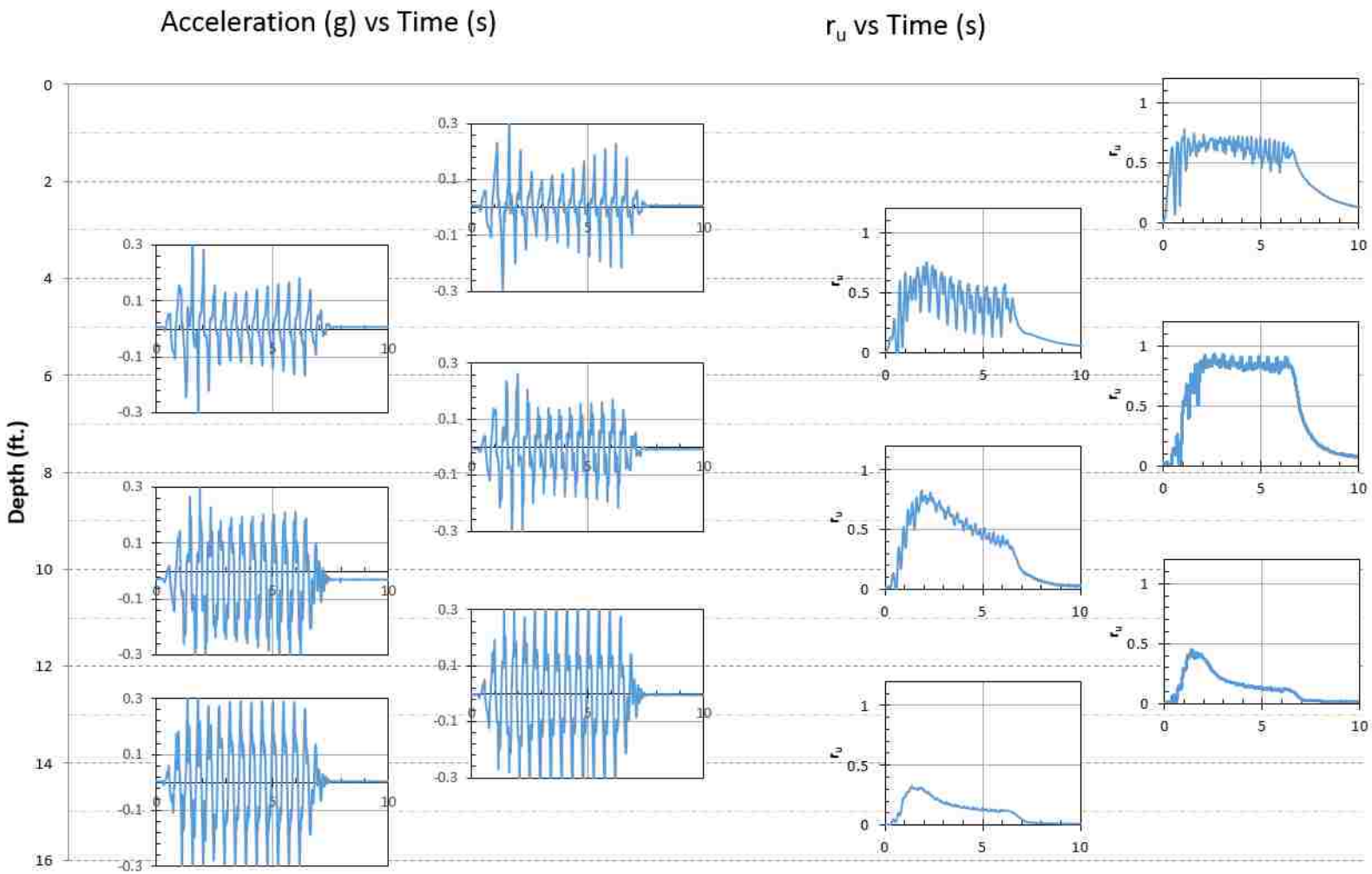

Figure 88 Acceleration Versus Time Paired with Excess Pore Pressure Ratio Versus Time for Round 2, a_{max} = 0.2g

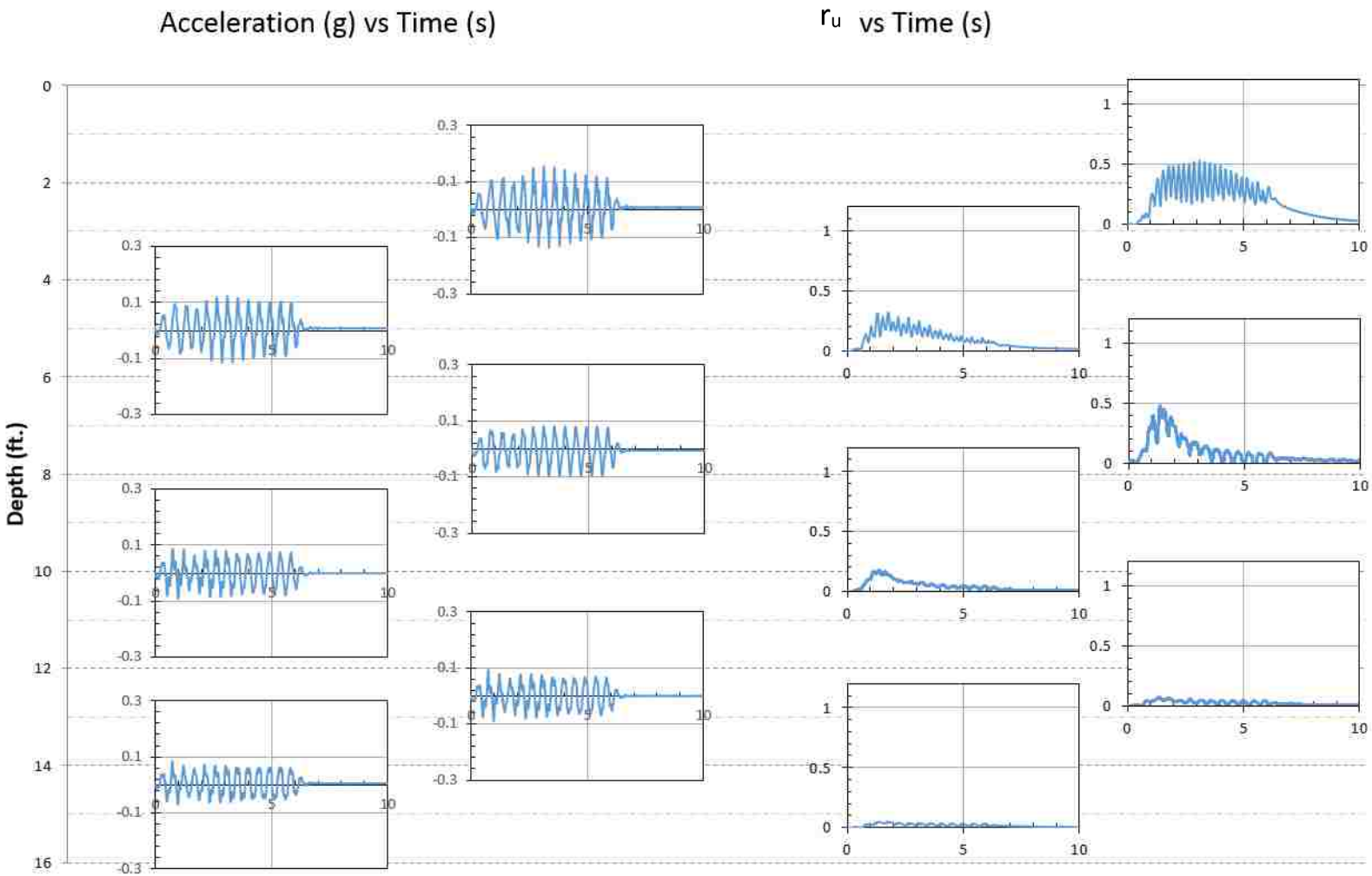

Figure 89 Acceleration Versus Time Paired with Excess Pore Pressure Ratio Versus Time for Round 3, a_{max} = 0.05g

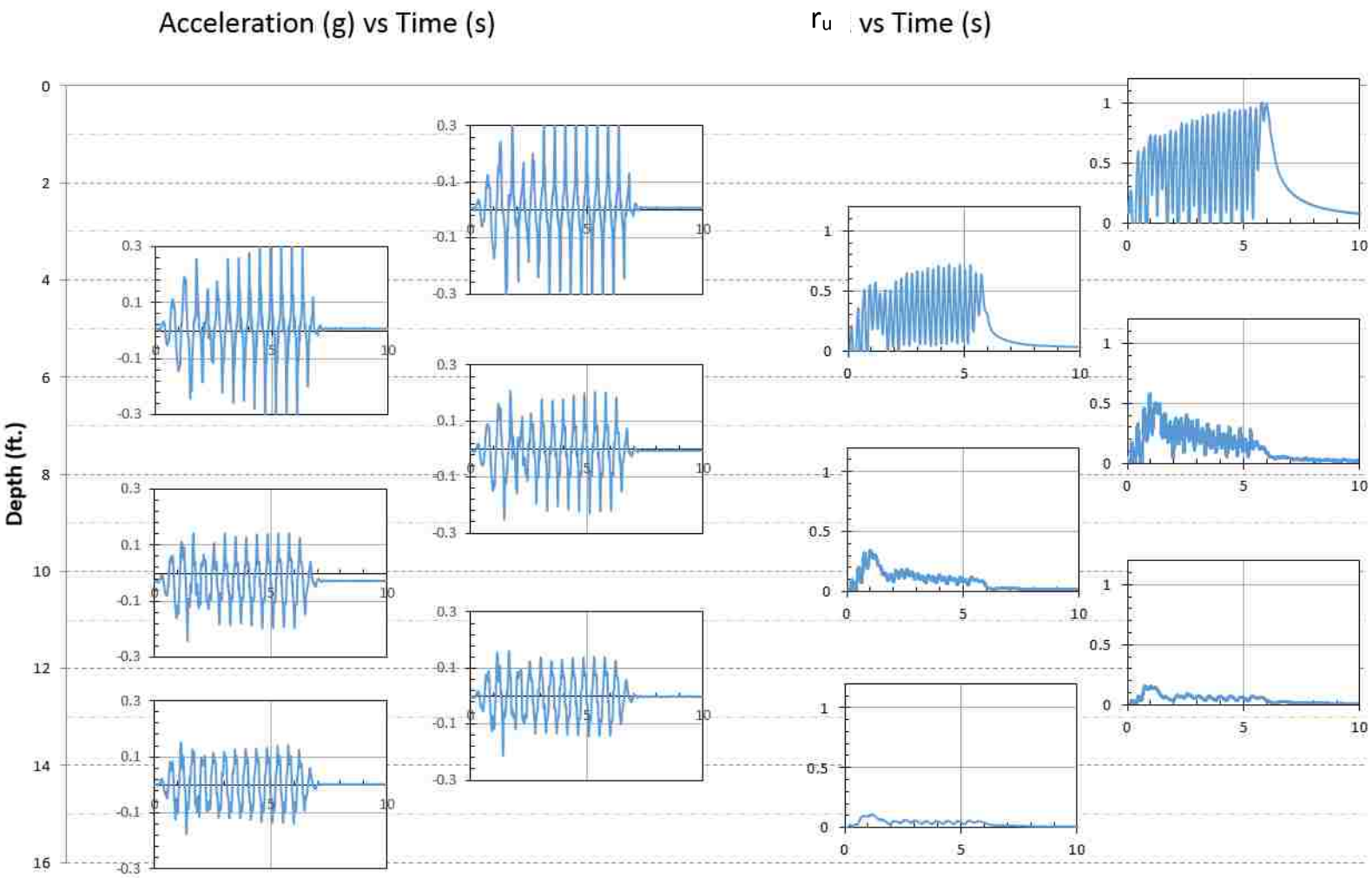

Figure 90 Acceleration Versus Time Paired with Excess Pore Pressure Ratio Versus Time for Round 3, a_{max} = 0.1g

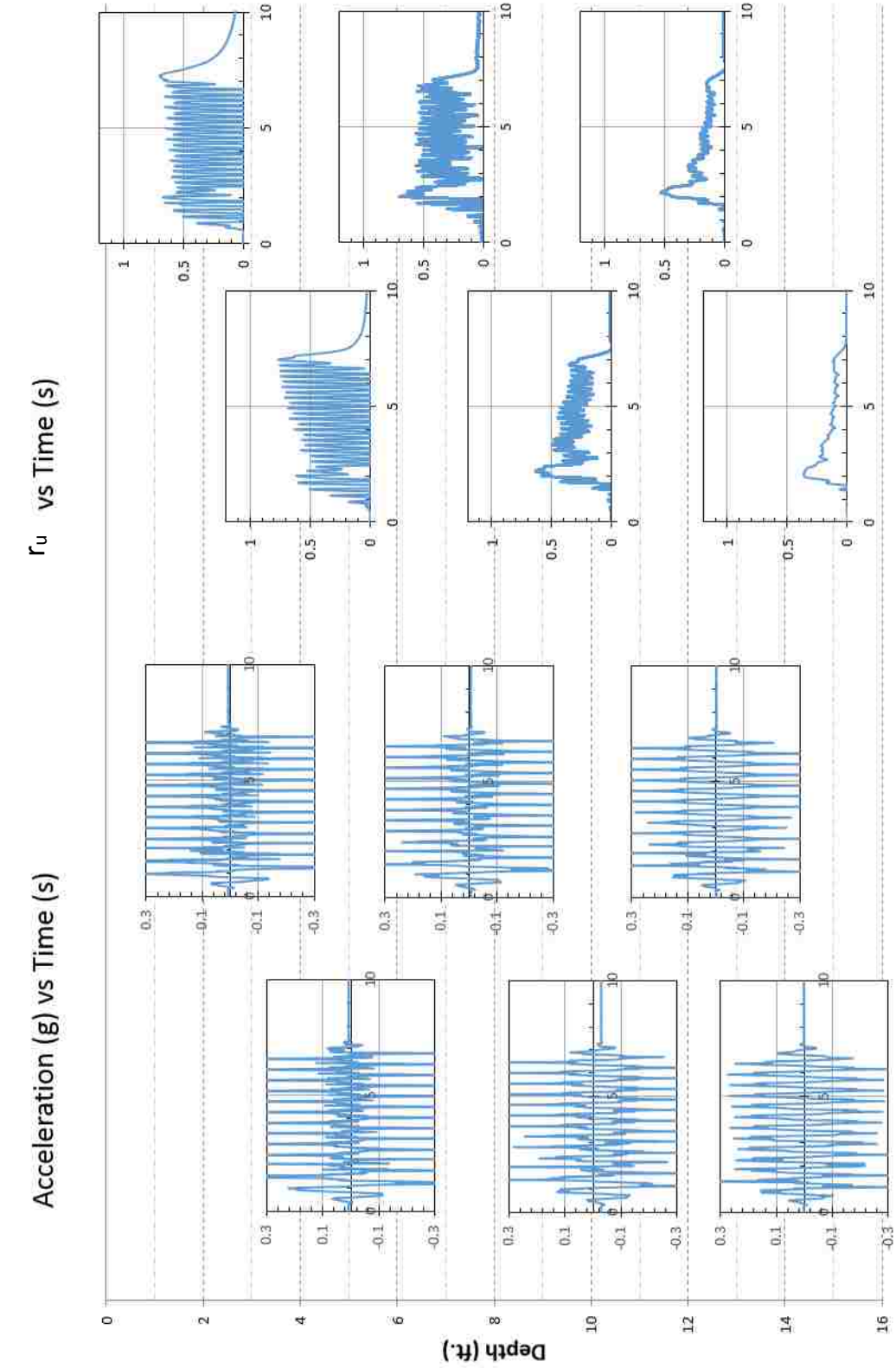

Figure 91 Acceleration Versus Time Paired with Excess Pore Pressure Ratio Versus Time for Round 3, a_{max} = 0.2g

Some pore pressure transducers experience large variation in excess pore pressure, which can be attributed to dilation (Howell et al, 2012). Similar results were obtained by Howell when using sinusoidal acceleration inputs with drains in centrifuge tests (see Figure 15).

Pore pressures build up rapidly during shaking with liquefaction or peak excess pore pressure ratios typically developing in 1 to 2 seconds or 2 to 4 acceleration cycles. During shaking, some pore pressure transducers experienced large oscillations in excess pore pressure. For the first round of tests, the decreases in r_u from the mean were typically less than r_u=10%; however, the magnitude of oscillations increased with each round of testing, as occurred in the PVD-1 series of tests. For the third round of tests, the decreases in r_u were as much as r_u=100%. In addition, the oscillations decreased substantially for the transducers located deeper in the box. These observations are consistent with dilation effects. As shear strains increase during cyclic loading, dilation would lead to a decrease in the excess pore pressure ratio. The potential for dilation increases as the sand becomes denser and the confining pressure decreases. Therefore dilation would be expected to increase as the sand became denser with each progressive round of testing. In addition, dilation would be expected to decrease as the confining pressure increased with depth in the box. This dilation occurred similarly in PVD-1, as noted in section 4.4.2. This dilation also occurred during testing by Howell et. al. (2012) when using sinusoidal acceleration inputs with drains in centrifuge tests.

Generally, liquefaction occurs near the surface, but deeper in the sand layer pore pressures were somewhat less than 50%, depending on the magnitude of the test.

Pore pressure ratios decrease rapidly immediately after shaking, especially as depth increases. In some cases, more so than in PVD-1, excess pore pressures dissipate during the shaking, especially at depths below 6 feet with 0.05g or 0.1g acceleration, or below 8 feet for tests

with acceleration of 0.2g. The time to reach a pore pressure ratio of 0.2 after shaking is very short in PVD-2. The longest is 6 seconds during the very first test. To compare with PVD-1, which had pore pressure monitors closer to the surface, the surface excess pore pressure would reach 0.2 just below the surface about 12 seconds after shaking stopped. Every other test besides the very first test at 0.5g during PVD-2 had a shorter time to reach 0.2 than any tests during PVD-1. This suggests that the closer spacing was much more effective at reducing excess pore pressures. Pore pressure ratios appear to decrease faster in later rounds than in the first round, which is most likely due to the denser soil in later rounds. Although the reduction in void space would be expected to reduce permeability and thus the dissipation rate, the compressibility also decreases with densification. The rate of dissipation is proportional to the permeability but inversely proportional to the compressibility and the reduction in compressibility more than compensate for the reduced permeability. This is consistent with previous findings that densification of liquefiable soils can be used as a mitigation technique.

Acceleration appears to be less uniform in PVD-2 than in PVD-1. In round 1, acceleration increases with depth, with the surface measuring lower accelerations than the input accelerations. Round 2 shows a slight increase in acceleration with depth, but not as significant as in round 1. In round 3 the acceleration is higher at the surface and decreases with depth. Dilation increases significantly in round 3, with excess pore pressures oscillating from $r_{u,max}=1$ to $r_u=0$ at the surface.

Figure 92 through Figure 100 provide plots of settlement versus depth profiles and peak excess pore pressure ratios ($r_{u,max}$) versus depth for each of the nine shaking tests. Settlement data is shown from three sources. First, two Sondex settlement profilometers provide settlement data for each test with data at two foot depth intervals as discussed in section 3.3. Second, three string potentiometers were attached to plates sitting on the ground surface. Finally, the amount of water

which flowed to the surface was measured to give a volume, which, when averaged over the surface area of the box gives an average settlement for the box. This calculation assumes that the water volume expelled is equal to the settlement of the sand. Excess pore pressure ratio profiles were provided by three vertical arrays of pore pressure transducers located at approximately 2.5 foot depth intervals.

Note that, as in PVD-1, in some cases the settlement versus depth has a settlement reading less than both the reading above and below it. This may be due to incorrect reading of a measurement, an artifact of reading at increments of 0.01 feet, or due to the Sondex tube not grabbing correctly in one area. This does not reflect the true settlement, and was corrected by creating a "smoothed" settlement curve. The smoothed curve represents a combination of both Sondex profilometers in a way that removes negative settlement from any zone. Surface settlement from the string pots and volume measurement are factored into the smoothed curve to include the best value for settlement near the surface.

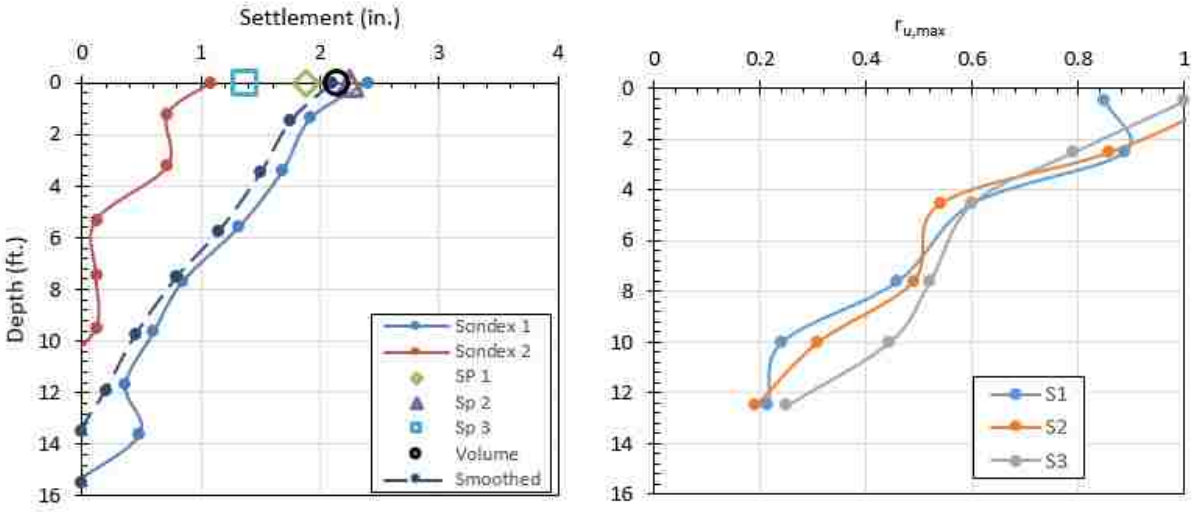

Figure 92 Profiles of Liquefaction Induced Settlement and Maximum Excess Pore Pressure Ratio ($r_{u,max}$) for Round 1 with a_{max} = 0.05 g.

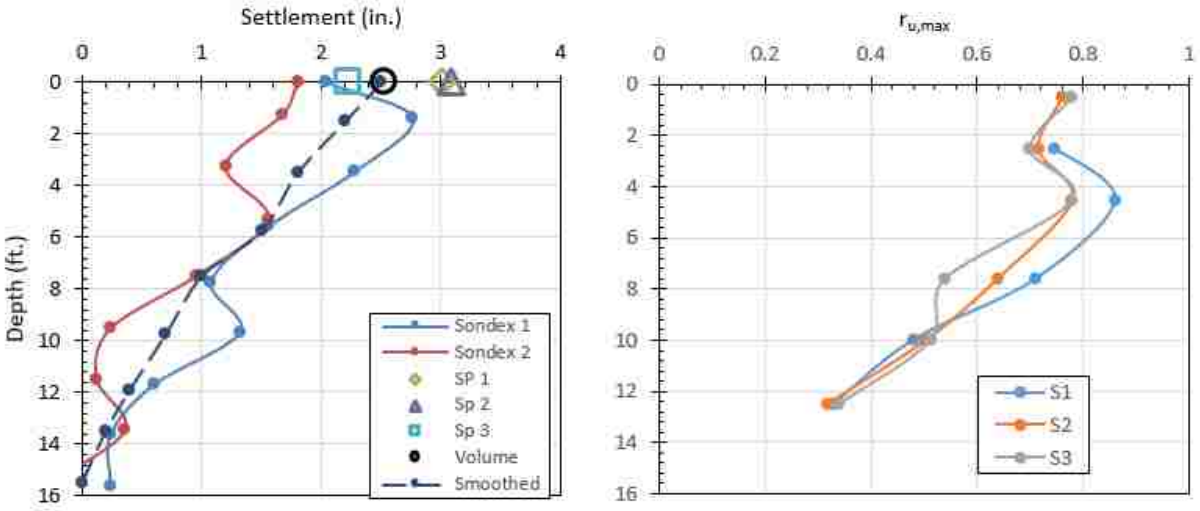

Figure 93 Profiles of Liquefaction Induced Settlement and Maximum Excess Pore Pressure Ratio ($r_{u,max}$) for Round 1 with a_{max} = 0.1 g.

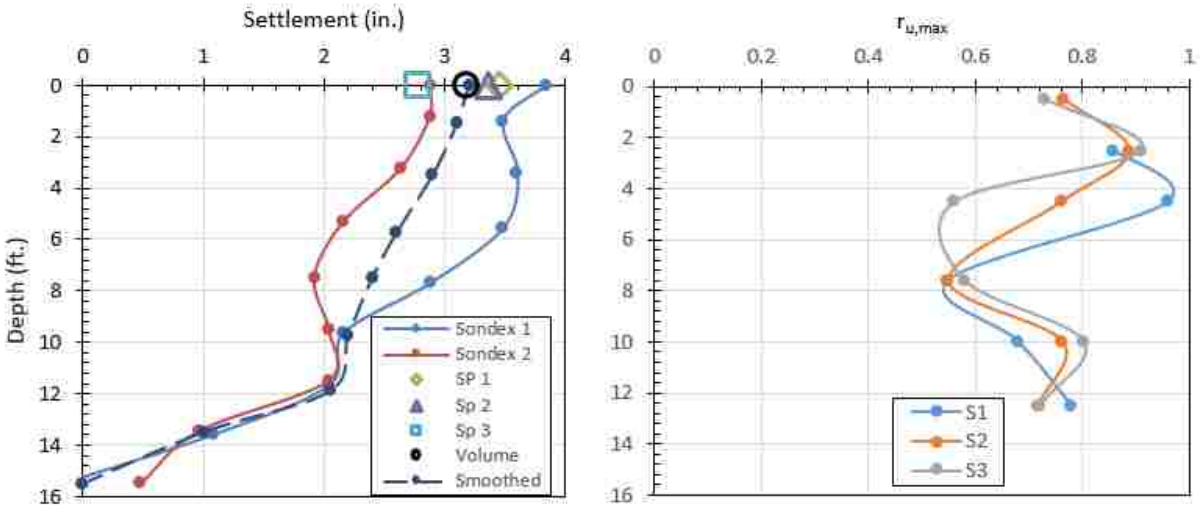

Figure 94 Profiles of Liquefaction Induced Settlement and Maximum Excess Pore Pressure Ratio ($r_{u,max}$) for Round 1 with a_{max} = 0.2 g

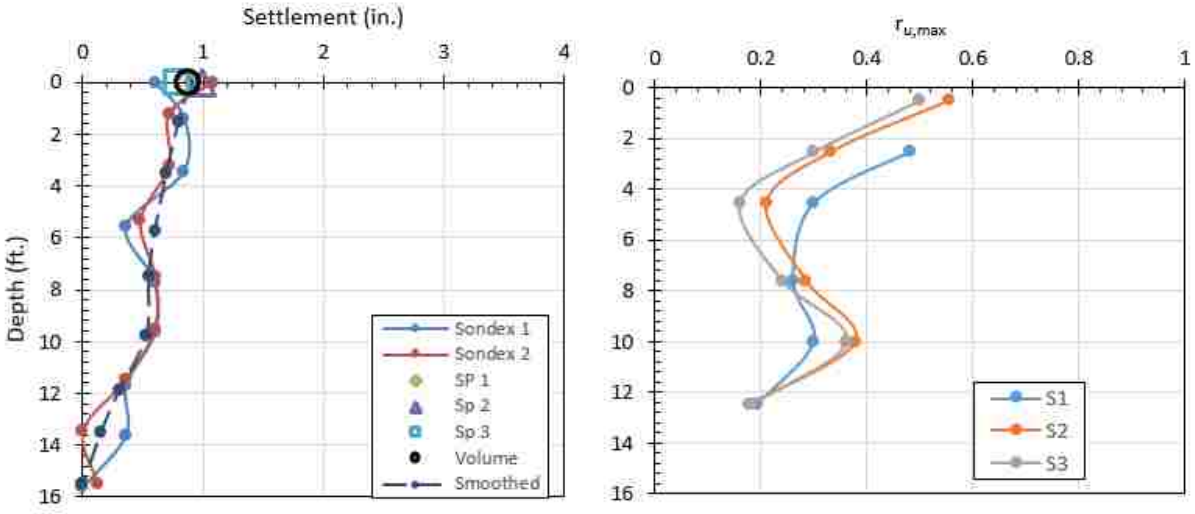

Figure 95 Profiles of Liquefaction Induced Settlement and Maximum Excess Pore Pressure Ratio ($r_{u,max}$) for Round 2 with a_{max} = 0.05 g

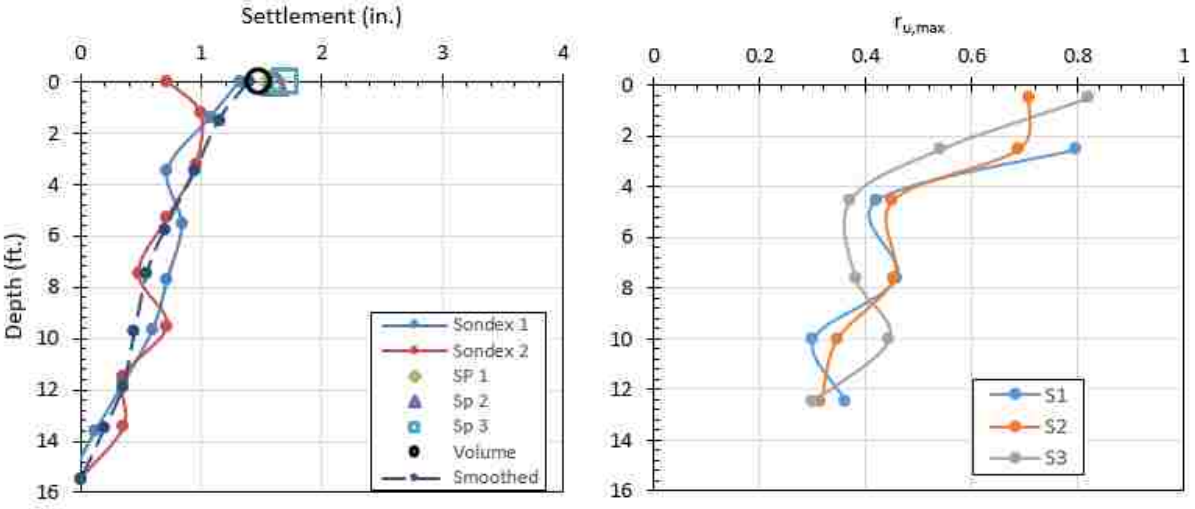

Figure 96 Profiles of Liquefaction Induced Settlement and Maximum Excess Pore Pressure Ratio ($r_{u,max}$) for Round 2 with a_{max} = 0.1 g

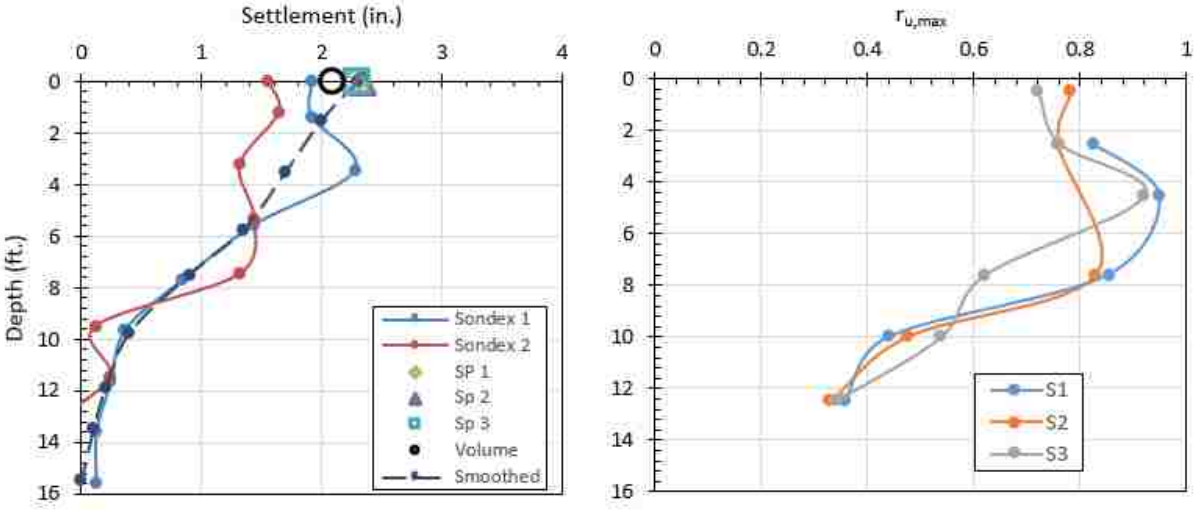

Figure 97 Profiles of Liquefaction Induced Settlement and Maximum Excess Pore Pressure Ratio ($r_{u,max}$) for Round 2 with a_{max} = 0.2 g

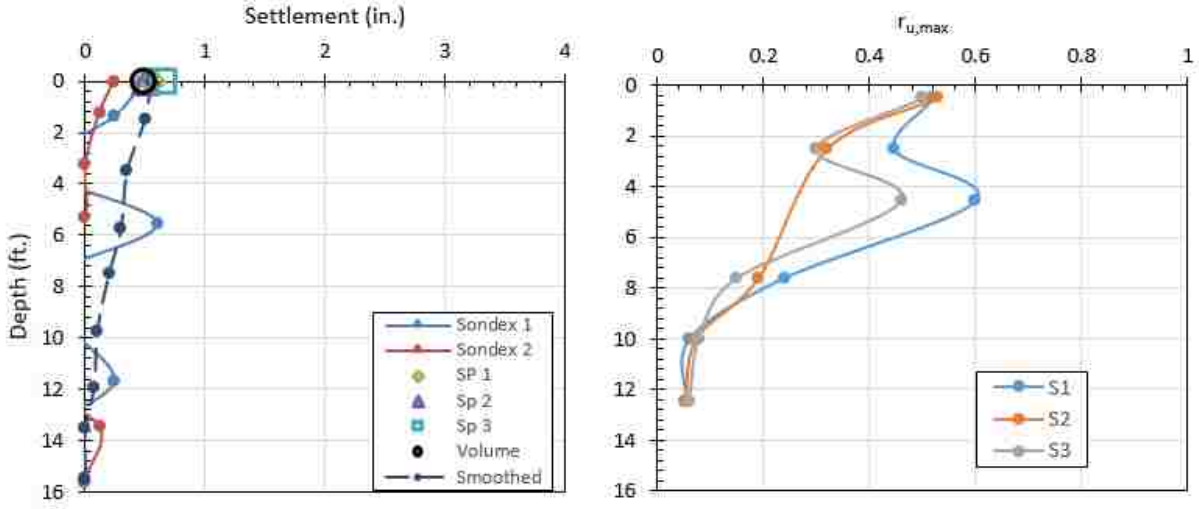

Figure 98 Profiles of Liquefaction Induced Settlement and Maximum Excess Pore Pressure Ratio ($r_{u,max}$) for Round 3 with a_{max} = 0.05 g

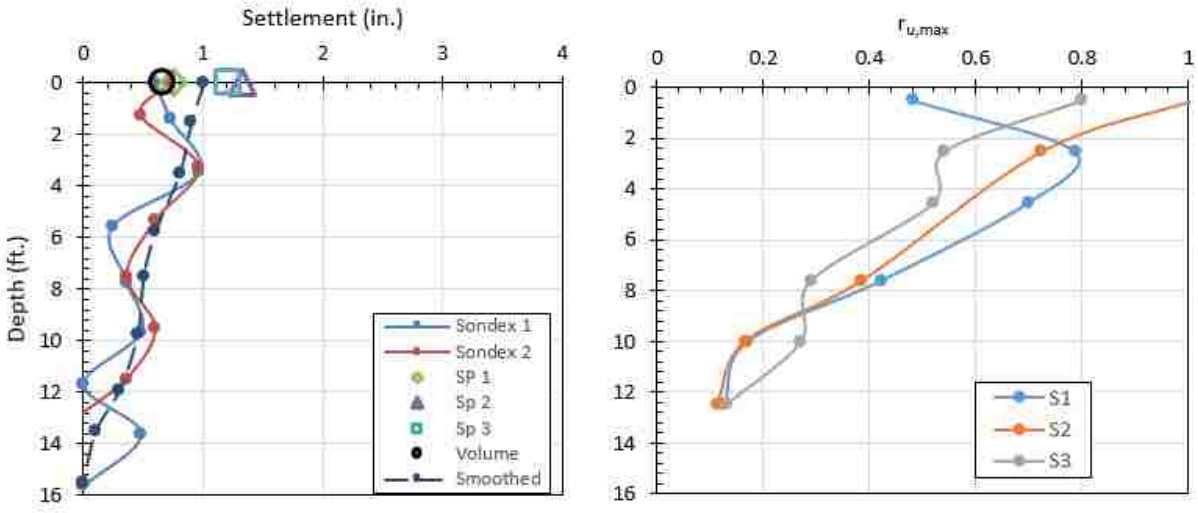

Figure 99 Profiles of Liquefaction Induced Settlement and Maximum Excess Pore Pressure Ratio ($r_{u,max}$) for Round 3 with a_{max} = 0.1 g

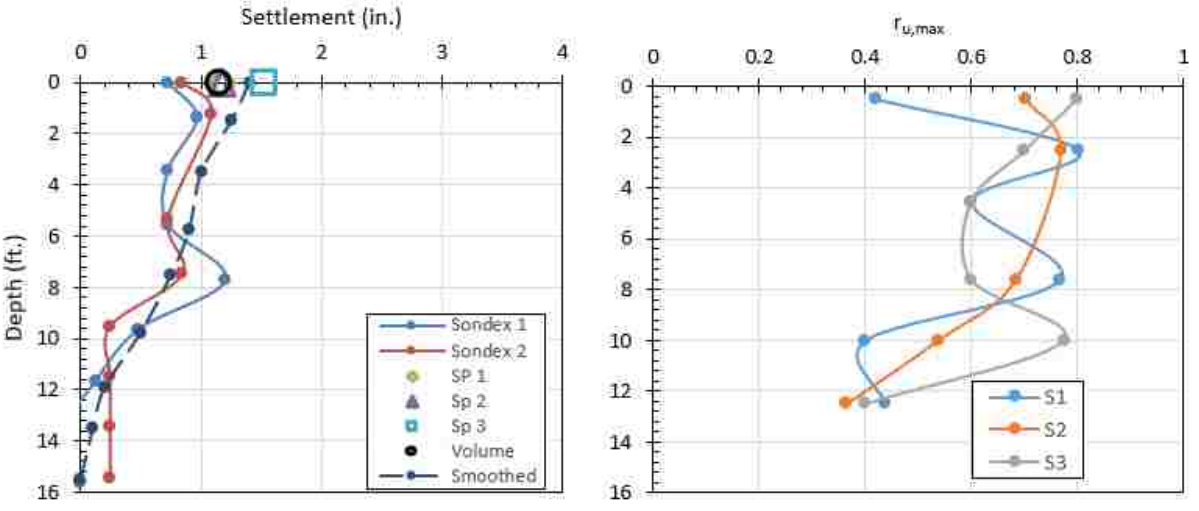

Figure 100 Profiles of Liquefaction Induced Settlement and Maximum Excess Pore Pressure Ratio ($r_{u,max}$) for Round 3 with a_{max} = 0.2 g

In round one, (Figure 92 through Figure 94), the excess pore pressure ratio, r_u, does not reach 1.0 at any depth in the profile. This is in contrast to PVD-1, which had r_u=1.0 nearly the full depth during shaking. The closer spacing of drains appears to be more effective at reducing pore pressures even during shaking, making the fully liquefied zone much thinner or non-existent. This is even more significant when compared with tests without drains, which experienced liquefaction throughout the entire depth after only a few cycles of loading (Dobry and Thevanayagam, 2013). This result indicates that the drains are producing increased liquefaction resistance, which, while more effective at depth is also more effective at all depths than drains spaced further apart. The pore pressures reach above 0.5 in the upper zone, which is where the majority of the settlement occurs, within the top 8 feet of the soil profile. The 0.1g test induced approximately 2.5 inches of settlement in about 14 feet of soil, which is equivalent to a strain of about 1.5. The first 0.1g test in the Dobry and Thevanayagam series of tests had about 3.5 inches of settlement over 16 feet of soil, equivalent to a strain of about 1.8%. This result suggests that even in the liquefied zones, the drains have reduced the liquefaction induced settlement to some extent.

Round 2 (Figure 95 through Figure 97) had lower values of $r_{u,max}$ and much less settlement than in round 1, as much as 40 to 50% less settlement. In the 0.05g test in round 2, only the top 3 feet of the soil profile reached $r_{u,max}$ of 0.5. Despite only the surface reaching $r_{u,max}$ of 0.5g, the settlement appears to be spread throughout the profile. When liquefaction does occur, or zones of the sand have $r_{u,max}$ values significantly higher than 0.5, more settlement does occur in those zones than in the rest of the profile. In the round 2 test with maximum acceleration of 0.2g, the zone between the surface to 8 feet reached $r_{u,max}$ of 0.8, and the majority of the settlement occurred between 4 to 8 feet, with almost all of the rest occurring between 8 and 10 feet, where $r_{u,max}$ was 0.5.

Settlement occurs deeper into the soil profile during higher acceleration tests. Much less settlement occurs where $r_{u,max}$ does not reach above 0.5 (see Figure 97 and Figure 98). The various settlement measurement techniques were relatively close in determining the settlement for each test; however, there are certainly variations. The Sondex measurements at the surface were either similar or smaller than the other methods. In a couple of instances, the Sondex measurements were significantly different near the surface. It may be that one of the Sondex tubes was closer to a drain which was ejecting significant amounts of water during the test. The flow of water directly next to the Sondex profilometer may have caused the difference in readings. After the first round of testing less settlement occurred, meaning less water coming from the drain, leading to less variation between the Sondex readings in later tests. Generally, water pumped from the box after the shaking seems to give a settlement very similar to the measurement obtained from the string pots. The water volume is probably a better measure of the average settlement volume lost across the entire box, whereas the string pots occasionally measured extreme values, possibly due to the non-uniformity of the soil profile or due to the plate sinking into the softened ground at the surface..

In comparing the 0.2g tests from each round, the majority of the settlement in round 1 is between depths of 12 to 15 feet. In rounds two and three the majority of the settlement is between depths of 6 to 12 feet. As in PVD-1, the settlement profiles during the first round have similar slope throughout the profile, while in later rounds there are flat sections where little settlement occurs near the surface. The settlement from the previous tests in the upper zone may prevent subsequent settlement in that zone.

5.4.3 Volumetric Strain Versus Depth Using Sondex Profilometers

Volumetric strain was calculated using settlement data obtained from the Sondex profilometers. Data was collected at intervals of approximately 2 feet. To reduce scatter in the strain plots, the settlement data used to calculate the volumetric strain versus depth was taken from the smoothed settlement curves. This removed any negative strain from settlement readings that are lower than the readings both above and below it which do not reflect the true conditions. Strain was calculated between each Sondex measurement by taking the difference in the settlement between the two readings above and below, and dividing by the distance between the two readings. Because the length and width of the box at all points remains the same, this strain is equal to the volumetric strain. Figure 101 through Figure 103 show the volumetric strain profiles for each round of testing.

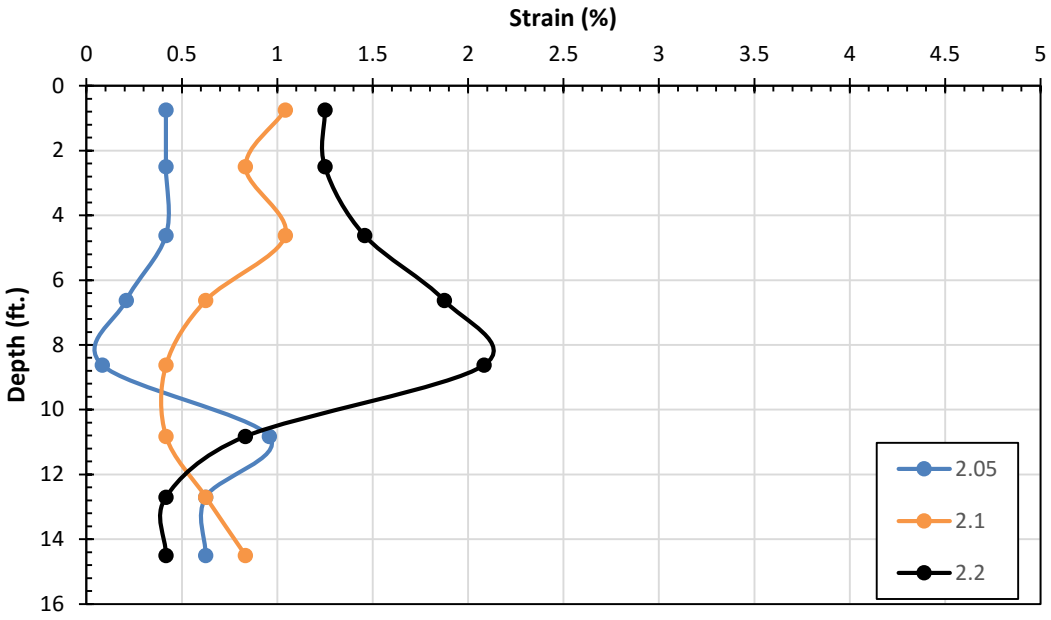

Figure 101 Profiles of Strain Versus Depth Using Smoothed Sondex Measurements for Round 1

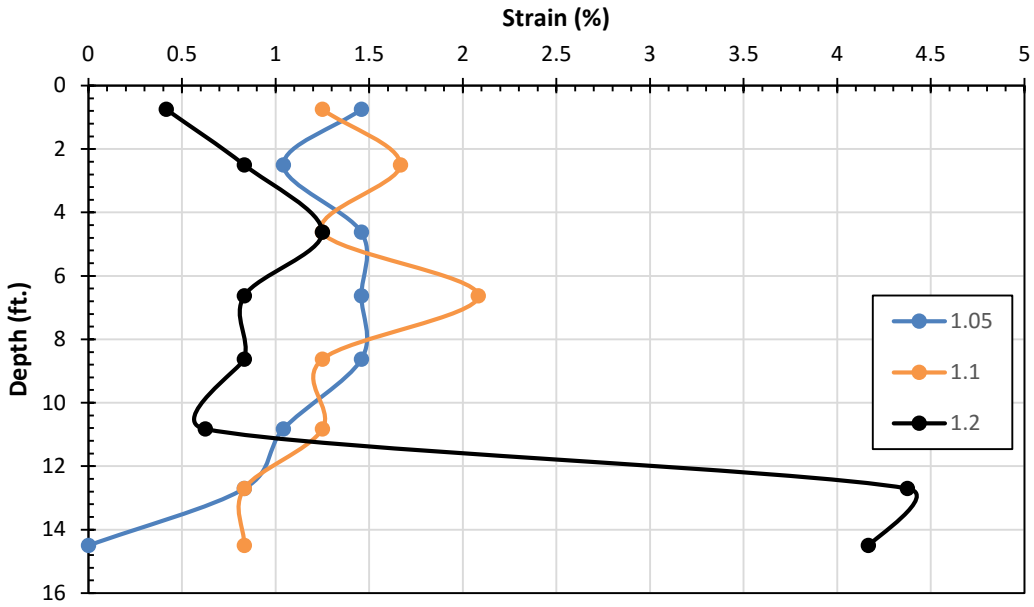

Figure 102 Profiles of Strain Versus Depth Using Smoothed Sondex Measurements for Round 2

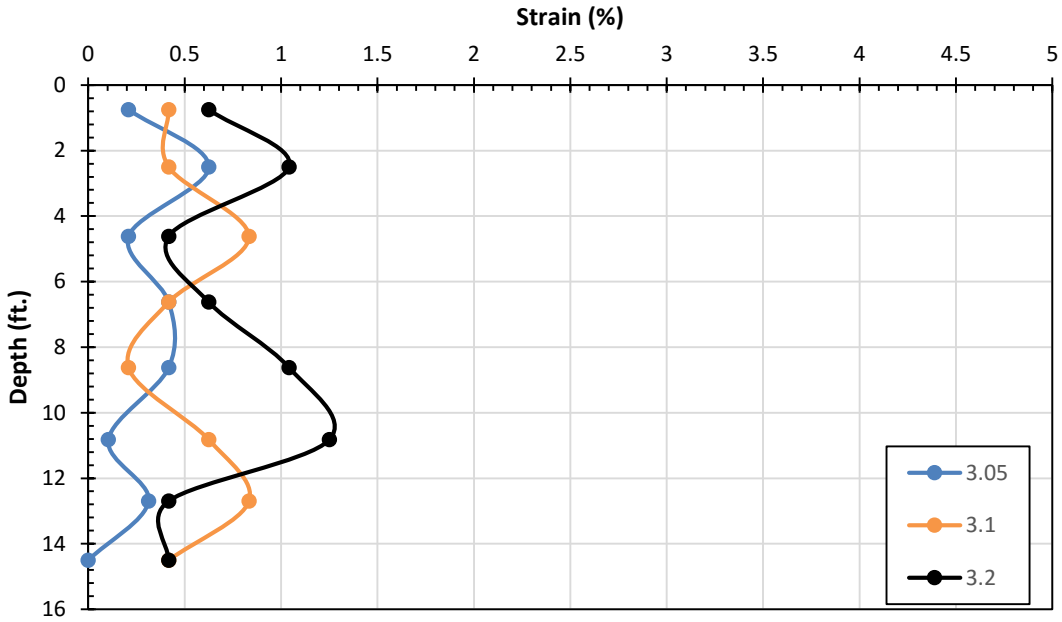

Figure 103 Profiles of Strain Versus Depth Using Smoothed Sondex Measurements for Round 3

Strain appears to be higher with higher acceleration, especially at lower elevations. The strain at the lowest acceleration level has the least variation through the depth profile. The overall

strain in round 3 is lower than in other rounds because there is less settlement during that round. The maximum strain gives an idea of where the most amount of settlement occurs in the soil profile. In Figure 101 the maximum strain in the 0.2g test for round 1 is between 10 and 14 feet, which is consistent with the settlement in Figure 94. The round 1 test at 0.2g experienced the most amount of settlement at this depth for any test in PVD-2. The maximum strain for the 0.2g tests in both round 2 and round 3 were at about 8 to 10 feet. In almost all cases, the 0.2g tests had the highest strain at depths below 8 feet, while the other tests may have had higher strain at shallower depths. This means that higher acceleration was required to liquefy the soil deeper in the profile, and it is most likely that the lower acceleration tests increased the density in the shallower soil before the large test occurred, so less settlement was recorded in those sections during the higher acceleration tests.

5.4.4 Surface Settlement Versus Time with Excess Pore Pressure Ratio Versus Time Surrounding the Liquefied Layer

Surface settlement was measured using string potentiometers connected to plates sitting on the sand at three locations (see Figure 73 for locations of string potentiometers). Settlement versus time plots are shown in Figure 104 through Figure 106. The settlement plots are in groups of three for each round. The left plot represents the settlement from the 0.05g test from that round, the center plot represents the 0.1g test, and the right plot shows the 0.2g test results. Below each settlement plot are two excess pore pressure ratio versus time plots that represent the excess pore pressure ratio at the top and bottom of the liquefied layer. The majority of the settlement occurred in the first 20 seconds, with less than 5% of settlement occurring afterward in almost all cases.

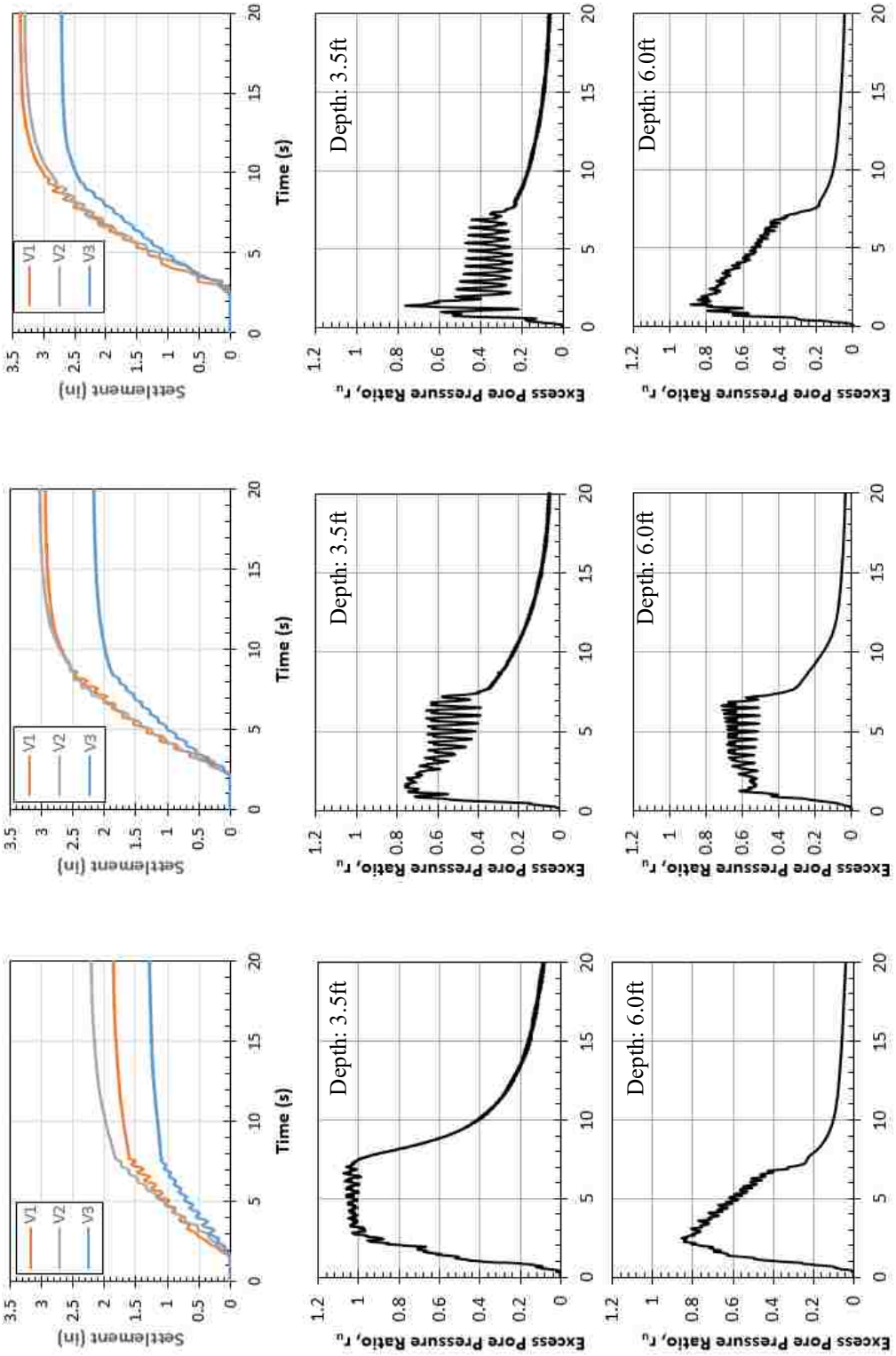

Figure 104 Surface Settlement Versus Time Paired with Excess Pore Pressure Ratio (r_u) Versus Time for Round 1, Left a_{max}=0.05 g, Middle a_{max}=0.10 g, Right a_{max}=0.20 g

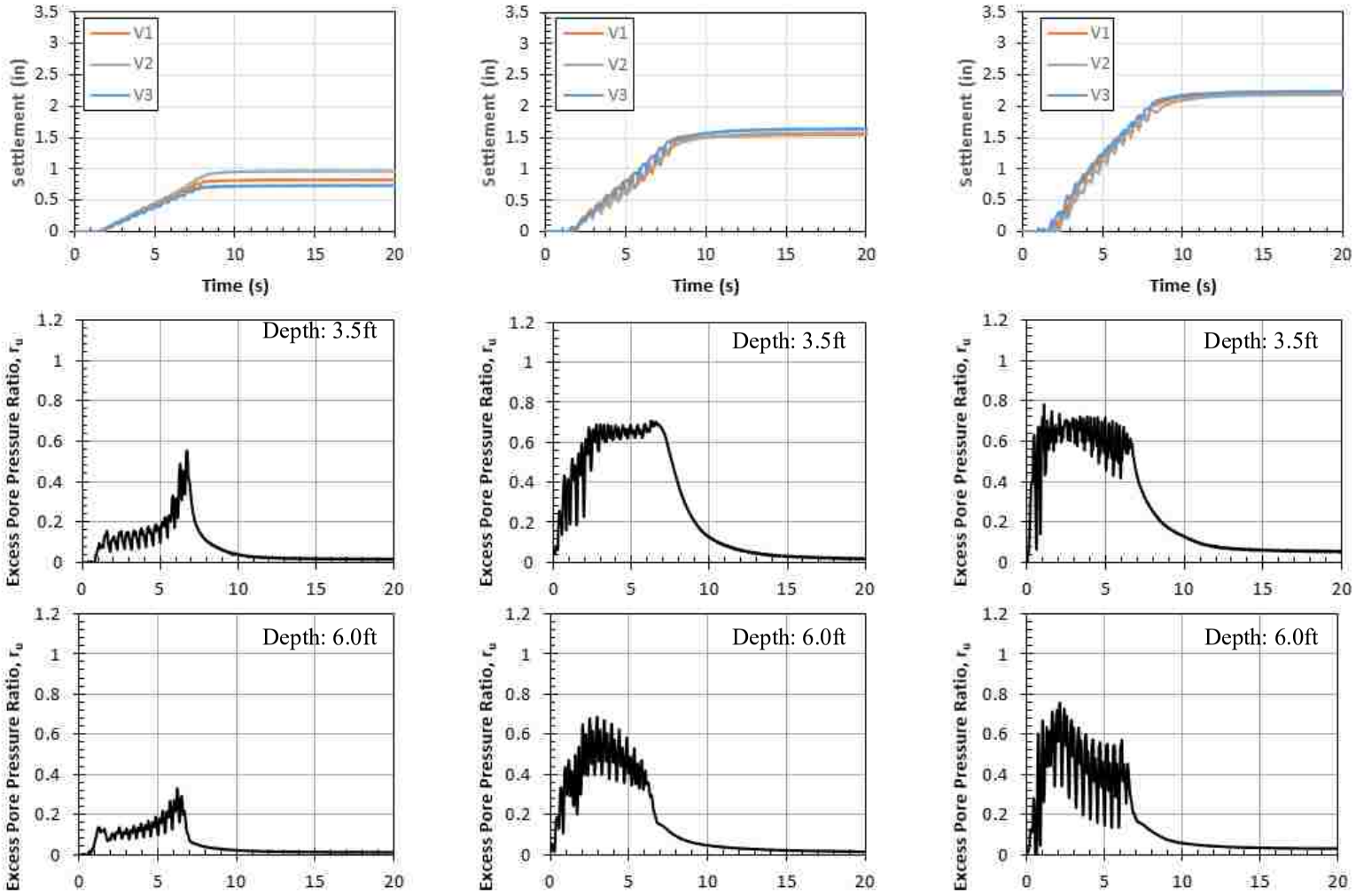

Figure 105 Surface Settlement Versus Time Paired with Excess Pore Pressure Ratio (r_u) Versus Time for Round 2, Left a_{max}=0.05 g, Middle a_{max}=0.10 g, Right a_{max}=0.20 g

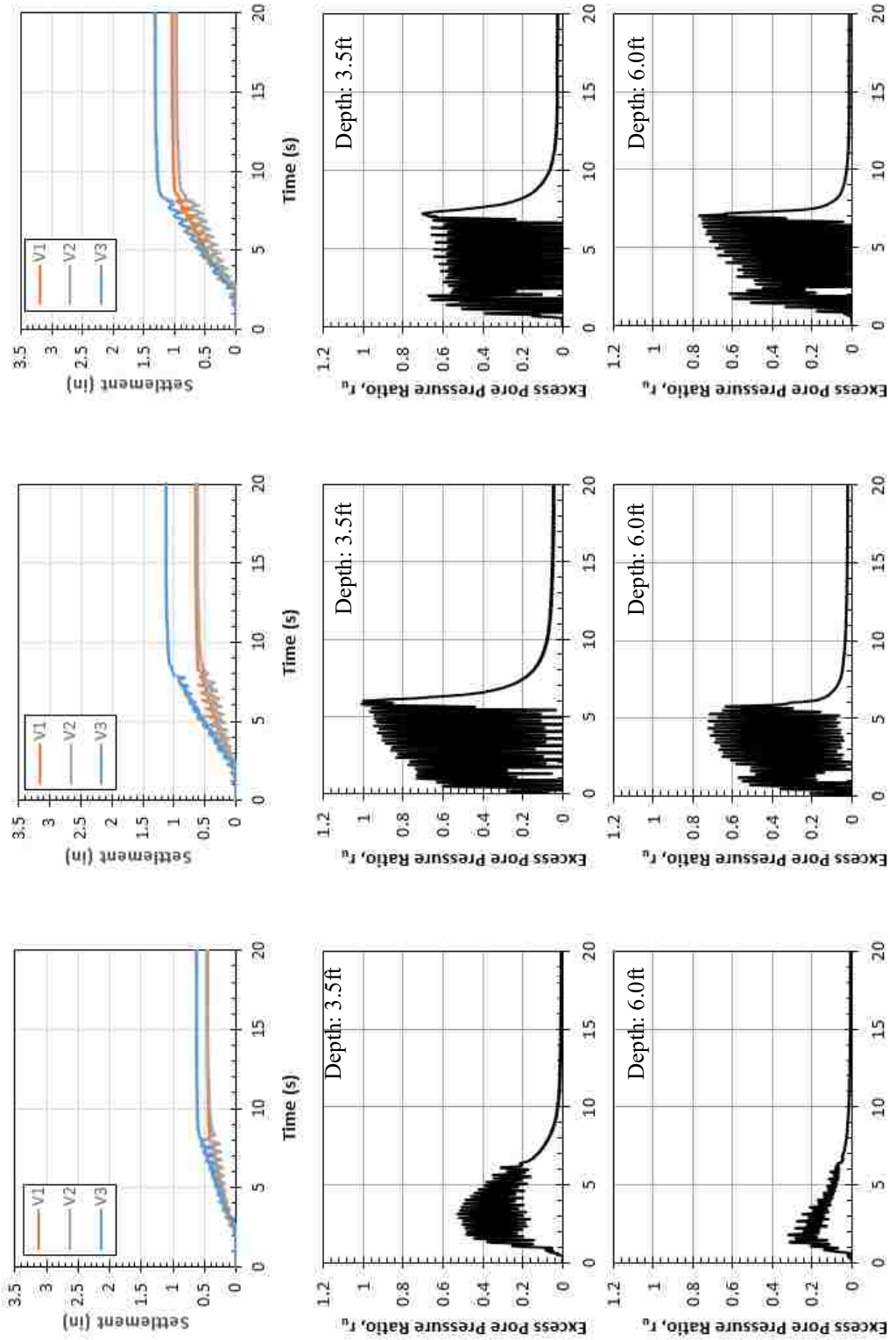

Figure 106 Surface Settlement Versus Time Paired with Excess Pore Pressure Ratio (r_u) Versus Time for Round 3, Left a_{max}=0.05 g, Middle a_{max}=0.10 g, Right a_{max}=0.20 g

Settlement increases with increasing acceleration. This is expected, as more energy is being introduced into the sand. In addition, settlement decreases with each progressive round of testing. Each round of testing has densified the sand from the settlement of the previous rounds, also evidenced by the increased cone tip resistance in the CPT (see Figure 77). The settlement from the final round is much less than the settlement from the first round, and even the second round.

Most of the settlement occurs during shaking (0 to 7.5 seconds), and the remainder occurs mainly within the next 10 seconds as pore pressures dissipate. Very little settlement occurs after r_u goes below 0.5. The tests in round 2 and round 3 all have very flat curves after the shaking is finished because the time for r_u to go below 0.5 is extremely short. The summary of time for r_u to dissipate to 0.2 after shaking is found in Table 15, and the time for r_u to dissipate to 0.5 after shaking is found in Table 16. These values are an average of the three sensor arrays.

Table 15 Time in Seconds for r_u to Dissipate to 0.2 After Shaking.

	Round 1			Round 2			Round 3		
depth (ft)	Acceleration (g)			Acceleration (g)			Acceleration (g)		
	0.05	0.1	0.2	0.05	0.1	0.2	0.05	0.1	0.2
3	6	2	2	1	2	3	0.5	1	1
5.5	1	1.8	1.1	0	0.666667	1	0	0.666667	1
7.5	0	1.2	0.8	0	0	1	0	0	0.666667
10	0	0.5	1	0	0	0.5	0	0	0.5
12.5	0	0	2.7	0	0	0	0	0	0
15	0	0	1.7	0	0.333333	0	0	0	0

Table 16 Time in Seconds for r_u to Dissipate to 0.5 After Shaking.

Round 1				Round 2				Round 3			
depth (ft)	Acceleration (g)			depth (ft)	Acceleration (g)			depth (ft)	Acceleration (g)		
	0.05	0.1	0.2		0.05	0.1	0.2		0.05	0.1	0.2
3	6	0.5	0	3	0	2	0.5	3	0	1	0.5

The time to reach 0.5 is only measured at a depth of 3 feet because many pore pressure transducers did not measure a value above 0.5, and the surface remained above 0.5 the longest. There was not a pore pressure transducer at a depth of 1 foot to compare to PVD-1. The time for r_u to each 0.5 at a depth of 3 foot was multiplied by two to estimate the time for the surface to reach 0.5, despite not having a pore pressure transducer at that location. This estimation of pore pressure at the surface follows the pattern found in PVD-1 and PVD-2 follows the same pattern near the surface as well. The total amount of settlement for each test taken from string pots, water volume, and Sondex measurements is given in Table 17. The percentage of settlement that occurs during shaking is summarized in Table 18. The percentage of settlement that occurs while r_u is greater than 0.5 at the surface is summarized in Table 19.

The amount of time for excess pore pressure ratios to dissipate reduces significantly after round 1. The time to reach r_u=0.5 is less impacted by acceleration than time to reach r_u=0.2 at the same depths. The higher acceleration tests cause higher excess pore pressures deeper in the soil profile, as found in previous sections.

Table 17 Settlement for Each Test from Sondex, String Pots, and Water Volume

		Average Sondex (in)	Average string pot (in)	Water volume (in)
Round 1	0.05	1.74	1.83	2.14
	0.1	1.92	2.78	2.52
	0.2	3.36	3.20	3.18
Round 2	0.05	0.84	0.88	0.88
	0.1	1.02	1.63	1.48
	0.2	1.74	2.30	2.08
Round 3	0.05	0.36	0.58	0.49
	0.1	0.66	1.10	0.66
	0.2	0.78	1.29	1.15

Table 18 Percentage of Settlement that Occurs During Shaking.

Acceleration (g)	Settlement (%)		
	Round 1	Round 2	Round 3
0.05	80.9	94.7	88.6
0.1	83.3	89.1	81.5
0.2	86.2	88.8	80.5

Table 19 Percentage of Settlement that Occurs While r_u>0.5.

Acceleration (g)	Settlement (%)		
	Round 1	Round 2	Round 3
0.05	98.9	97.8	92.5
0.1	96.4	98.2	96.5
0.2	98.6	93.8	94.8

All rounds at all levels for PVD-2 have at least 90% of settlement occur while the surface had r_u>0.5. Round 3 with 0.05g and 0.2g experienced 92.5% and 94.8% of the total settlement one second after shaking. In comparison, PVD-1 round 3 with 0.05g experienced only 86.3% of the total settlement two seconds after shaking, compared to 92.5% from the same test in PVD-2 in only one second after shaking. This shows that the drains with closer spacing are making an impact on the settlement and the time to reduce excess pore pressures. As in PVD-1, time to dissipate to r_u=0.5 is not a perfect indicator of the total settlement. Time to dissipate to r_u=0.5 is a better indicator of total settlement when including acceleration level and density, with higher acceleration causing more settlement, and denser sand causing less settlement to occur.

5.4.5 Settlement Comparisons

Figure 107 shows settlement of the sand versus acceleration level normalized by the settlement for the 0.05g test from each round. Round 1 had lower normalized settlement with higher acceleration, but in rounds 2 and 3, an increase from 0.05g to 0.1g gives a 50% increase in

settlement. Increasing from 0.1g to 0.2 g gives a similar 40% increase. The settlement reductions are generally consistent with the results obtained by Marinucci et al. (2008) comparing drains versus no drains in centrifuge models (Figure 10).

Figure 108 plots the incremental settlement of the sand for each test as a function of acceleration for each round of testing. For all acceleration levels the settlement decreases significantly from the first round of tests to the final round. Increased density should account for some of this decrease; however, the drainage function appears to be more effective as the density of the sand increases. Figure 109 plots settlement of the sand at a given peak acceleration after normalization by settlement for the first test. This normalization shows that the second round tests had 30% less settlement than the first round, and the third round tests had 70% less settlement

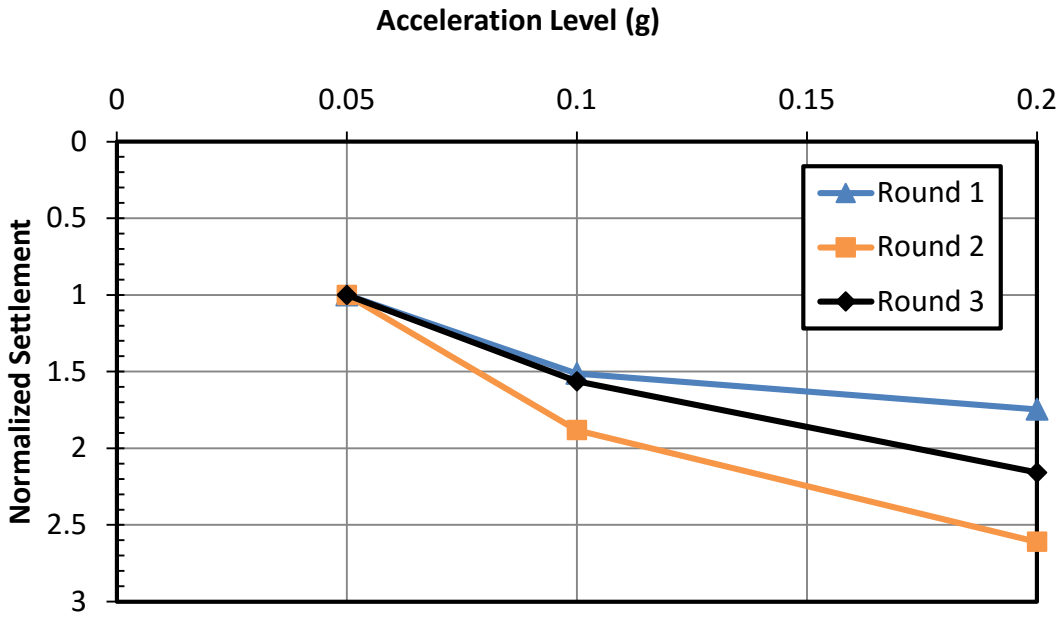

Figure 107 Settlement of Sand Versus Acceleration Level by Round After Normalizing by Settlement for the 0.05g Test for Each Round

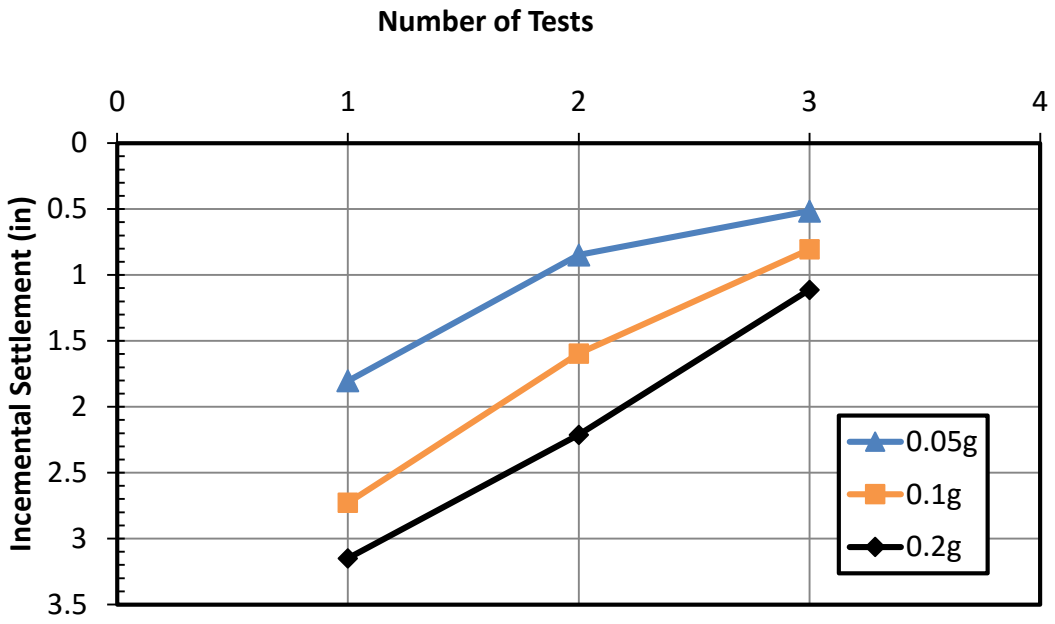

Figure 108 Incremental Settlement at a Given Peak Acceleration

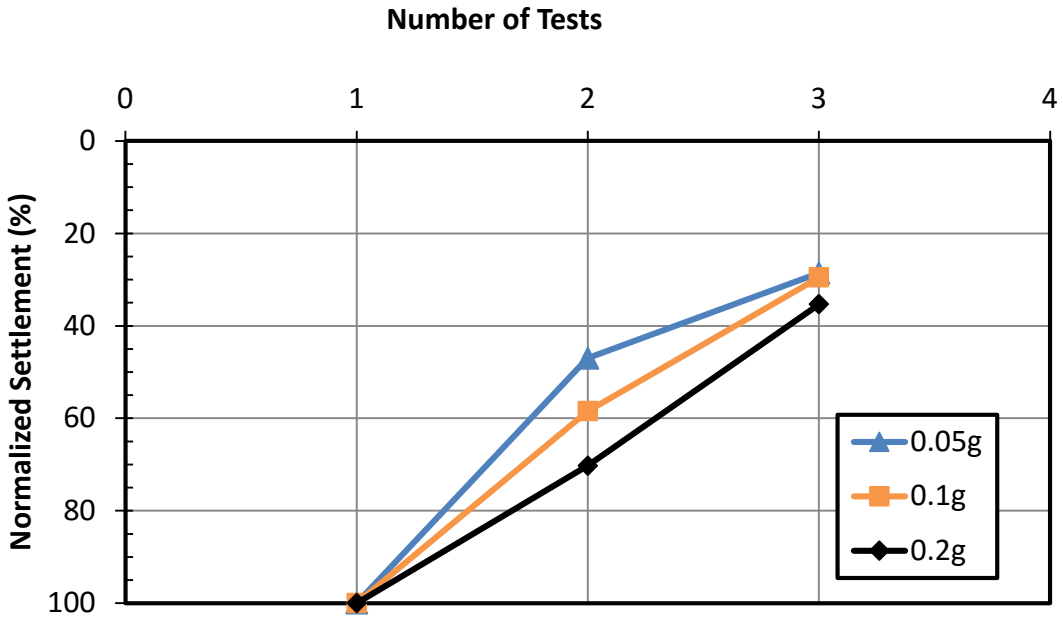

Figure 109 Settlement of Sand with Number of Tests at a Given Acceleration Level After Normalization by Settlement for the First Round

5.5 Comparison with Other Tests

5.5.1 Laminar Box Tests

Figure 110 provides a comparison of the cumulative settlement as a function of the number of tests for the first set of nine tests with drains spaced at three feet intervals, PVD-2 Test, in comparison with previous studies without drains as well as PVD-1. All settlement has been scaled to match a soil depth of 16 feet. PVD-2 settlement was not scaled, as it was already 16'. PVD-1 settlement was scaled up from 13 feet to 16 feet, accounting for the dense sand at the bottom of the box that was not removed from previous testing. The LG1 test involves repeated tests with a peak acceleration of 0.1g with an untreated sand layer 16 feet deep. The IPS1 test result involved testing with induced partial saturation treatment in a 10 foot layer of the total 16 foot thickness. Settlement has been scaled up proportionally assuming that the untreated sand was responsible for the majority of the settlement. In the IPS1 testing the sand was subjected to 0.1g acceleration for six tests and 0.2g acceleration for two tests. Significantly more settlement was observed for tests where 0.2g accelerations were applied. While the comparisons are not perfect nor completely direct because of differing acceleration levels, using 0.05g, 0.1g, and 0.2g accelerations in PVD-1, it is clear that the cumulative settlement curve for the profile with vertical drains is significantly lower than without. In many cases the settlement is only 50 to 60 percent of the settlement for the untreated sand. Considering that the untreated test curves are generally for 0.1g, while the treated sand experienced three 0.2g cycles, the reduction produced by the drains may be even greater than represented in Figure 110. PVD-2 had very similar results to PVD-1, with approximately 2% less settlement than PVD-1 for most of the tests. This reduction in settlement is small, but may be attributed to the closer spacing of drains.

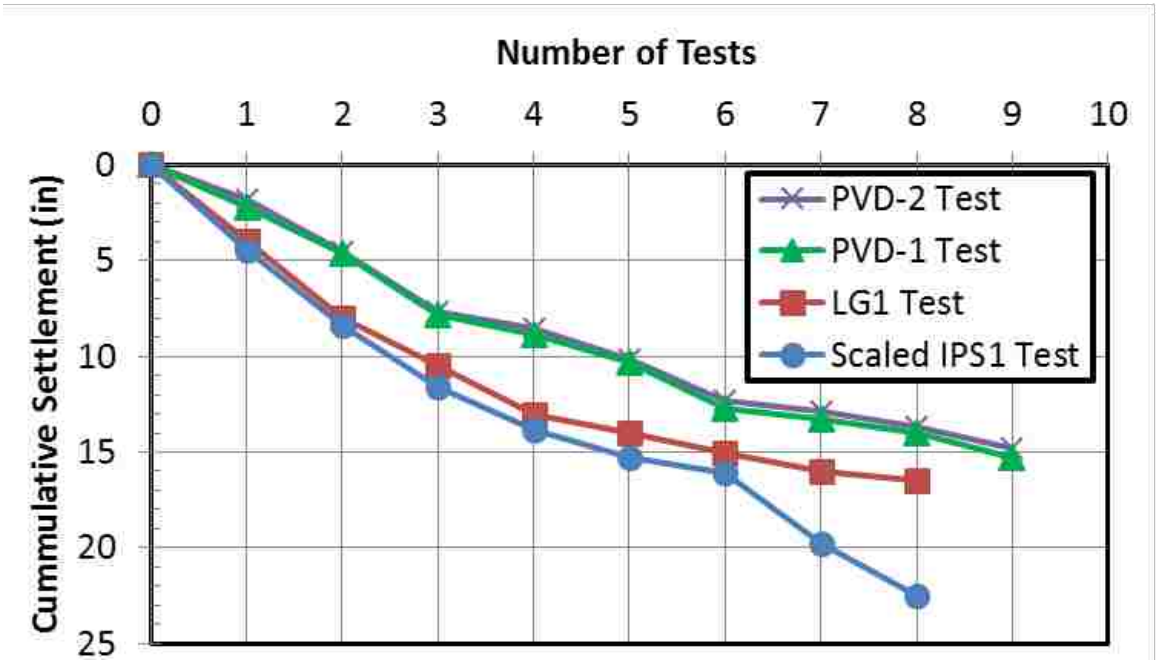

Figure 110 Comparison of Cumulative Settlement from PVD-2 with Other Tests

Figure 111 and Figure 112 show excess pore pressure ratio versus time plots at the depth of the pore pressure transducers for PVD-1 and PVD-2 side by side for the 0.2g tests in round 1 and round 3 respectively. These plots are useful to show the effect of the drains and drain spacing on excess pore pressures both during and after shaking.

Figure 113 shows $r_{u,max}$ profiles for PVD-1 and PVD-2 from round 1 with 0.05g acceleration, round 1 with 0.2g acceleration, and round 3 with 0.2g acceleration. The maximum excess pore pressure ratios are lower in PVD-2 at nearly all depths in all three cases. Because the maximum excess pore pressures are generally higher during shaking, this suggests that drains spaced closer together are more effective at reducing excess pore pressures during shaking.

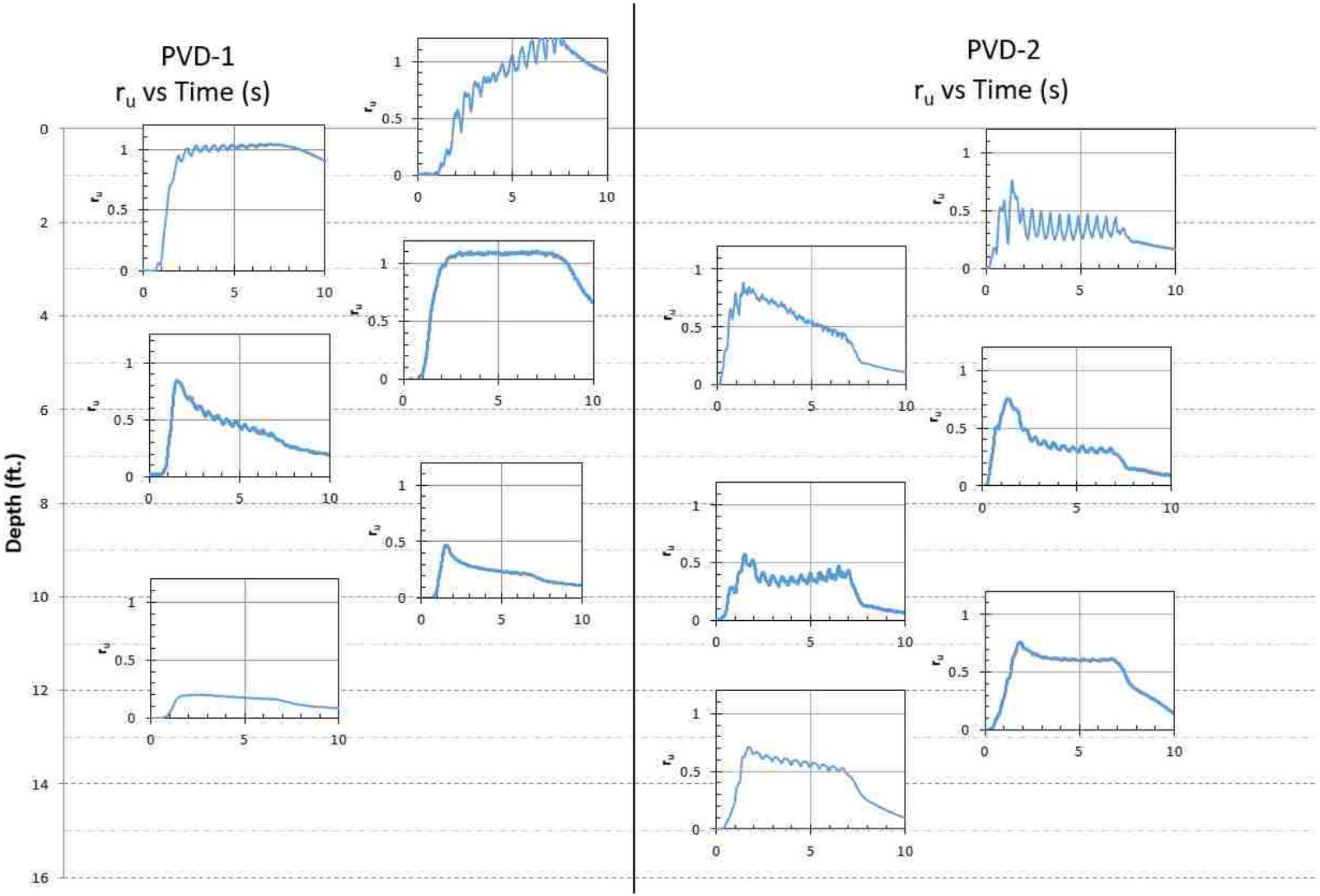

Figure 111 Excess Pore Pressure Versus Depth Profiles for PVD-1 and PVD-2 for Round 1, a_{max}=0.2g

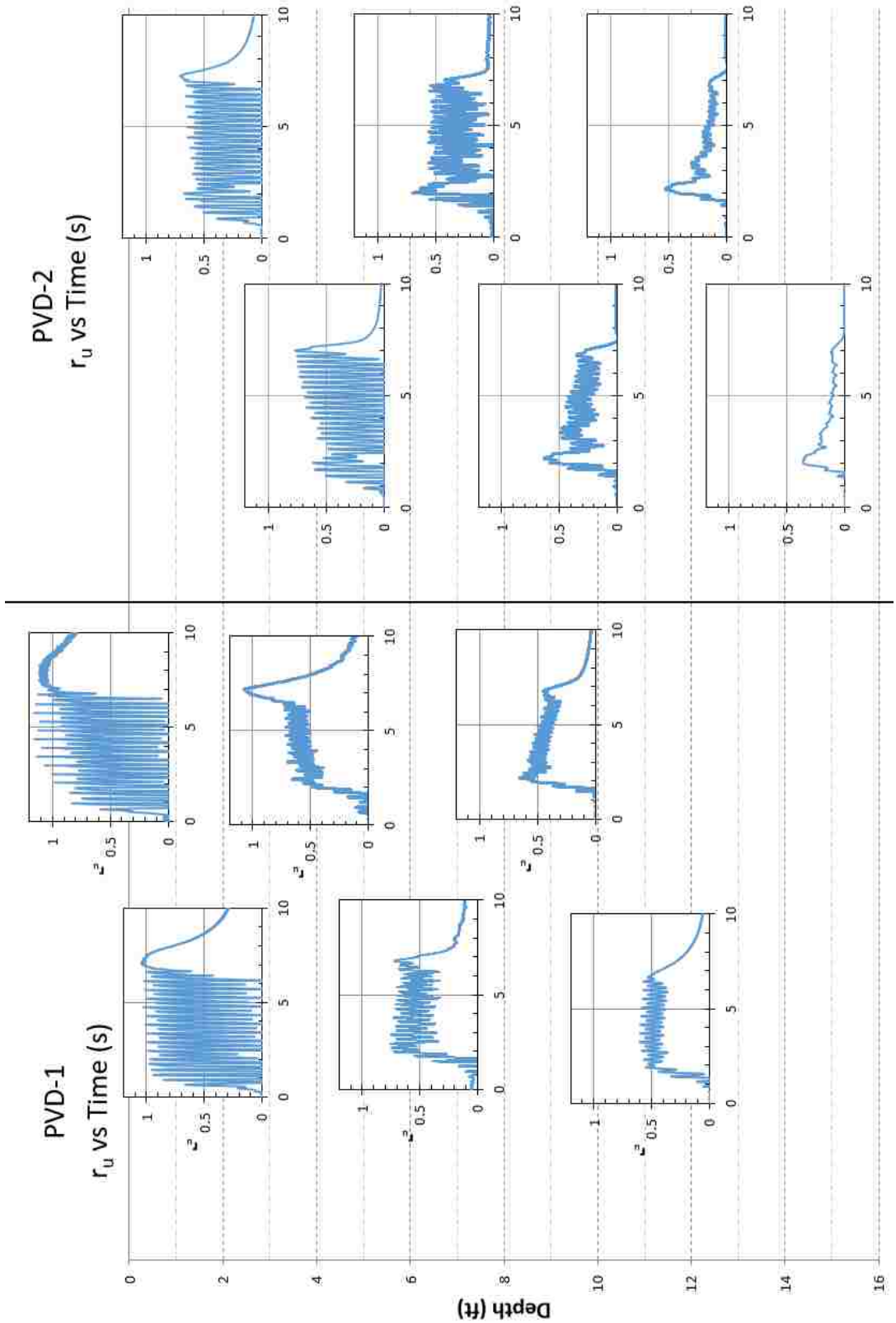

Figure 112 Excess Pore Pressure Versus Depth Profiles for PVD-1 and PVD-2 for Round 3, a_{max}=0.2g

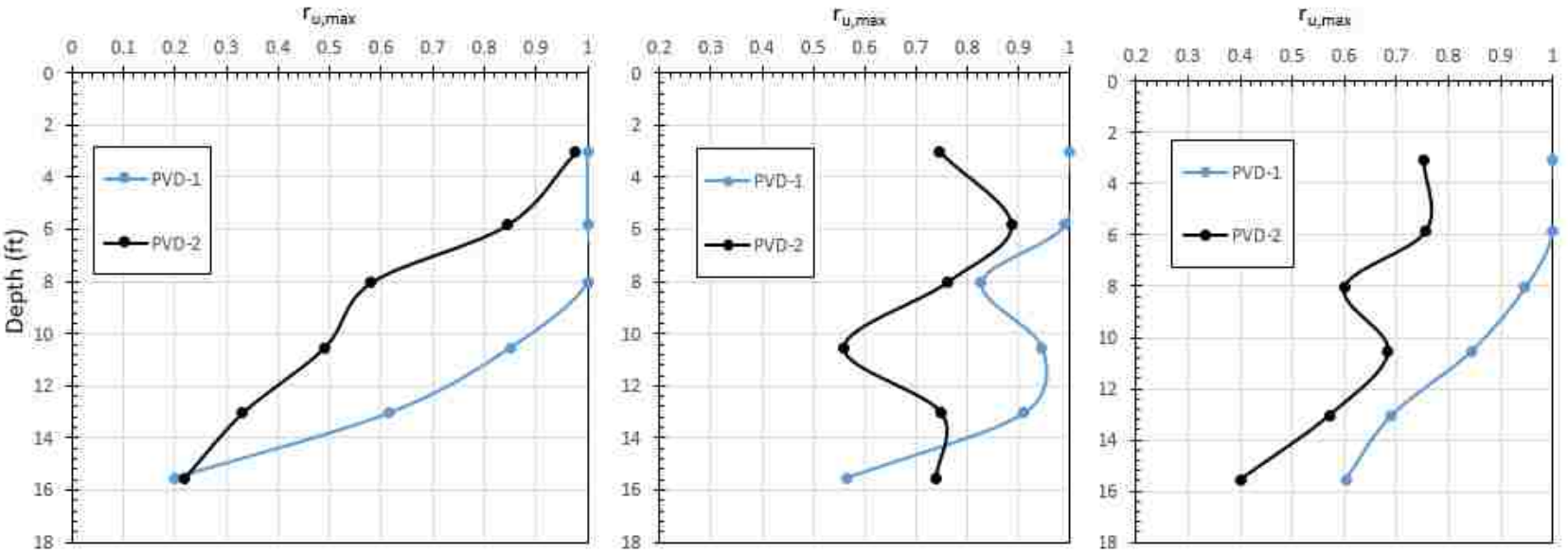

Figure 113 Comparisons of $r_{u,max}$ Versus Depth Profiles for PVD-1 and PVD-2

PVD-1 had higher excess pore pressures near the surface than PVD-2 during the 0.2g test in round 1, but lower excess pore pressures at depths below 10 feet. The excess pore pressures dissipate more rapidly after shaking, and even during shaking in some cases, in PVD-2 than in PVD-1. This is expected because with smaller drain spacing there should be shorter paths and more capacity for water to exit the soil profile. In the comparison of the third round test at 0.2g for PVD-1 and PVD-2, the excess pore pressures are lower in PVD-2 at most or all depths, with faster dissipation of excess pore pressures as well. The excess pore pressure ratio in PVD-2 is almost immediately below 0.5 at all depths, while in PVD-1 it takes a few seconds near the surface to dissipate to 0.5.

LG0 had acceleration levels and shaking time much longer than in PVD-2, making comparisons with settlement difficult, but LG0 does have records of excess pore pressure dissipation without drains which are useful for comparison. The side-by-side excess pore pressure dissipation for LG0 (left) and PVD-2 is shown in Figure 114. Note that LG0 shows excess pore pressure, while PVD-2 shows excess pore pressure ratios. The scales are such that r_u=1 is equal to o'_{v0}. The excess pore pressure ratios are taken from round 1 at 0.2g to compare with LG0, which had a maximum acceleration of 0.3g. The shaking lasts 35 seconds in LG0 and only 7 seconds in PVD-2.

The pore pressures remain at r_u=1 in LG0 for up to one minute at 4.33 feet, or about 20 seconds at 12.41 feet. The excess pore pressures are not reduced to r_u=0.5 in LG0 until approximately 125 to 160 seconds, depending on depth. In comparison, the excess pore pressure ratios from PVD-2 immediately begin to dissipate, and are completely dissipated within 30 seconds after shaking. At lower depths the excess pore pressure ratio does not even reach r_u=1.

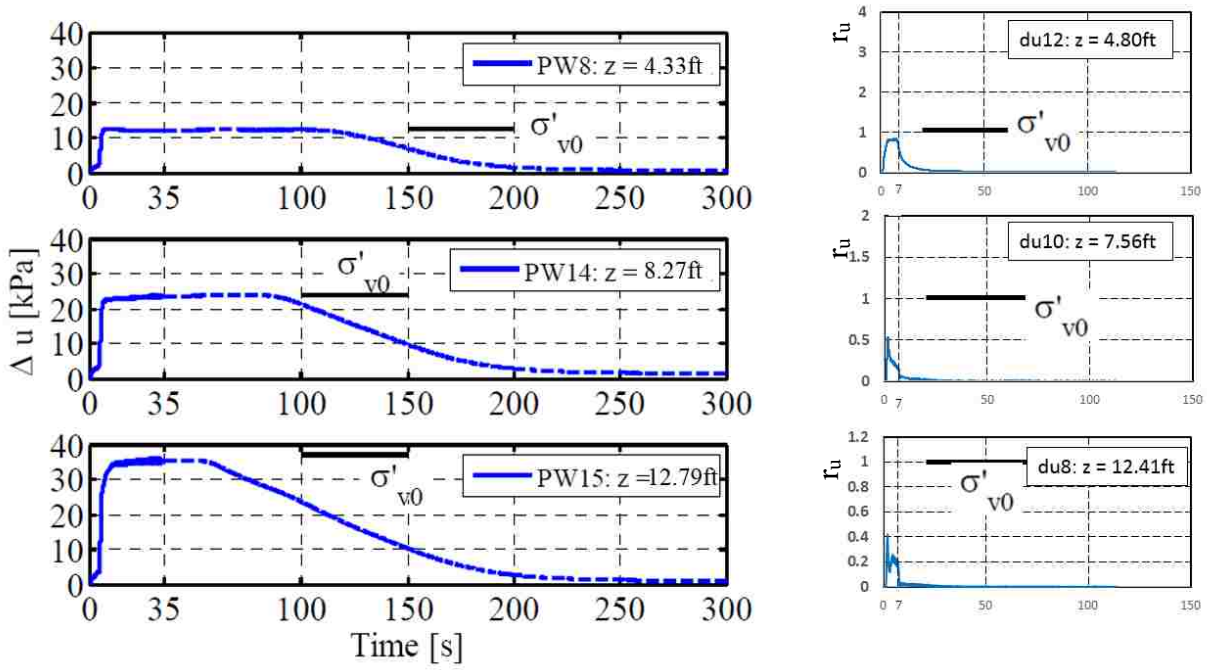

Figure 114 Comparison of Excess Pore Pressures from LG0 and PVD-2.

Figure 18 shows pore pressure generation during shaking for LG0. After 10 seconds of shaking, with only 5 seconds of shaking at 0.05g, the excess pore pressure ratio had reached r_u=1 down to 11.5 feet. In the first test at 0.05g in PVD-2 (see Figure 83), r_u at 8.5 feet depth never reached above 0.5, and after 5 seconds of shaking, r_u at 5.5 feet depth was reduced to 0.6 after peaking at 0.9 after a couple cycles of shaking.

5.5.2 Centrifuge Tests

Earthquake drains used in centrifuge testing were successful at reducing vertical settlement as much as 50% (see Figure 12). After 8 tests, the reduction in cumulative settlement versus LG1 is 20%. Comparing with the scaled IPS1 test, the reduction in cumulative settlement is 43%, which

matches very well the previous centrifuge testing. Individual comparisons are difficult because there is not an exact match with acceleration levels between the tests, but drains do appear to provide decreased settlement in agreement with previous centrifuge testing.

As in PVD-1, dilation spikes are noticeable in the later tests (see Figure 90 and Figure 91), which Howell (2012) attributes to dilation. Also, the drains continue to be more effective at reducing pore pressures deep in the soil profile in most cases, rather than at the surface. In Figure 81 and Figure 82, $r_{u,max}$ for each test shows a trend of high $r_{u,max}$ near the surface which drops off at depth.

6 FINAL DISCUSSIONS

6.1 Project Summary

Liquefaction of loose saturated sand results in significant damage in nearly every major earthquake event. Typically vibrocompaction, stone columns, compaction grouting, dynamic compaction, or explosives are used as liquefaction mitigation. An alternative to densifying the sand is providing drainage so that excess pore water pressures are dissipated quickly, thereby preventing liquefaction. Testing of prefabricated vertical drains has been done using centrifuges has been successful at reducing excess pore water pressures, but no full scale testing of prefabricated vertical drains has been done previously.

The main objective of this project is to confirm the results of previous centrifuge testing with prefabricated vertical drains by performing a full scale testing. The results will show whether prefabricated vertical drains can effectively reduce excess pore pressures and settlement due to liquefaction. The effect of spacing on drain effectiveness will also be determined in this project. A major portion of this project includes setup and performance of this test at the University at Buffalo Network for Earthquake Engineering Simulation (NEES) facility, as well as data reduction to produce case histories of earthquake loading. Further evaluation of the test data to match the results with current models will be done in the future, and is not included in this thesis.

Test equipment for this project was provided by the NEES laboratory at the University at Buffalo campus. Instrumentation and details concerning the laminar shear box are provided in Chapter 3. Instrumentation specific to each test, including drain, pore pressure transducer, and settlement string pot locations are given in Chapters 4 and 0 for PVD-1 and PVD-2 respectively. The sand used was Ottawa F55 sand, which was provided by the NEES facility. The sand was deposited in the laminar shear box by pluviation. Three rounds of testing were done for PVD-1 and PVD-2 separately. Each round consisted of three tests with sinusoidal acceleration inputs of 0.05g, 0.1g, and 0.2g. CPT testing was performed before each round and after all testing was completed to determine the density of the soil during each round of testing.

6.2 Conclusions

PVD-1 consisted of testing with drains spaced at 4 feet intervals. Liquefaction occurred during shaking with excess pore pressures dissipating quickly after shaking stopped. Within 15 seconds after shaking only the surface continued to r_u above 0.2. With increased density r_u dissipated more rapidly. Most settlement occurred during shaking, when r_u was above 0.5. Because r_u dissipated so quickly after shaking, very little settlement occurred after shaking except during the first round, which had the slowest dissipation. Higher acceleration tests had more settlement, and settlement occurred deeper in the profile during higher acceleration tests. When compared to previous laminar shear box testing without drains, settlement was reduced by 20% to 60% (see Figure 69), which matches previous centrifuge testing results (see Figure 12).

PVD-2 consisted of testing with drains spaced at 3 feet intervals. The results were similar to PVD-1, liquefaction occurring during shaking, and excess pore pressures dissipating even more quickly after shaking stopped. Only five seconds after shaking all excess pore pressure ratios from

all tests were below 0.5, and after 15 seconds all were below 0.2, including the surface. Most settlement occurred during shaking, when r_u was above 0.5. Because r_u dissipated so quickly after shaking, very little settlement occurred after shaking except during the first round, which had the slowest dissipation. Higher acceleration tests had more settlement, and settlement occurred deeper in the profile during higher acceleration tests. When compared to previous laminar shear box testing without drains, settlement was reduced by 20% to 64% (see Figure 110), which matches previous centrifuge testing results (see Figure 12). The closer spacing does decrease the time to dissipate pore pressures, as well as reduce settlement by up to 2%.

In summary:

1. Excess pore pressures dissipated rapidly after shaking, with higher density in later tests increasing the rate of dissipation
2. Excess pore pressures dissipated significantly faster than previous laminar shear box testing without drains, taking seconds rather than minutes for excess pore pressures to fully dissipate.
3. Higher acceleration caused more settlement to occur and caused settlement deeper in the soil profile.
4. Settlement was reduced by 20-64% when compared to previous laminar shear box testing without drains. This matches previous results from centrifuge testing.
5. Drains spaced closer together are more effective at reducing excess pore pressures, and may have slightly reduced settlement.

REFERENCES

Adalier, K., and Elgamal, A. (2004). "Mitigation of liquefaction and associated ground deformations by stone columns." Eng. Geology, 72(3-4), 275-291.

Assimaki, D. (2004). "Topography effects in the 1999 Athens earthquake: Engineering issues in seismology." Cambridge.

Bethapudi, R. (2008). Liquefaction Induced Lateral Spreading in Large-Scale Shake Testing, Master's thesis, State University of New York at Buffalo.

Boulanger, D.P., Hashish, Y. and Schmidt, B. (1997). "Drainage capacity of stone columns or gravel drains for mitigating liquefaction." 2nd Geotechnical Earthquake Engineering and Soil Dynamics Conference, Seattle, Vol. I, 678-690.

Chang, W, Rathje, E.M., Stokoe, K.H., and Cox, B.R. (2004). "Direct evaluation of effectiveness of prefabricated vertical drains in liquefiable sand." Soil Dynamics and Earthquake Engineering, Vol. 24, Issues 9-10,723-731.

Chiou, B., Darragh, R. Gregor, N., & Silva, W. (2008). NGA Project Strong-Motion Database. Earthquake Spectra, 24(1), 23-44.

Cook, R.D., Malkus, D.S., Plesha, M.E., and Witt, R.J. (2002). Concepts and Applications of Finite Element Analysis, 4th ed, John Wiley & Sons, New York.

Cornell, A., Jalayer, F., Hamburger, R., & Foutch, D. (2002). Probabalistic basis for 2000 SAC federal emergency management agency steel moment frame guidelines. Journal of Structural Engineering, 128(4), 526-532.

Cox, B.R. (2006). Development of a Direct Test Method for Dynamically Assessing the Liquefaction Resistance of Soils In Situ, Ph.D. dissertation, The University of Texas at Austin.

Dafalias, Y., & Manzani, M. (2004). Simple Plasticity Sand Model Accounting for Fabric Change Effects. Journal of Engineering Mechanics, 130(6), 622-634.

EQE (1995). "The January 17, 1995 Kobe Earthquake" Summary Report, www.eqe.com/publications/kobe/economic.htm.

Gallagher, P.M., Conlee, C.T. and Rollins, K.M. (2007). Full-Scale Field Testing of Colloidal Silica Grouting for Mitigation of Liquefaction Risk. Journal of Geotechnical and Geoenvironmental Engineering, 133(2), p. 186-196.

Hayden, R.F., and Baez, J.I. (1994). "State of practice for liquefaction mitigation in North America." Proc., Int. Workshop on Remedial Treatment of Liquefiable Soils, Public Works Research Institute, Tsukuba City, Japan.

Holzer, TL. (1998). "Introduction". The Loma Prieta, California, Earthquake of October 17, 1989-Liquefaction, U.S. Geological Survey Professional Paper 1551-B, U.S. Government Printing Office, B1-B8.

Holzer, TL., Tinsley, JC., Bennett, MJ., Mueller, CS. (1992). "Observed and predicted ground deformation-Millter Farm lateral spread, Watsonville, California," Procs. 5th US-Japan Workshop on Earthquake Resistant Design of Lifeline Facilities and Countermeasures Against Soil Liquefaction, Snowbird Utah, MCEER, Tech. Report NCEER-94-0026, p. 79-99.

Howell, R. et al. (2009a). "Centrifuge modeling of liquefaction sites treated with prefabricated drains." IS-Tokyo 2009 Int. Conf. on Performance Based Design in Earthquake Geotechnical Engineering, CRC, Balkema, Netherlands.

Howell, R. et al. (2009b). "Evaluation of the effectiveness of prefabricated vertical drains for liquefaction remediation: Centrifuge data report for RLH01." Data Rep. UCD/CGMDR-0801, Center for Geotechnical Modeling, Univ. Of CA, Davis, CA.

Howell, R., Rathje, E.M., Kamai, R. and Boulanger, R. (2012). "Centrifuge modeling of prefabricated vertical drains for liquefaction remediation." J. of Geotech. and Geoenviron. Engineering. ASCE, Vol.138, no. 3, p. 262-271.

Iai, S., & Koizumi, K. (1986). Estimation of earthquake induced excess pore water pressure for gravel drains. Proc. 7th Japan Earthquake Engineering Symposium, (pp. 679-684).

Iai. S. et al. (1994). "Effects of remedial measures against liquefaction at 1993 Kushiro-Oki earthquake." Proc., 5th U.S.- Japan Workshop on earthquake Resistant Design of Lifeline Facilities and Countermeasures against Soil Liquefaction, Technical Rep. NCEER-94-0026, T. D. O'Rourke and M. Hamada, eds. 135-152.

Iai, S., Koizumi, K., Noda, S., and Tsuchida, H. (1998). "Large scale model tests and analysis of gravel drains." Proc. 9th World Conf. on Earthquake Engineering, Vol. III, Japan Association for Earthquake Disaster Prevention, Tokyo, Japan.

Idriss, I., and Boulanger, R. (2008). Soil liquefaction during earthquakes, Earthquake Engineering Research Institute (EERI), Oakland, CA.

Ishihara, K. and Yoshimine, M. (1992). "Evaluation of settlements in sand deposits following earthquakes," Soils and Foundations, JSSMFE, v. 32, no. 1, p. 1-22.

Japanese Geotechnical Society, ed. (1998). Remedial measures against soil liquefaction, A.A. Balkema, Rotterdam, Netherlands.

Jamiolkowsky, et al. (1985). New developments in field and laboratory testing of soils, International Conference on Soil Mechanics and Foundation Engineering, San Francisco, CA. 1985. Vol. 1 A. A. Balkema, Boston, 985.

Kamai, R., and Boulanger, R.W. (2010). "Characterizing localization processes during liquefaction using inverse analyses of instrumentation arrays." Meso-Scale shear physics in earchquake and landslide mechanics. Leiden, Y. H. Hatzor, J. Sulem, and I. Vardoulakis, eds., CRC Press, 219-238.

Kamia, et al. (2008). Evaluation of the Effectiveness of Prefabricated Vertical Drains for Liquefaction Remediation – Centrifuge Data Report for RNK01, Center for Geotechnical Modeling Data Report UCD/CGMDR. Univ. of California, Davis.

Kamai, R., Kano, S., Conlee, C., Marinucci, A., Rathje, E., Boulanger, R. and rix, G. (2007). Evaluation of the Effectiveness of Prefabricated Vertical Drains for Liquefaction Remediation – Centrifuge Data Report for SSK01, Center for Geotechnical Modeling Data Report UCD/CGMDR. Univ. of California, Davis.

Knappett, J.A. and Madabhushi, S.P.G. (2008). Liquefaction-Induced Settlement of Pile Groups in Liquefiable and Laterally Spreading Soils." J. Geotech. and Geoenv. Engrg. 134(11), 1609-1618.

Kulasingam, R., Malvick, E.J., Boulanger, R.W. and Kutter, B.L. (2004). "Strength loss and localization at silt interlayers in slopes of liquefied sand." J. Geotech. and Geoenv. Engrg. ASCE, 130(11) 1192-1202.

Lee, K.L. and Albaisa, A. (1974). "Earthquake induced settlements in saturated sands," J. of Geotechnical Engineering, ASCE, v. 100 no. GT4, p. 387-406.

Kutter, B. (1995). "Recent advances in centrifuge modeling of seismic shaking. State-of-the-art paper." Proc., Third Int. Conf. on Recent Advances in Geotechnical Earthquake Engineering and Soil Dynamics, St. Louis, Vol. 2, 927-942.

Lysmer, J., & Kuhlemeyer, A. (1969). Finite dynamic model for infinite media. Journal of the Engineering Mechanics Division, 95(EM4), 859-877.

Makdishi F, S. H. (1978). Simplified procedure for estimating dam and embankment earthquake-induced deformations. Journal of Geotechnical Engineering, 104(7), 849-867.

Marinucci, A. (2010). "Effectiveness of prefabricated vertical drains on pore water pressure generation and dissipation in liquefiable sand." Ph.D. dissertation, Univ. of TX at Austin, Austin, TX.

Marinucci, A., Rathje, E., Kano, S. Kamai, R., Conlee, C., Howell, R., Boulanger, R., and Gallagher, P. (2008). "Centrifuge testing of prefabricated vertical drains for liquefaction remediation." Soil Dynamic s and Earthquake Engineering, Geotechnical Special Publication 181, ASCE, p. 1-10.

Mazzoni, S., McKenna, F., & Fenves, G. (2005). Opensees Command Language Manual.

Mitchell, J.K. and Wentz, F.J., Jr. (1991). "Performance of improved ground during the Loma Prieta earthquake." Earthquake Engineering Research Center, Rep. No. UCB/EERC-91/12, College of Engineering, Univ. of CA, Berkeley, CA.

National Research Council (1985). Liquefaction of Soils During Earthquakes, National Academy Press, 240 p.

Oishi, H., and Tanaka, Y. (1992). "Densification of surrounding soils due to gravel drain construction." Proc., 4th U.S.- Japan Workshop on Earthquake Resistant Designs of Lifeline Facilities and Countermeasures against Soil Liquefaction, Technical Rep. NCEER-92-0019, Buffalo, NY.

Onoue, A. (1988), "Diagrams Considering Well Resistance for Designing Spacing Ratio of Gravel Drains," *Soils and Foundations*, Japanese Soc. of Soil Mechanics and Foundation Engineering, 28(No. 3), 160-168.

Onoue, A., Mori, N., and Takano, J. (1987). "In-situ experiment and analysis on well resistance of gravel drains." *Soils and Foundations*, Japanese Soc. of Soil Mechanics and Foundation Engineering., 27(2), 42-60.

Papadimitriou, A., Moutsopoulou, M., Bouckovalas, G., & Brennan, A. (2007). Numerical Investigation of Liquefaction Mitigation using Gravel Drains. 4th International Conference on Earthquake Geotechnical Engineering. Thessaloniki – GREECE 2007:4ICEGE.

Pedersen, L. (2004). "Centrifuge features and limitations." http://nees.org/data/get/facility/UCDavis/Equipment/220/Centrifuge%20description.pdf.

Pedersen, L., and Kutter, B. (2004). "Horizontal shaking table features and limitations." http://nees.org/data/get/facility/UCDavis/Equipment/221/HorizontalShaker.pdf.

Pestana, J., Hunt, C., Goughnour, R., & Kammerer, A. (n.d.). Effect of Storage Capacity on Vertical Drain Performance in Liquefiable Sand Deposits.

Pestana, J.M., Hunt, C.E. and Goughnour, R.R. (1997). "FEQDrain: A Finite Element Computer Program for the Analysis of the Earthquake Generation and Dissipation of Pore Water Pressure in Layered Sand Deposits with Vertical Drains," *Report No. EERC 97-15*, Earthquake Engineering Research Ctr., Univ. of Calif., Berkeley, CA.

Pestana, J.M., Hunt, C.E. and Goughnour, R.R. (1997). "FEQDrain: A Finite Element Computer Program for the Analysis of the Earthquake Generation and Dissipation of Pore Water Pressure in Layered Sand Deposits with Vertical Drains," *Report No. EERC 97-17*, Earthquake Engineering Research Ctr., Univ. of Calif., Berkeley, CA.

Rathje, E. M., Chang, W. J., Cox, B. R., & Stokoe II, K. H. (January 7-9, 2004). Effect of Prefabricated Vertical Drains on Pore Pressure Generation in Liquefiable Sand. The 3rd

International Conference on Earthquake Geotechnical Engineering (3rd ICEGE). Berkeley, CA: University of California.

Rollins, K.M. Joshua K.S. Anderson, McCain, A.K., Goughnour, R.R. (2003). "Vertical composite drains for mitigating liquefaction hazard." 13th Intl. Conference on Offshore and Polar Engineering, Intl. Society for Offshore and Polar Engineering, paper 2003-SAK-01, 8. pp.

Rollins, K.M., Goughnour, R.R., Anderson J.K.S. and McCain, A. (2004). "Liquefaction hazard mitigation using vertical composite drains." Procs. 13th World Conf. on earthquake Engineering, EERI, Vancouver.

Rollins, K.M., Goughnour, R.R., Anderson, J.K.S. and Wade, S.F. (2004). Liquefaction Hazard Mitigation by Prefabricated Vertical Drains. Proc., Fifth Int'l Conference on Case Histories in Geotechnical Engineering, N.Y., 8pp.

Rollins, K.M. and Anderson, J.K.S. (2008). "Cone penetration resistance variation with time after blast liquefaction testing." Procs. Geotechnical Earthquake Engineering and Soil Dynamics-IV, Geotechnical Special Publication 181, ASCE, 10 p, CD-ROM.

Sasaki, Y., and Taniguchi, E. (1982). "Shaking table tests on gravel drains to prevent liquefaction of sand deposits." Soils Found., 22(3), 1-14.

Seed, H.B., and Booker, J.R. (1977). "Stabilization of Potentially Liquefiable Sand Deposits Using Gravel Drains," J. Geotech Engrg. Div., ASCE, 103(GT7), 757-768.

Seed, H., Mori, K., and Chan, C, (1975). "Influence of seismic history on the liquefaction characteristics of sands." Earthquake Engineering Research Center, Rep. No. EERC 75-25, College of Engineering, Univ. of CA, Berkeley, CA.

S&ME, Inc. (2006). Design Geotechnial Exploration Report. S&ME Project No. 1633-06-680.

Tokimatsu, K. and Seed, HB. (1987). "Evaluation of settlements in sands due to earthquake shaking," J. Geotechnical Engrg., ASCE, v. 11, no. 12, p. 1425-1445.

Vytiniotis, A. (2009). Numerical Simulations of the Response of Sandy Soils Treated with Pre-fabricated Vertical Drains. Cambridge.

Yang, D., Naesgaard, E., Byrne, P.M., Adalier, K., and Abdoun, T. (2004). "Numerical model verification and calibration of George Massey tunnel using centrifuge models." Can Geotech. J. NRC Canada, 41(5): 921-942.

Yegian, M, et al. (2015). "IPS UB NEES Report," https://nees.org/resources/13610.

Youd, T.L, Carter, B. (2005) "Influence of Soil Softening and Liquefaction on Spectral Acceleration" J. Geotech. Geoenviron. Eng., ASCE 131(7), 811-825.

Youd, T.L., Idriss, I.M., Andrus, R., Arango, I., Castro, G., Christian, J., Dobry, R., Finn, W.D.L., Harder, L., Jr., Hynes, M.E., Ishihara, K., Koester, J., Liao, S.S.C., Marcuson, W., III, Martin, G., Mitchell, J., Moriwaki, Y., Power, M., Robertson, P., Seed, R., and Stokoe, K.H. II. (2001). Liquefaction Resistance of Soils: Summary Report from the 1996 NCEER and 1998 NCEER/NSF Workshops on Evaluation of Liquefaction Resistance of Soils, ASCE, Journal of Geotechnical and Geoenvironmental Engineering, Vol. 127, No. 10, p. 817-833.

Youd, T.L., Hansen, C.M., and Bartlett, S.F. (2002). "Revised multilinear regression equations for prediction of lateral spread displacement, J. Geotech. and Geoenviron. Engrg., ASCE, 128(12) 1007-1017.

Zeghal, M, and Elgamal, A. W. (1994) "Analysis of Site Liquefaction Using Earthquake Records", Journal of Geotechnical Engineering, ASCE, 120*6), 666-1017.

Zhang, G., Robertson, P.K., and Brachman, R.W.I. (2002) "Estimating liquefaction-induced ground settlements from CPT for level ground" Canadian Geotechnical Journal, Canadian National Research Council, 39(5): 1168-1180.

Zienkiewicz, O., & Bettess, P. (1978). Fluid-structure dynamic interaction and wave forces. An introduction to numerical treatment. International Journal for Numerical Methods in Engineering, 13(1), 1-16.